SUMOylation as a fine-tuner of mitochondrial homeostasis and ageing in *Caenorhabditis elegans*

Investigating the role of eIF4E beyond translation initiation

PhD Thesis

Andrea Princz

Supervisor: Prof. Nektarios Tavernarakis

2018

University of Crete, Biology Department
FORTH, Institute of Molecular Biology and Biotechnology

Acknowledgements

First of all, I would like to thank my supervisor, Prof. Nektarios Tavernarakis for putting his faith in me and accepting me to be a member of his lab and mentoring me throughout my PhD years. The experience I gained here is invaluable regarding my future career. During these years I developed a sharper scientific sense and I learnt how to be an independent researcher. I couldn't have achieved this without his supervision and guidance. I thank to my Three Member Committee members, Prof. Charalampos Spilianakis and Prof. Kostas Tokatlidis for advising me on the progress of my work, and providing a "fresh eye" to the problematic situation when it was needed. I would also like to thank all the past and current lab members for their companionship and scientific discussions. I am especially thankful that I got to know and befriend Matthias, who helped me through the start of my PhD. I found a real friend in him. Importantly, through him I met Rena, who also became one of my best friends, supported me in everything and just showed incredible kindness and understanding towards me.

I am thankful for all my old and new friends as well. I left my home country to seek a career in a foreign country; still my oldest, best friend, Veroni, stayed next to me and supported me during the hard times; thank you for everything you did for and with me throughout these ~16 years of friendship. Starting a new life in Crete meant to meet with a lot of new, unique and interesting people. I am most grateful for the friendship of Giulia, who was my flat-mate for more than 2 years; and Ruth, with whom we made some amazing trips around the island and supported each other in private and professional life. I couldn't have made it through the hardest, last couple of months without Natalie. I will never forget your support, and your unconditional faith in me; without your friendship it would have been much harder to reach to this point. Thank you for coming to my tennis matches, cheering for me and thank you for understanding when I needed space and alone-time.

My eternal gratitude goes to my family. They made all of this possible, worked relentlessly to support me not just throughout these last few years but my entire life. Without them I couldn't have reached to this point in my life. They achieved to raise a biologist, starting from a small village in Hungary, but ending up in a different country pursuing her PhD. Their love was sometimes the only thing keeping me away from depression during the difficult times. I can only hope that I could become as good as a parent like they are at some point in the future. I am thankful for my brother as well, who could always advise me or solve my computer science problems; he was a life-saver on more than one occasion. I am thankful beyond words that I can have the best family and friends anybody could ever wish for.

"When someone you love becomes a memory, the memory becomes a treasure."

Περίληψη

Το σηματοδοτικό μονοπάτι της ινσουλίνης/προσομοιάζοντος στην ινσουλίνη αυξητικού παράγοντα επηρεάζει τη διάρκεια της ζωής απομακρυσμένων εξελικτικά τάξεων, ελέγχοντας την δράση μεταγραφικών παραγόντων. Στο νηματώδη *Caenorhabditis elegans* και σε καταστάσεις χαμηλής σηματοδότησης του μονοπατιού της ινσουλίνης/ προσομοιάζοντος στην ινσουλίνη αυξητικού παράγοντα και στρες, οι μεταγραφικοί παράγοντες DAF-16/FOXO και SKN-1/Nrf επάγουν τη μακροζωία. Η δράση και ο υπο-κυτταρικός εντοπισμός των DAF-16 και SKN-1 καθορίζονται περαιτέρω από συγκεκριμένες μετα-μεταγραφικές τροποποιήσεις, όπως η φωσφορυλίωση και η ουβικουϊτίνωση. Σ' αυτή τη διδακτορική διατριβή, δείχνουμε ότι η γήρανση προκαλεί μια αξιοσημείωτη αύξηση στα επίπεδα της πρωτεΐνης SUMO στον *C. elegans*. Με τη σειρά της, η SUMO συντονίζει τη δράση των DAF-16 και SKN-1 σε συγκεκριμένους ιστούς του νηματώδη, ώστε να ενισχύσει την αντοχή στο στρες. Η σουμοϋλίωση του DAF-16 διαμορφώνει την ομοιόσταση των μιτοχονδρίων παρεμβαίνοντας στη μιτοχονδριακή δυναμική και τη μιτοφαγία. Τα ευρήματά μας αποκαλύπτουν ότι η SUMO είναι ένας σημαντικός ρυθμιστής της διάρκειας ζωής και παρέχει νέες ιδέες σχετικά με την πολυπλοκότητα των σηματοδοτικών μηχανισμών οι οποίοι επηρεάζουν την γονιδιακή έκφραση ώστε να καθορίσουν την επιβίωση του οργανισμού στα μετάζωα.

Summary

SUMOylation (the attachment of a small ubiquitin related modifier (SUMO) to a target protein) is employed by the cell to govern diverse and vital processes. The consequences of SUMOylation vary from changing the localization of proteins within the cell, through influencing protein-protein interactions to determining protein stability. The function of SUMO has already been implicated in DNA damage response, cell division, development and carcinogenesis, among others. However, our understanding of SUMOylation in relation to ageing remains elusive. Here we show that the amount of SUMOylated proteins is increasing in *C. elegans* during ageing. Reducing the expression of the sole SUMO protein (SMO-1) by RNAi, leads to a shortened lifespan, while a modest overexpression of SUMO extends the life expectancy of *C. elegans*. Furthermore, we find that the shortened lifespan is conveyed via the intestine and the nervous system. The regulation of lifespan is achieved via conserved signaling pathways, and there are several main transcription factors, like DAF-16/FOXO, SKN-1/NRF and HSF-1 which influence the process of ageing. The SUMOylated status of HSF-1 and its inhibitory function has been already demonstrated. *In silico* analysis predicted putative SUMOylation sites in the other two transcription factors, DAF-16 and SKN-1, as well. We find that the lifespan influencing effect of SUMOylation is achieved via DAF-16 and SKN-1. In order to show that SUMOylation affects the transcriptional activity of DAF-16 and SKN-1, we analyzed the expression of their target genes, using reporter constructs, in animals subjected to *smo-1* RNAi and we found an increased expression under normal conditions. Moreover, in a SMO-1 overexpressing background, the mRNA levels of DAF-16 target genes are significantly reduced. Intriguingly, this change in the mRNA levels of SKN-1 target genes did not happen in the same genetic background. Using transgenic lines, we were able to observe co-localization of DAF-16 and SMO-1 in the nucleus. Furthermore, SMO-1 overexpression confers stress resistance; these animals survived longer under oxidative and heat stress conditions due to their ability to mount a more robust stress response in early adulthood compared to wild type. Besides their role as master regulators of lifespan, DAF-16 and SKN-1 regulate mitochondrial homeostasis as well. Interestingly, reduced *smo-1* expression causes the preservation of interconnected mitochondrial network in the intestine of aged animals and this phenotype is DAF-16 dependent. Moreover, we find that SUMOylation is required for the fission of mitochondria. As a consequence, the process of mitophagy is blocked upon *smo-1(RNAi)*. Additionally, *smo-1(RNAi)* treated animals have more active mitochondria and they produce more ROS as well in a DAF-16 dependent manner. At the same time, animals with reduced expression of *smo-1* display no change in their mitochondrial DNA copy number compared to control levels. We conclude that SUMOylation is required for healthy ageing and maintenance of mitochondrial homeostasis.

Contents

Acknowledgements **2**

Περίληψη **3**

Summary **4**

Introduction **6**

Caenorhabditis elegans as a model organism for ageing 6

The SUMOylation pathway 12

Materials and Methods **16**

Results **23**

SUMOylation levels increase during ageing in *C. elegans* 23

SUMO modulates *C. elegans* lifespan 24

The transcriptional activity of DAF-16 and SKN-1 is regulated by SUMO 28

SUMO facilitates mitochondrial homeostasis 35

Discussion **44**

Part 2: Investigating the role of eIF4E beyond translation initiation **48**

Introduction **48**

Results **50**

HSF-1 promotes the degradation and prevents the nuclear accumulation of IFE-2 50

XPO-1 influences lifespan but not the nuclear localization of IFE-2 53

Heat stress sequesters IFE-2 in stress granules but not in the nucleus 54

Outlook **56**

References **57**

Introduction

Caenorhabditis elegans as a model organism for ageing

As human life expectancy keeps increasing (https://ourworldindata.org/life-expectancy), the need for preserving health at older ages is becoming more imperative. In order to achieve longer health-span, first we need to have a good understanding of the molecular mechanisms which regulate the process of ageing. Since studies in humans are rarely possible and take impractically long time, we take advantage of small model organisms with short lifespans to decipher the basic mechanisms of ageing. One of the most popular model organisms for ageing studies is the nematode *Caenorhabditis elegans* (*C. elegans*). There are several features which make this animal an ideal model organism: *C. elegans* has a median lifespan of two weeks, it has a transparent body, its population is made up from self-fertilizing hermaphrodites, however males are also naturally occurring (~0.2 %), its cell lineage is invariable and described (http://www.wormatlas.org/), its genome is sequenced and well-annotated (https://wormbase.org/#012-34-5), it is small (~1.2 mm) and easily maintained under laboratory conditions (1) and its genome can be easily manipulated either by RNA interference (RNAi) (2) or transgenes (3).

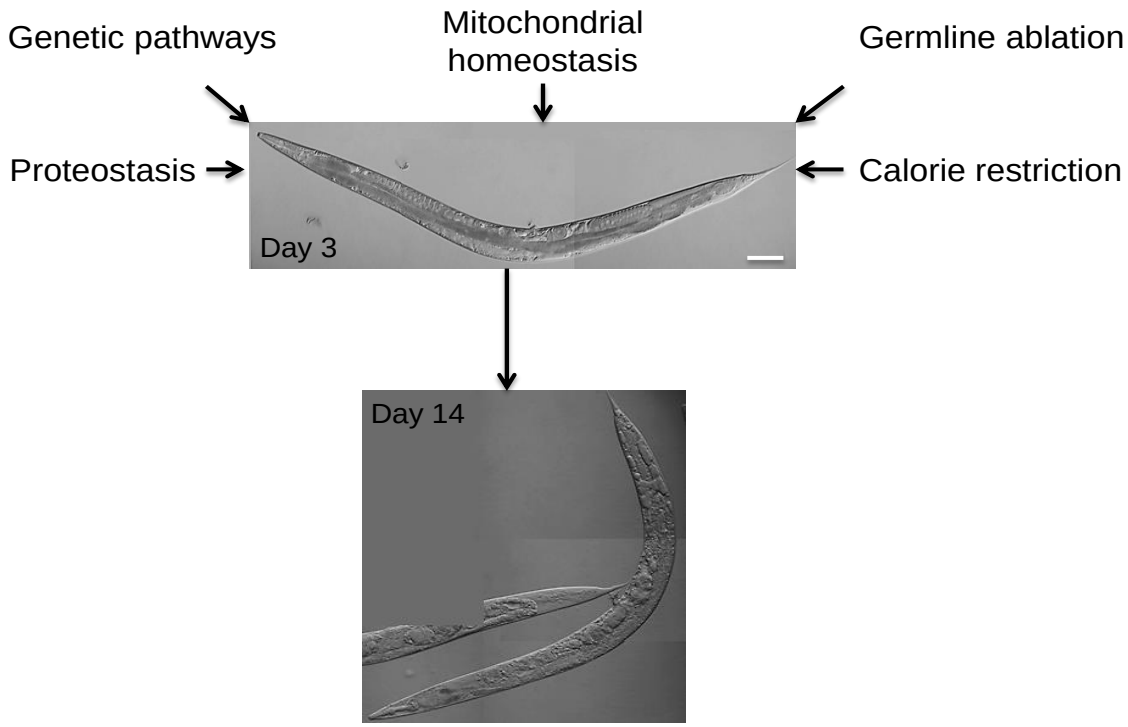

Figure 1: Main factors that regulate ageing in *C. elegans*. The lifespan of an animal will be determined as an outcome of genetic and environmental factors that the animal will encounter. The loss of proteostasis and impairment of mitochondrial homeostasis promotes ageing, while calorie restriction and germline ablation can extend lifespan. Pictures represent the phenotypical changes during ageing, scale bar: 100 µm.

The lifespan of *C. elegans* is determined by evolutionarily conserved signaling pathways and external stimuli such as insulin/IGF-1 signaling, germline ablation, dietary restriction, mTOR activity and mitochondrial signaling (4) (Figure 1). The effectors of these stimuli are the transcription factors which will initiate the proper transcriptional program as an answer to the diverse signals from the environment. The most influential, conserved transcription factors are: DAF-16 (FOXO), HLH-30 (TFEB), PHA-4 (FOXA), HIF-1 (HIF1), HSF-1 (HSF1), SKN-1 (NRF2) and nuclear hormone receptors. Importantly, these transcription factors not always act alone; depending on the stress signal they can form complexes to mount the appropriate stress response. DAF-16 (dauer formation abnormal) is the terminal transcription factor of the insulin/IGF-1 pathway and its activity is regulated on multiple levels via posttranslational modifications. Under normal, growth promoting conditions the activation of insulin receptor, DAF-2, initiates a phosphorylation cascade in the cytoplasm which ends with the phosphorylation of DAF-16 by the AKT-1 kinase and promotes its cytoplasmic retention (5) (Figure 2). Similarly, acetylation by CBP-1 (CBP/p300 homolog) also causes the accumulation of DAF-16 in the cytoplasm (6). The phosphorylation by AKT-1 can be counteracted by DAF-18/PTEN which can dephosphorylate DAF-16 and promote its nuclear localization (7). Another protein, PRMT-1, a protein arginine methyltransferase, helps to keep DAF-16 in the nucleus (8). The stability of DAF-16 is regulated via ubiquitination by RLE-1 (9) and deubiquitination by MATH-33 (10) (Figure 2).The cell non-autonomous action of DAF-16 on lifespan has also been proposed, based on evidence that showed the intestine specific rescue of *daf-16* deficiency is capable to restore the normal lifespan of the animals (11). Moreover, DAF-16 is required for the longevity effect of intermittent fasting (12) and calorie restriction initiated in middle-aged animals (13). On the other hand, the activity of DAF-16 is not needed under chronic calorie restriction (14) or under continuous fasting regime (15, 16) for the extended lifespan phenotype.

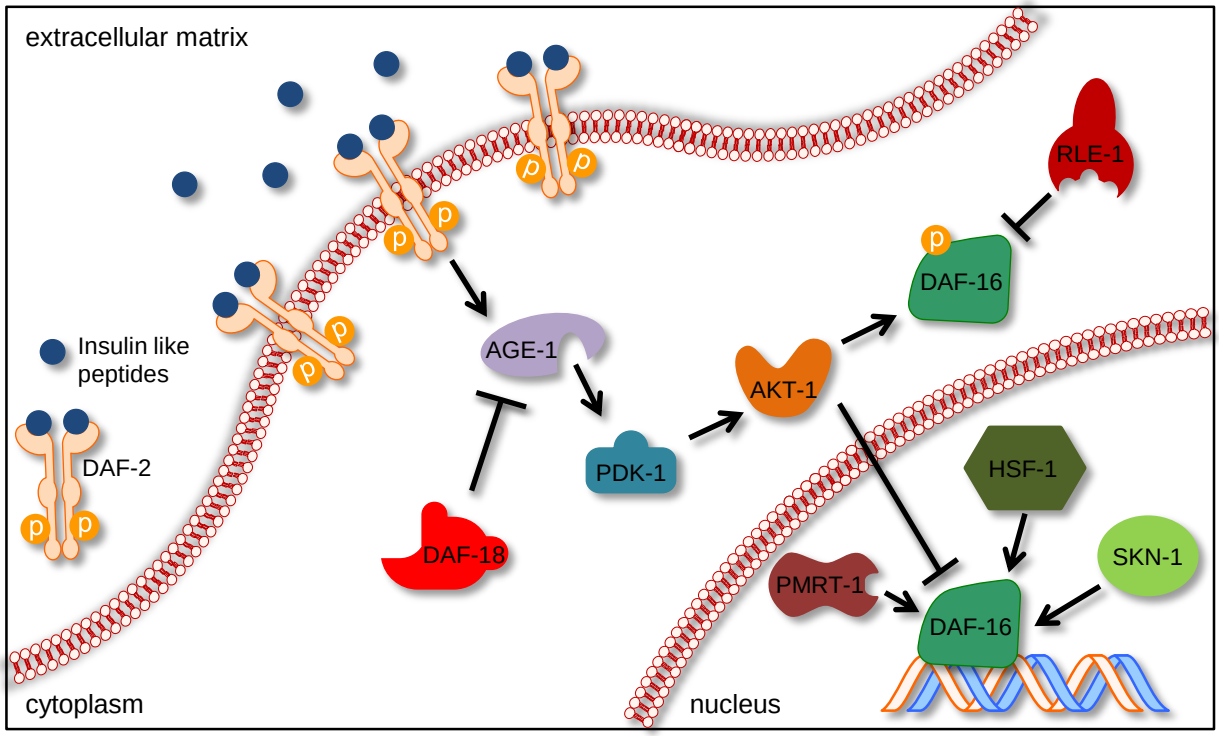

Figure 2: Insulin/IGF-1 signaling in *C. elegans*. Under normal conditions the binding of insulin like peptides to the DAF-2 receptor leads to its auto-phosphorylation and activation of other cytoplasmic kinases which results in the phosphorylation of DAF-16 and its cytoplasmic localization. DAF-18 inhibits this phosphorylation cascade and initiates the nuclear translocation of DAF-16. PMRT-1 promotes the nuclear retention of this transcription factor and HSF-1 and SKN-1 are influencing the transcriptional activity of DAF-16.

SKN-1 (skinhead-1) is another main stress responsive transcription factor and its role has been implicated in oxidative, ER (endoplasmic reticulum) stress and starvation; it is also important for metabolic processes and the maintenance of protein homeostasis (proteostasis) under normal conditions (17). Under favorable conditions the activity of SKN-1is suppressed via phosphorylation by AKT-1/2, SGK-1 and GSK-3 (18, 19). Oxidative stress induces the activation of SKN-1 via phosphorylation by PMK-1(p38) which leads to the nuclear localization of the protein in the intestine of the animals (20). Reduced insulin signaling is also able to trigger SKN-1 activity and it is required for the long lifespan of *daf-2* mutants (18). Phosphorylation by MPK-1 (ERK) initiates the nuclear translocation of SKN-1 and the suppression of the expression of insulin-like peptides (21). Interestingly, DAF-16 is able to induce *skn-1* expression in a DAF-16 overexpressing background, where SKN-1 is dispensable for the regulation of lifespan but not for the oxidative stress response (22).

HSF-1 is the sole heat shock transcription factor encoded in the *C. elegans* genome. Heat stress leads to the trimerization and activation of HSF-1 which induces the heat shock response (23). Besides having a pivotal role in the heat shock response, HSF-1 also plays a role in development and metabolism (24-26). Phosphorylation of HSF-1 initiates its function upon heat stress (23) while under reduced insulin

signaling the phosphorylation of the HSF-1 regulatory complex, DDL-1/DDL-2 results in the activation of HSF-1 (27). During larval development HSF-1 can be activated indirectly via HPK-1 (homeodomain-interacting protein kinase-1) which prevents the inhibitory SUMOylation of HSF-1 (28). Recently it was demonstrated that HSF-1 is required for the maintenance of actin cytoskeleton during ageing (29, 30). HSF-1 is also essential for the long lifespan of *daf-2* mutants together with DAF-16 (31) and it extends lifespan under hormetic heat stress conditions (32) (Figure 2).

HLH-30 (basic helix-loop-helix transcription factor) is the master regulator of autophagy which also plays a vital role in lifespan regulation. HLH-30 governs the autophagic response to starvation (33), innate immunity (34) and it is also indispensable for the long lifespan of several longevity mutants (35). The activity of HLH-30, similarly to DAF-16, is regulated by posttranslational modifications. Phosphorylation by LET-363 (mTOR) inhibits HLH-30 function by keeping it in the cytoplasm (36). Recently it has been shown that HLH-30 is a target of the nuclear export protein, XPO-1, which functions to halt the activity of this transcription factor (37). Importantly, DAF-16 and HLH-30 can act together to promote longevity in a reduced lipoprotein synthesis regime (38). Recently, a more general interaction between the two transcription factors was demonstrated in order to regulate lifespan and oxidative stress response, but not the heat shock response (39).

Lifespan extension via dietary restriction requires the transcription factor PHA-4 (40) (defective pharynx development) which was initially described to function in the development of foregut (41). The role of PHA-4 is also important in the longevity of germline-less animals. LET-363/TOR can phosphorylate and thereby suppress the activity of PHA-4 (42).

The hypoxia inducible factor-1 (HIF-1) has a complex and context dependent influence on the lifespan of *C. elegans* (43). Under normal oxygen conditions HIF-1 is ubiquitilated by VHL-1 (von Hippel-Lindau tumor suppressor homolog), signaling for degradation, however low oxygen levels inhibit VHL-1, allowing for HIF-1 stabilization and nuclear translocation (43). Stabilization of HIF-1 extends lifespan (44); it has also been reported to promote the extended lifespan of mitochondrial mutants (45) and it is required for mitophagy, induced upon iron starvation (46). Another study found that HIF-1 stabilization only in neurons is sufficient to promote longevity via serotonin signaling to the intestine (47).

Nuclear hormone receptors, like DAF-12, NHR-80 and NHR-49 are also determinants of the ageing process. DAF-12 can be activated by specific steroids, called dafachronic acids, and it is required for the extended lifespan of germline-less animals (48, 49). Additionally, NHR-80 and NHR-49 have been reported to be upregulated and interact physically in animals which lack their germline (50, 51).

Moreover, NHR-49 regulates the transcriptional programs in response to oxidative stress, starvation and the expression of fatty acid β-oxidation genes (52, 53).

LET-363 (lethal) is the *C. elegans* homolog of mTOR (mechanistic target of rapamycin) which is a serine/threonine kinase and it functions under normal nutrient conditions to promote cell growth, protein synthesis and inhibit autophagy (54). Upon calorie restriction, TOR signaling is inhibited and the lifespan of the animals is increased in a DAF-16 (55, 56) and PHA-4 (57) dependent way. Inhibition of *rsks-1* (ribosomal protein S6 kinase), a target of LET-363, is able to further extend the long lifespan of *daf-2* mutant, indicating that these two lifespan influencing pathways act in parallel in the regulation of longevity (58).

Sirtuins encode a family of NAD-dependent protein deacetylases which are linked to cellular nutrient availability and they can influence lifespan. The *C. elegans sir-2.1* (yeast SIR related) has a positive effect on longevity. Its overexpression extends lifespan (59) via the activation of DAF-16 (60). Moreover, it has been shown that under chronic calorie restriction, *sir-2.1* does not have a further effect on lifespan (61). Nonetheless, calorie restriction initiated in middle-aged animals does not require the function of SIR-2.1 (62), indicating a condition dependent involvement of SIR-2.1 in mediating the lifespan of *C. elegans*. Recently, crosstalk has been shown between this nutrient sensing pathway and proteostasis. It has been demonstrates that HSP-90 stabilizes SIR-2.1, allowing to perform its proper function. Loss of HSP-90 results in the proteosomal degradation of SIR-2.1 (63).

Another protein that serves as a cellular energy sensor is AMPK (AMP-activated protein kinase), encoded by *aak-2* (AMP activated kinase) in *C. elegans*. Similarly to SIR-2.1, AAK-2 also acts through DAF-16 in a reduced insulin signaling regime (14). Furthermore, DAF-16 regulates the expression of *aakg-4* (AMP activated protein kinase gamma subunit), a regulatory subunit of AAK-2, creating a feedback loop between AAK-2 and DAF-16 (27). Additionally, reducing *aak-2* expression shortens, while overexpression of the gene extends lifespan (13).

Initially, the production and accumulation of reactive oxygen species (ROS) during ageing was associated with macromolecular damage and as a cause of cellular senescence (64). In recent years however, the role of ROS as signaling molecules are emerging. There are several species of ROS which can be produced in the mitochondria (electron transport chain) or cytoplasm (enzymatic reactions) and they can have different consequences on cellular physiology (64). For instance, it has been demonstrated that in long-lived mitochondrial mutants and germline-less animals ROS convey lifespan extension (65, 66). Additionally, treatment with low concentrations of paraquat, which will cause oxidative stress through a

mild elevation in ROS production, also extends lifespan (65); this phenomenon is called mitohormesis. Recent evidence suggests that ROS from the mitochondria or endoplasmic reticulum (ER) is able to suppress the unfolded protein response of ER (UPR^{ER}) and initiate the oxidative stress response via SKN-1 activation (67).

The ability of the cell to maintain proteostasis gradually declines during ageing. This is a consequence of the collapse of several surveillance mechanisms, like autophagy, unfolded protein response (in the ER or mitochondria), proteasome system, heat shock response and protein synthesis. Autophagy is one of the main degradation mechanisms in the cell. It involves the formation of a double membrane which engulfs part of the cytoplasm or even whole organelles, like mitochondria (68). Autophagy is involved in several longevity pathways, like insulin/IGF-1 signaling (69), calorie restriction (70) and TOR signaling (71).

It is important to note that most of the lifespan modulating genes have additional phenotypes in the organism. It was suggested that in some cases the effect on lifespan is only a “side-effect” of a loss of a gene, e.g. it is well known that insulin signaling mutants have altered metabolism, development and stress resistance (72).

Over the course of ageing, not only proteostasis, but mitochondrial function decreases as well (73). Depending on the age, type, developmental stage and environmental conditions of the cell, mitochondrial number, shape and size are subject to change. Healthy mitochondrial function is heavily dependent on mitochondrial dynamics, which can influence the quality of the organelles and mitochondrial DNA (mtDNA) stability; moreover, it is a prerequisite of mitophagy (mitochondria specific autophagy) (74). Mitochondrial dynamics is determined by fusion and fission events, orchestrated by dynamin related GTPases: FZO-1/Mitofusin1 (Fzo mitochondrial fusion protein related) is required for the fusion of outer mitochondrial membrane, EAT-3/OPA1 (eating abnormal pharyngeal pumping) controls the inner mitochondrial membrane fusion event and DRP-1 (dynamin-related protein 1) coordinates the fission of mitochondria (75) (Figure 3). Proper mitochondrial function involves a balance between elimination of damaged mitochondria and mitochondrial biogenesis. Recently, it has been suggested that changes in mitochondrial dynamics can lead to the accumulation of mitochondrial defects which can cause reduced mitochondrial activity. Moreover, alterations in mitochondrial dynamics can also impair the clearance of damaged organelles, further increasing the detrimental effects of the dysregulation of mitochondrial dynamics which will eventually lead to ageing and age-related diseases (76) (Figure 3).

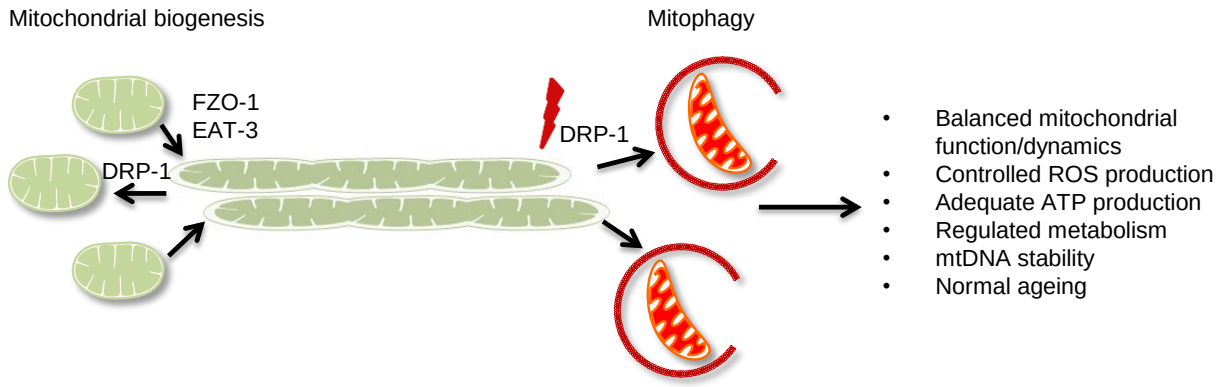

Figure 3: Schematic representation of mitochondrial dynamics. The mitochondrial number in a cell is determined by the ratio of biogenesis and degradation/mitophagy. FZO-1 and EAT-3 initiates the fusion of individual mitochondria, while DRP-1 participates in the process of fission. Proper balance of mitochondrial dynamics ensures correct function of the organelle, including ROS and ATP production, metabolism and mtDNA stability. All these processes allow for normal ageing of the cell/organism.

The SUMOylation pathway

Posttranslational protein modifications (PTMs) play pivotal roles in all cellular processes under normal and stress conditions. SUMOylation, a posttranslational modification through which a small ubiquitin like modifier (SUMO) gets attached to a target protein, has an invaluable function in the cell; it regulates protein-protein interactions, DNA damage response, mitochondrial dynamics, development and cellular senescence, among others (77, 78). The process of SUMO modification is analogous to the ubiquitin pathway; however, it uses its own set of enzymes which cannot be substituted with the enzymes of the ubiquitin pathway. The SUMO pathway starts with the translation of the immature SUMO protein. The activation of the protein requires a proteolytic cleavage by a SUMO protease and it results in the exposure of a di-glycine motif. Through the di-glycine motif the dimer E1 enzyme binds and activates the SUMO protein. In the next step the activated SUMO is transferred to the E2 conjugating enzyme. There is only one E2 enzyme identified up to date, UBC9. This complex binds to the E3 SUMO ligase and SUMOylates the target protein *in vivo*. Under *in vitro* conditions the E3 enzyme could be dispensable, but this depends on the target and experimental conditions. The target protein usually possesses a consensus SUMOylation site: ψKXD/E, where ψ is a large hydrophobic amino acid, K is the target lysine, X is any amino acid and D/E is aspartate or glutamate (79, 80). Nevertheless, SUMOylation can also occur on non-canonical, extended SUMOylation sites (81-83). Protein modification by SUMO is a transient process; SUMO proteases (called SENPs in mammals and Ulps in yeast and *C. elegans*) are responsible for the cleavage of SUMO from the target protein after it has fulfilled its function (Figure 4).

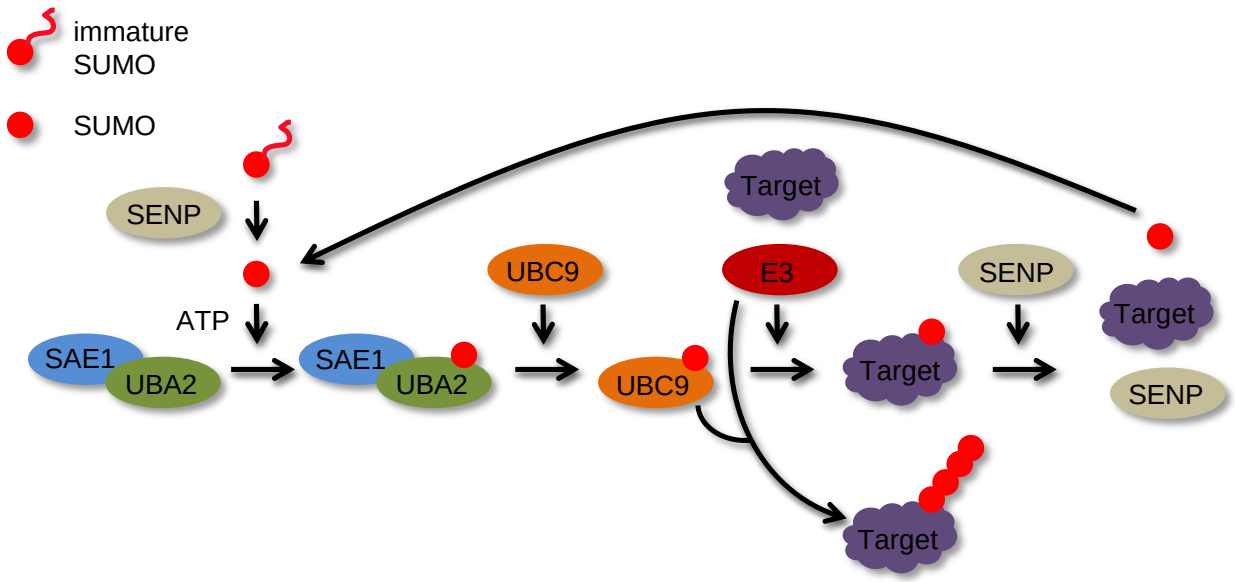

Figure 4: SUMOylation pathway. SUMO is translated as an immature protein, a C-terminal cleavage by a SUMO protease (SENP) is needed for its maturation. The E1 enzyme, which is a heterodimer consisting of SAE1 and UBA2, will activate SUMO through and ATP dependent reaction, and transfer it to the E2 enzyme, UBC9. UBC9, together with the E3 ligase will attach SUMO to the target protein. A protein can be mono- or polySUMOylated, and the process is reversible: a SENP will cleave SUMO from the target protein and the components can enter a new SUMOylation cycle.

Although in yeast the SUMO modified target proteins can measure up to 10% of all the proteins, the described pathway consists of only a few enzymes. This raises the question how specificity is achieved, especially because the ubiquitin pathway possesses more than a hundred E3 ligases which provide substrate specificity (84). Three ways of actions have been proposed for SUMO: competition with other posttranslational modifications, interfering with and promoting protein-protein interactions. In the case of IκBα, SUMO competes with ubiquitilation, protecting IκBα from degradation (85). SUMO can also compete with acetylation of MEF2A (myocyte-specific enhancer factor 2A), where acetylation is needed for the transactivation activity of the protein (86). Whenever the yeast PCNA (cell proliferation nuclear antigen) is SUMOylated at the residue K127, the interaction with Eco1 is blocked, therefore this protein cannot activate sister chromatid cohesion during S phase (87). The most widely studied function of SUMO is the positive regulation of protein-protein interactions. This is achieved through the interaction between SUMO and SUMO-interaction motifs (SIMs) in the target/partner protein. This interaction can strengthen protein associations and promote group SUMOylation; it is also called SUMO glue (88). Interestingly, SUMO-SIM interactions can be exploited in an intramolecular manner as well; as it has been shown with the example of thymine DNA glycosylase, where the SUMO-SIM interaction within the protein causes conformational change and it is promoting the enzymatic turnover of the protein (89). Most of the times, functionally and physically interacting protein complexes are target for group

SUMOylation. These proteins harbor several SUMOylation sites and SIMs which will enhance protein-protein interactions. This phenomenon also provides robustness to the system, since it is less likely that a mutation in the modification site will have detrimental effect on the whole protein complex and its function (84). These SUMOylated protein groups can be regulated by SUMO-targeted ubiquitin ligases (STUbLs) which control the function of SUMOylated proteins through ubiquitilation (90).

There are several *in silico* tools for the prediction of SUMO modification. The GPS-SUMO prediction site gives results about the SUMOylation sites and SIMs of a protein (http://sumosp.biocuckoo.org/). We initially used SUMOplot for our *in silico* analysis (http://www.abgent.com/sumoplot) to predict SUMOylation in our proteins of interest. Recently a new, more reliable tool became available: SUMOgo (http://predictor.nchu.edu.tw/SUMOgo/). The advantage of this method is that it is able to take into account other posttranslational modifications that a protein might possess (e.g. phosphorylation, acetylation) and make predictions about SUMOylation based on this information as well. The tests of this new method showed that it is generating even more reliable predictions than Biocuckoo (91).

The *C. elegans* genome encodes a sole SUMO gene, *smo-1*, a feature which renders the nematode an ideal model organism for dissecting the process of SUMOylation in regards to ageing. While there is increasing interest regarding the role of SUMOylation in cellular senescence (92-94); there is only one, recent study showing a link between SUMOylation and ageing up to date. Under reduced insulin signaling conditions, the SUMOylated status of an RNA binding protein in the germline (CAR-1) is reduced and this leads to the promotion of longer lifespan through reduction in *glp-1* levels (95). SUMOylation in *C. elegans* has been mainly studied in the context of development; its role has been shown in embryonic, vulval and muscle development and in DNA damage response. During oocyte meiosis and embryonic development, SUMOylation is needed for chromosome congression (96), cell cycle progression (97), the anchoring of telomeres to the nuclear envelope (98), the assembly of cytoplasmic intermediate filaments (99) and the repression of Hox genes (100). In vulval development, SUMOylation of transcription factors inhibits their function and thereby allows the induction of proper developmental programs in specific cells (101-103). SUMOylation is needed for the development of pharyngeal muscles (104, 105) and later in adulthood for the maintenance of muscle myosin levels (106). During DNA damage response, SUMOylation protects POLH-1 from degradation, ensuring to carry out its function (107).

Here we show a direct link between SUMOylation and the regulation of ageing in *C. elegans*. Perturbation of SUMOylation levels causes alterations in lifespan and mitochondrial homeostasis in a DAF-16 and SKN-1 dependent manner. Reduced *smo-1* expression leads to shortened lifespan, while a

modest overexpression promotes a longer lifespan. We report for the first time that DAF-16 is SUMOylated. SUMOylation represses the transcriptional activity of DAF-16. At the same time, lack of SUMOylation causes the over-activation of stress response genes under normal conditions, while under stress conditions these animals are mounting a less effective stress response. Moreover, mitochondrial homeostasis is altered upon knocking down *smo-1*; ATP and ROS production is increased, mitochondrial fission is reduced and the process of mitophagy is blocked. These results demonstrate that the balance in protein SUMOylation/deSUMOylation is needed for normal ageing and mitochondrial homeostasis in *C. elegans*.

Materials and Methods

C. elegans Strains and Genetics

We followed standard procedures for maintenance of *C. elegans* strains and transgenic lines (108). Animals were grown at 20°C unless noted otherwise. The following strains were used for this study: N2: wild type Bristol isolate, CB1370: *daf-2(e1370)III*, MQ887: *isp-1(qm150)IV*, CF1038: *daf-16(mu86)I*, SJ4143: N2;*Is*[p_{ges-1}mtGFP], CL2166: N2;*Is*[p_{gst-4}GFP], CF1553: N2;*Is*[p_{sod-3}GFP], TJ356: N2;Is[p_{daf-16}DAF-16a/b::GFP;*rol-6(su1006)*], FGP14: *unc-119(ed3);fgpIs35*[*unc-119*(+);p_{smo-1}*::6xHis::smo-1::smo-1 3' UTR*], VP303: *rde-1(ne219)V;kbIs7*[p_{nhx-2}*::rde-1;rol-6(su1006)*], NR350: *rde-1(ne219)V;kzIs20*[p_{hlh-1}*::rde-1*;p_{sur-5}::NLS::GFP], NR222: *rde-1(ne219)V;kzIs9*[p_{lin-26}::NLS::GFP;p_{lin-26}*::rde-1;rol-6(su1006)*], TU3401: *sid-1(pk3321)V;uIs69*[p_{myo-2}::mCherry;$p_{unc-119}$*::sid-1*], MQ1333: *nuo-6(qm200)I*, CB4876: *clk-1(e2519)III*, KX15: *ife-2(ok306)X,* NL2099: *rrf-3(pk1426)II*, JRIS1: N2;Is[p_{rpl-17}HyPer].

Molecular cloning

To create a p_{smo-1}DsRed::SMO-1 construct, we utilized the pPD95.77(DsRed) construct, previously generated in the lab. Briefly, GFP was excised from pPD95.77(GFP) vector using the AgeI/EcoRI restriction enzymes, and was replaced with the fragment coding DsRed, isolated from p_{col-12}DsRed (109). We amplified the *smo-1* ORF from *C. elegans* genomic DNA, using the following primer pair: 5'-GAATTCCAACATGGCCGATGATGCAG-3' and 5'-GGATCCCGTTTATAGCGGGAGTCTC-3' and the 560 bp product was first subcloned into pCRII-TOPO vector (Invitrogen). Using the restriction enzyme EcoRI, the fragment was excised and inserted into pPD95.77(DsRed) and was sequenced to check for possible mutations and orientation. The correct construct was introduced to *unc-119(ed3)* worms, together with pRH21 (110), using biolistic transformation. To generate the p_{vha-6}SMO-1 construct, we amplified the *smo-1* ORF from *C.elegans* genomic DNA, using the following primer pair: 5'-GTTTCAGAGACTCCCGCTATAAAC-3' and 5'-GCTAGCCGAAGAGTTTATTTGTAAG-3' and the 570 bp product was subcloned into pCRII-TOPO vector. Using the restriction enzymes BamHI/NheI, the fragment was inserted in pPD96.52 vector, containing the *myo-3* promoter. The promoter was removed, using the HindIII/XbaI restriction enzymes and the 950 bp coding sequence of *vha-6* promoter was inserted from pCRII-TOPO. To amplify the *vha-6* promoter from *C. elegans* genomic DNA, we used the following primer pair: 5'-GAGAAGATGTGATGAGATGGAGAGAAAG-3' and 5'-TGAGCACTTTACAGTTCTTGTTGATTTG-3'. The construct, together with the pRH21 plasmid, was introduced to *unc-119(ed3)* worms, using biolistic transformation. To generate the p_{rab-3}SMO-1 construct, we amplified the *smo-1* ORF from *C. elegans* genomic DNA, using the following primer pair: 5'-CCCGGGGTTTCAGAGACTC-3' and 5'-

GGTACCCGAAGAGTTTATTTGTAAG-3' and the 580 bp product was subcloned into pCRII-TOPO vector. We inserted the Xma/KpnI fragment in pPD95.77, containing the *rab-3* promoter. The construct and the pRH21 plasmid were introduced to *unc-119(ed3)* worms, using biolistic transformation. The generation of $p_{ife\text{-}2}$IFE-2::GFP transgenic strain has been described previously (111). For the generation of *smo-1*, *ubc-9* , *ulp-1*, *ulp-2*, *ulp-4*, *ulp-5* and *xpo-1* RNAi construct, the following primer pairs were used: 5'-TAAACGATGGCCGATGATGC-3' and 5'-GGATCCCGAAAGAGTTTATTTGTAAG-3', 5'-ATGTCGGGAATTGCTGCAGG-3' and 5'- GTCCAGAAGCAAATGCTCGAGTAG-3', 5'-CCACAGTTGTTACAGAACAAG-3' and 5'- GGATCCCACATTAGTTTCTCTGCTTC-3', 5'-ATGAGTGATTCAACTCAAATGGAGG-3' and 5'- CATACAGCAGTTGCCACAAACG-3', 5'-ATGGAAGTGTCAACGTCTTACTGTACG-3' and 5'- GATTTTTGCTGTCTCCAGGAGAAG-3', 5'-ATGCCTCATCCTAAGCTCACTCC-3' and 5'- GCCTGGTTCATTCAAAAAAATACAG-3', 5'-CATCCATGGGTGTCTCGGAGCAGGATG-3' and 5'-CATCCATGGACGCATATCCTCATCTTCCAC-3', respectively. The resulted fragments were cloned into the vector pL4440 and the constructs were transformed into HT115(DE3) *Escherichia coli* strain, which is defective for RNase III. Bacteria carrying the pL4440 empty vector alone were used for control experiments. RNAi constructs against *daf-2*, *eat-3*, *daf-16*, *skn-1, drp-1, fzo-1* and *hsf-1* have been described previously (112-114). Double RNAi against *skn-1* and *smo-1* was constructed by digesting the *skn-1(RNAi)* and *smo-1(RNAi)* plasmids with BamHI restriction enzyme and ligating the *smo-1* fragment (~1000 bp) into *skn-1(RNAi)* plasmid, treated with Alkaline Phosphatase, Calf Intestinal (CIP, New England Biolabs).

Epifluorescence and confocal microscopy

Transgenic worms were placed in a drop of 10mM levamisole on a microscope slide and sealed with a cover slip. Images were taken with a Zeiss AxioImager Z2 epifluorescence microscope. At least 25 worms were imaged and quantified per condition; each experiment was repeated at least 3 times. Mean fluorescence intensity was measured using the software Image J.

For confocal microscopy, animals were immobilized on a 5% agarose pad, in a 5μl drop of Nanobeads (Nanobeads NIST Traceable Particle Size Standard 100 nm, Polysciences). Images were taken with an LSM710 Zeiss confocal microscope, Axio-observer Z1.

Western blot analysis

Synchronized animals were collected in M9 buffer and after a short spin, the buffer was exchanged to the lysis buffer (50 mM Tris-HCl pH: 7.4, 150 mM NaCl, 1 mM EDTA, 1% Triton X-100, 1 mM PMSF, 30mM NEM) supplemented with protease inhibitor cocktail (cOmplete mini protease inhibitors cocktail

tablets – ROCHE) just before use. Animals were frozen at -80°C and then boiled at 95°C together with 1X Laemmli sample buffer (70 mM SDS, 1.5 mM bromophenol blue, 0.8% glycerol, 10 mM Tris-HCl pH: 6.8, 100 mM DTT). The lysates were spun down at 4°C, then loaded and separated by SDS-PAGE and transferred to PVDF membrane (Amersham-GE Healthcare). The membrane was blocked using 5% non-fat milk for 1 hour and then incubated overnight with anti-SUMO antibody (115) (DSHB, 1:250) and with anti-α-tubulin antibody (AA4.3 – DSHB, 1:5000) in 5% non-fat milk at 4°C. The next day the membrane was washed with 1XPBS-T (0.1% Tween 20) and incubated with horseradish peroxidase-conjugated secondary antibody for 1 hour at room temperature. After washes with 1XPBS-T, the membrane was developed by chemiluminescence (Supersignal chemiluminescent substrate pico and femto, Thermo Fisher Scientific).

For the analysis of SUMO conjugated proteins upon *smo-1(RNAi)* and SMO-1 overexpression (FGP14 strain), animals were washed and collected from 2 plates in M9 buffer with 0.1% Triton-X 100. Animals were washed 1 time with M9 buffer with 0.1% Triton-X 100 and transferred to a new tube. 200 µl of 40% trichloroacetic acid (TCA) (Sigma-Aldrich) and 300 µl glass beads (Sigma-Aldrich) were added to each sample. Samples were lysed by using a Beadbeater (Biospec), for 3 min (1 min on – 1 min off) in a cold room. Lysates were transferred to a new tube and the beads were washed with 5% TCA and mixed with the lysates. Samples then were centrifuged for 15 min at 13000 rpm at 4°C. The pellet was washed 3 times with 500 µl chilled acetone. Pellets were dried at room temperature and resuspended in 100 µl 1X Sample Reducing Agent (Thermo Fisher Scientific). Following a 5 min incubation at 70°C, samples were sonicated 2x for 10 sec (12% amplitude). Samples were incubated again at 70°C and then centrifuged for 10 min at 11000rpm. Samples were transferred to a new tube and loaded onto a 4-12% Bis-Tris gel for separation, transferred to a nitrocellulose membrane (Amersham-GE Healthcare). The membrane was blocked in a blocking solution (Invitrogen) for 1 hour and then incubated overnight with anti-SUMO antibody (sheep) (116) (1:1000) and with anti-α-tubulin antibody (DSHB Cat# AA4.3, RRID:AB_579793, 1:5000) in 3% BSA at 4°C. The next day the membrane was washed with 1XPBS-T (0.1% Tween 20) and incubated with AlexaFluor™ 647 secondary antibody for 1 hour at room temperature. After washes with 1XPBS-T, the membrane was analyzed with Amersham Typhoon Biomolecular Imager (GE Healthcare).

Mitochondria isolation

Age matched animals were collected in M9 buffer, and incubated at 4°C with rotation in the presence of 10mM DTT. To remove the DTT from the sample, 3 washes were performed with M9. Worms were homogenized in incubation buffer (50mM Tris-HCl pH:7.4, 210mM mannitol, 70mM sucrose, 0.1mM

EDTA, 2mM PMSF, cOmplete mini protease inhibitors cocktail (ROCHE)) with 100 strokes in a 3ml Potter-Elvehjem homogenizer with PTFE pestle and glass tube (Sigma-Aldrich). The lysate was centrifuged at 200*g* for 1 min. The pellet was subjected to another round of homogenization. The lysate was combined with the supernatant from the previous centrifugation step, and they were centrifuged together for 1 min at 200*g*. The supernatant was centrifuged again at 12000*g* for 5 min. We kept the supernatant as the cytoplasmic fraction and resuspended the pellet/mitochondrial fraction in incubation buffer. Samples were analysed on 4-12% SDS-PAGE gradient gels with anti-SUMO (DSHB Cat# SUMO 6F2, RRID:AB_2618393), anti-MTCO1 (Abcam [1D6E1A8] (ab14705)) and anti-α-tubulin (DSHB Cat# AA4.3, RRID:AB_579793).

DAF-16 and SKN-1 purification

We codon optimized the sequence of isoform "a" of DAF-16 (UniProt number: O16850) and isoform "c" of SKN-1 (UniProt number: P34707) and inserted into a vector suitable for bacterial expression, pHis-TEV-30a (117). This vector also contains an N terminal 6xHis-MBP tag and a TEV cleavage site. The construct was transformed to BL21 Rosetta *E. coli* strain for protein expression. Bacterial cultures were grown at 37°C until OD_{600}=0.8, then cooled down and induced with 1mM IPTG at 20°C for 4 hours for DAF-16 expression and with 0,1mM IPTG at 37°C for 4 hours for SKN-1 expression. The cells were pelleted by centrifugation (4500 rpm, 30 min, 4°C) and resuspended in 50 ml lysis buffer (50mM Tris-HCl, 0.5M NaCl, 10mM imidazole, pH 7.5) supplemented with 0.5mM TCEP and cOmplete mini protease inhibitors cocktail tablets – ROCHE. Cells were lysed by sonication (Digital Sonifier, Branson) for 5X 20 sec pulses at 50% amplitude with 20 sec cooling period between pulses. Cell lysate was centrifuged (15000 rpm, 45 min, 4°C) to clear the sample from any insoluble material and supernatant was loaded onto a 2 ml Ni-NTA column (Qiagen) pre-equilibrated with lysis buffer. After sample binding, the column was washed with 10 column volume of lysis buffer and with 10 column volume of lysis buffer containing 30mM imidazole. The protein was eluted from the column with elution buffer (50mM Tris-HCl, 150mM NaCl, 150mM imidazole, 0.5mM TCEP). DAF-16 was further purified by size exclusion chromatography with Superose 6 Increase 10/300 column (GE Healthcare). Purified and concentrated protein was aliquoted and stored at -80°C.

***In vitro* SUMOylation assays**

Conjugation assays contained 50mM Tris-HCl, 0.5mM TCEP, 5mM $MgCl_2$, 2mM ATP, 5µg SUMO, 0.5µg SUMO-Alexa Fluor™ 680, 60ng SAE1/SAE2 (SUMO E1), 5 or 20ng UBC-9, 10, 50 or 100ng GEI-17 and 5µg DAF-16, SKN-1 or MBP. Reactions were incubated at 30°C for 4 hours and they were run parallel on 4-

12% Bis-Tris (better visualization of free SUMO) and 3-8% Tris-Acetate gels (better visualization of SUMO modified proteins). Gels were analyzed by Coomassie staining and Amersham Typhoon Biomolecular Imager (GE Healthcare) (116).

Mitochondrial imaging

For TMRE (tetramethylrhodamine, ethyl ester) staining, age-matched animals were placed overnight on an RNAi plate containing 150 nM TMRE and the next morning placed in a 10mM levamisole drop on a microscope slide, sealed with a cover slip. Images were taken with a Zeiss AxioImager Z2 epifluorescence microscope. For mitochondrial ROS staining, synchronized animals were placed on RNAi plates containing 150 nM MitoTracker Red CMXROS (Thermo Fisher Scientific) overnight and the next morning were mounted on microscope slides in a 10mM levamisole drop, sealed with a cover slip to assess mitochondrial ROS production. Images were taken with a Zeiss AxioImager Z2 epifluorescence microscope. Images were quantified using the software Image J. For paraquat treated TMRE staining, age-matched animals were placed on RNAi plates containing 4 mM paraquat for 1 day, and the next day were transferred to a fresh RNAi plate containing 4 mM paraquat and 150 nM TMRE. The next morning the animals were placed on microscope slides in a 10 mM levamisole drop, sealed with a cover slip. Images were taken with a Zeiss AxioImager Z2 epifluorescence microscope. Images were quantified using the software Image J. For monitoring mitophagy we used the previously described mitochondrial targeted Rosella biosensor in body wall muscle cells of the animals (113), with a minor modification. We created a new transgenic line with biolistic transformation and fed these animals with the test RNAi constructs. Animals were mounted on 5% agarose pads in a 10mM levamisole drop and sealed with a cover slip. Images were taken with an Invitrogen EVOS FL Auto 2 Cell Imaging System. Images were quantified using the software Image J.

Messenger RNA quantification

Total RNA was extracted from worms, using Trizol (Sigma). cDNA was synthesized using the iScript kit (BioRad). Quantitative Real Time PCR was performed using a Bio-Rad CFX96 Real-Time PCR system, and was repeated three times. The following primer pairs were used to quantify the expression of genes: for *ges-1*: 5'-TCGCCAAGAGGTATGCTTCACAAG-3' and 5'-TGCTGCTCCTGCACTGTATCCC-3', for *gst-4*: 5'-GGCAAGAAAATTTGGACTC-3' and 5'-GCCAAGAAATCATCACGGGC-3', for *sod-3*: 5'-ATTGCTCTCCAACCAGCGC-3' and 5'-GGAACCGAAGTCGCGCTTAA-3', for ife-2: 5'-GAGAATTGGAGGCGTCTTGA-3' and 5'-GAGACTGGAACTGGGGCTTT-3'.

ATP measurements

To quantify intracellular ATP levels, we followed the protocol described here (118). In short, 100 age matched animals were collected in 50µl of M9 buffer and frozen at -80 °C. Frozen worms were boiled at 95°C for 15 min. After a 10 min centrifugation step at 14000 rpm at 4°C, the supernatant was transferred to a fresh tube and diluted tenfold before measurement. ATP content was determined by using the Roche ATP bioluminescent assay kit HSII (Roche Applied Science) and a TD-20/20 luminometer (TurnerDesigns). ATP levels were normalized to total protein content.

Oxygen consumption rate measurement

To determine oxygen consumption rates, we followed a previously described protocol (119). In short, 4-day-old adult animals were collected in 1 ml M9, and transferred to the chamber of Oxygraph (Hansatech Instruments). Measurements were performed for 15 min at 20°C. The oxygen consumption rate was obtained by the slope of the straight portion of the plot. The animals were recovered after measurement and were subjected to sonication and protein determination. The oxygen consumption rates were normalized to total protein content.

Mitochondrial DNA quantification

mtDNA was quantified using quantitative real time PCR as described previously (120). 50 worms were collected per condition, lysed and diluted 10-fold before performing the PCR reaction. The following primer set was used for mtDNA (*mito-1*): 5'-GTTTATGCTGCTGTAGCGTG-3' and 5'-CTGTTAAAGCAAGTGGACGAG-3'. The results were normalized to genomic DNA using the following primers specific for *ama-1*: 5'-TGGAACTCTGGAGTCACACC-3' and 5'-CATCCTCCTTCATTGAACGG-3'. Quantitative PCR was performed using a Bio-Rad CFX96 Real-Time PCR system, and was repeated three times.

Lifespan Analysis

Experiments were carried out at 20°C, unless noted otherwise. Animals were synchronized by placing 7-8 gravid adults on control RNAi plates for overnight egg laying and they were removed the next morning. L4 larvae were placed on experimental plates (containing 2 mM IPTG and seeded with HT115 (DE3) bacteria comprising the control vector (pL4440) or the test RNAi construct) and they were transferred to a fresh plate every 2-3 days. Animals were scored for survival with movement provoking touch every second day. Those who crawled out of the plate or died due to internal egg-hatching were considered censored and incorporated into the dataset as such. Each lifespan assay was repeated at

least 2 times and figures represent typical assays. Statistical analysis was performed using the Prism software package (GraphPad Software), and the product-limit method of Kaplan and Meier.

Survival assays

For oxidative stress assays we grew synchronized animals until day 6 of adulthood on control or *smo-1(RNAi)* plates. At days 6 animals were transferred to control or *smo-1(RNAi)* plates containing paraquat (methyl viologen dichloride hydrate, Sigma) in 2mM final concentration. Additionally, bacteria were killed with UV before adding paraquat on the plates in order to prevent interference arising from bacterial metabolism.

For acute heat stress survival the animals were grown until day 4 of adulthood on control or *smo-1(RNAi)* plates at 20°C. At day 4 animals were subjected to 37°C for 2 hours and then placed back to 20°C. In both stress conditions animals were scored for survival with movement provoking touch every day. Those who crawled out of the plate or died due to internal egg-hatching were considered censored and incorporated into the dataset as such. Each stress survival assay was repeated at least 2 times and figures represent typical assays. Statistical analysis was performed using the Prism software package (GraphPad Software), and the product-limit method of Kaplan and Meier.

DAPI staining

For visualizing nuclei, we picked age-matched animals into 1 ml of 0.01% PBS-T and centrifuged them for 1 minute at 3000 rpm. After removing the supernatant, we performed 2 more washes with 1ml 0.01% PBS-T. After the last centrifuge the supernatant was removed and replaced with 1 ml ice cold methanol. The tube was incubated at -20°C for 5 minutes. After a 1 minute centrifuge at 3000 rpm we removed the methanol and washed the animals with 0.1% PBS-T and centrifuged them. DAPI solution was added to the animals in a final concentration of 100ng/ml. After 5 minutes of incubation in the dark the sample was washed with 0.1% PBS-T. Replacing the supernatant with 75% glycerol, the animals were placed on 2% agarose pads and sealed with a cover slip. Images were taken with a Zeiss AxioImager Z2 epifluorescence microscope.

Statistical Analysis

Statistical analyses were carried out using the Prism software package (GraphPad Software Inc., San Diego, USA) and the Microsoft Office 2010 Excel software package (Microsoft Corporation, Redmond, WA, USA). Mean values were compared using unpaired t-tests or one-way ANOVA.

Results

SUMOylation levels increase during ageing in *C. elegans*

There are growing numbers of studies showing that the protein SUMOylation levels are increasing during ageing (94, 121, 122). In order to examine the SUMOylation levels in *C. elegans*, we performed Western blot analysis. Using age matched, wild type animals, we report that the amount of SUMO conjugated proteins peaks at day 4 of adulthood in *C. elegans* (Figure 5a).

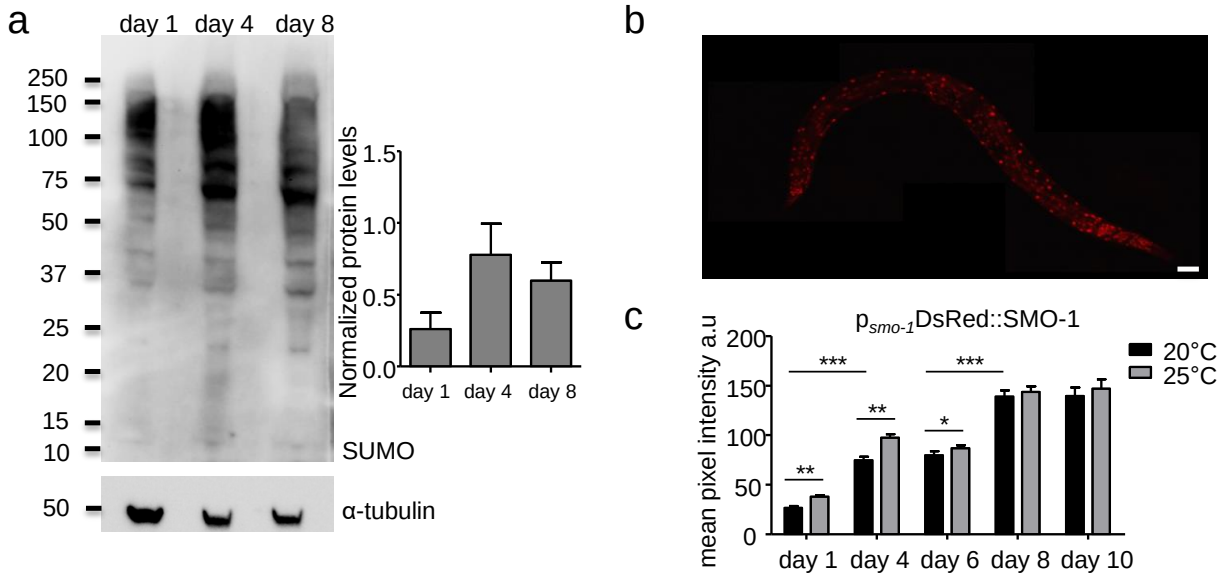

Figure 5: SUMOylated proteins are accumulating during ageing. a) Western blot showing protein SUMOylation levels in day 1, 4 and 8 wild type lysates. Protein levels were normalized to α-tubulin. b) p$_{smo-1}$DsRed::SMO-1 expression pattern, scale bar: 40 µm. Image was acquired using x20 objective lens. c) The expression of p$_{smo-1}$DsRed::SMO-1 is increasing during ageing and when the animals are grown at 25°C. (n=25, *p<0.05, **p<0.01, ***p<0.001, unpaired t-test). Error bars, S.E.M.

To visualize the endogenous expression pattern of SMO-1 we generated transgenic animals, expressing DsRed::SMO-1 under its own promoter (p$_{smo-1}$DsRed::SMO-1) (Figure 5b). We observed nuclear expression pattern in every tissue (e.g. neurons, seam cells, intestine and muscles) (Figure 5b). However, overexpression of SMO-1 leads to developmental and reproductive defects (123, 124), making it difficult to generate a stable and healthy transgenic line. Our overexpressing line displays a weak expression of SMO-1, explaining the viability of these animals, but the level of expression increases during ageing and upon a temperature shift to 25°C (Figure 5c). This data is in agreement with our finding about the accumulation of SUMOylated proteins with age (Figure 5a). A recent study confirms our results about SMO-1 cellular localization, and also finds that the localization of SMO-1 is not limited to the nucleus, but it can be found in the cytoplasm as well (9).

SUMO modulates *C. elegans* lifespan

We next sought to determine whether SUMO plays a role in the regulation of lifespan. Mutation of *smo-1* causes embryonic lethality (125, 126). This is due to the fact that SUMOylation is required throughout development to ensure proper cell division and organogenesis (124). However, *C. elegans* offers the possibility to silence any target gene (by RNAi) after the development is completed, when the organism reaches a post-mitotic state with the exception of its germline. Reducing *smo-1* expression from the L4 larval stage (Figure 6) causes a significant reduction in lifespan (Figure 7a). Interestingly, when we knocked down the E2 enzyme, UBC-9 by RNAi, we did not observe any effect on lifespan (Figure 7b). This is to be expected, taking into account that knocking down a gene by RNAi, starting at L4, does not completely abolish its expression, and the UBC-9 enzyme remnants are competent enough to perform SUMOylation. There are 4 SUMO proteases (ubiquitin-like proteases) encoded in the *C. elegans* genome (*ulp-1-2, ulp-4- 5*). Reducing the expression of these proteases did not influence the lifespan of wild type animals (Figure 7c-d).

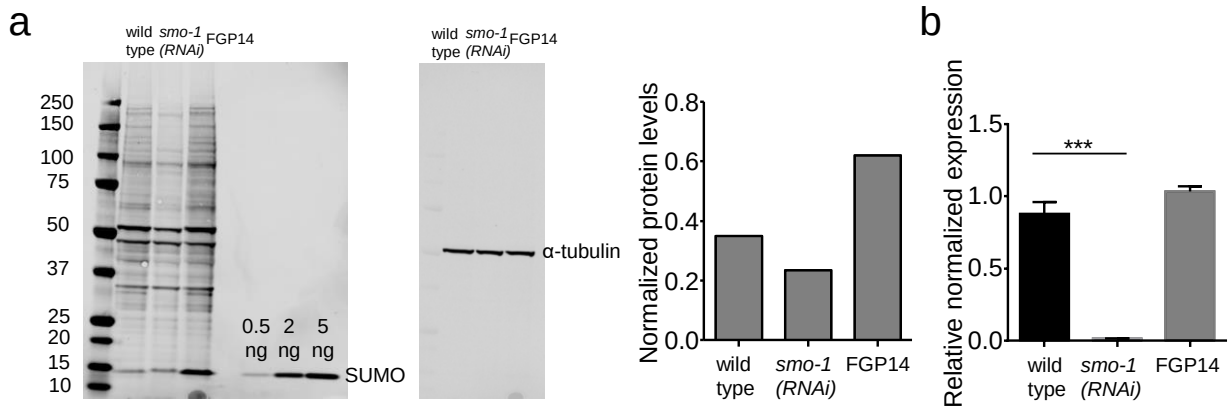

Figure 6: Changes in protein SUMOylation levels upon *smo-1* knock-down and overexpression. a) Western blot showing SUMO protein levels in wild type, *smo-1(RNAi)* and *smo-1* overexpressing (FGP14) background. Protein levels were normalized to α-tubulin. N=1. b) mRNA levels are diminished under *smo-1(RNAi)* conditions (***p<0.001, unpaired t-test). Error bars, S.E.M.

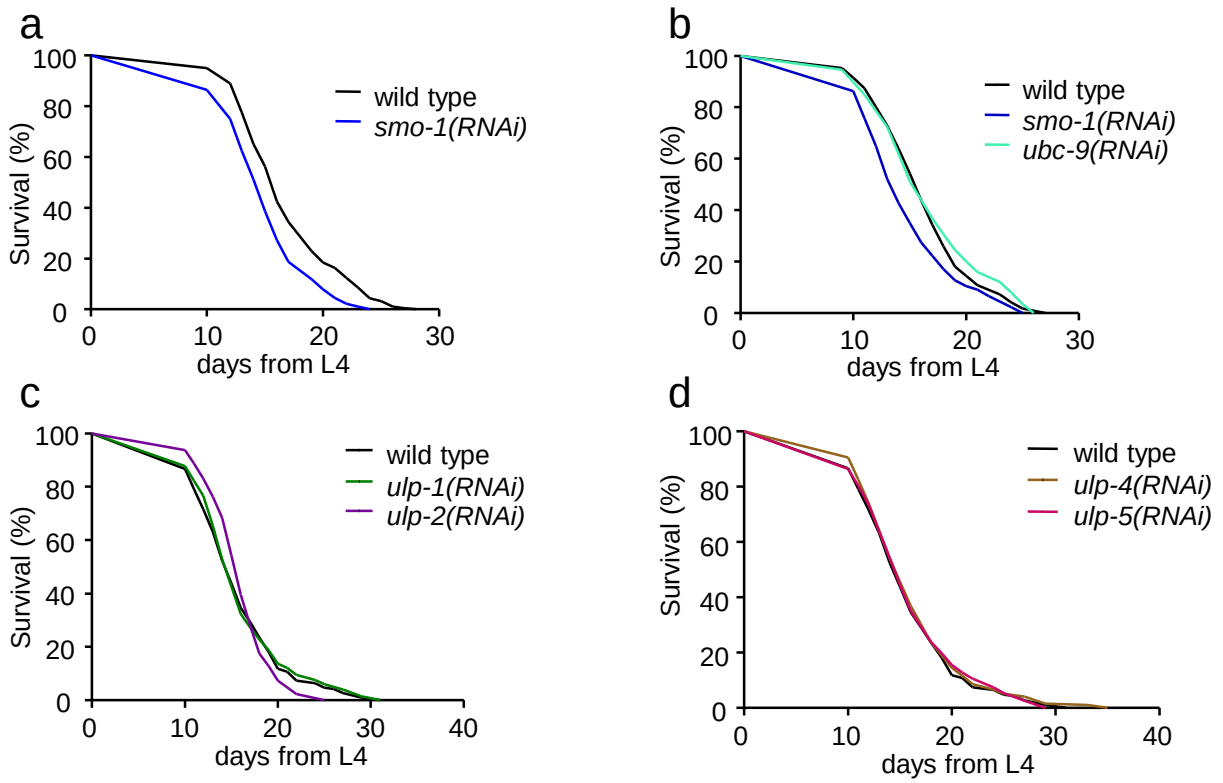

Figure 7: SUMO is required for wild type lifespan. a) Loss of *smo-1* shortens the lifespan of wild type animals. b) Loss of the E2 enzyme (*ubc-9*) does not influence wild type lifespan. c-d) Removing the SUMO proteases (*ulp-1-5*) does not have an effect on wild type lifespan. Lifespan assays were carried out at 20°C. The percentage of animals remaining alive is plotted against age.

In order to place SUMO in the longevity regulating pathways, we knocked down *smo-1* in various long- and short-lived mutants. Previous work has shown that reducing the rate of translation by mutation of the translation initiation factor, *ife-2*, extends the lifespan of *C. elegans* (127). The lack of SUMO in this genetic background also shortened the lifespan, similar to the wild type situation (Figure 8a). When we interfered with the insulin/IGF-1 signaling (IIS), using the long-lived insulin receptor mutant, *daf-2*, and the short-lived FOXO transcription factor mutant, *daf-16*, *smo-1(RNAi)* shortened the lifespan of animals (Figure 8b-c). Moreover, using a SMO-1 overexpressing strain, FGP14 (p_{smo-1}*::6xHis::smo-1*::*smo-1* 3' UTR) (110) (Figure 6), we observed a significant lifespan extension, compared to wild type. Loss of *daf-16* in this genetic background resulted in a shorter lifespan, but these animals were still long-lived compared to wild type subjected to *daf-16* RNAi (Figure 8d). This led us to the conclusion that SUMO must act partly through the IIS and partly in parallel or downstream of IIS in the regulation of longevity.

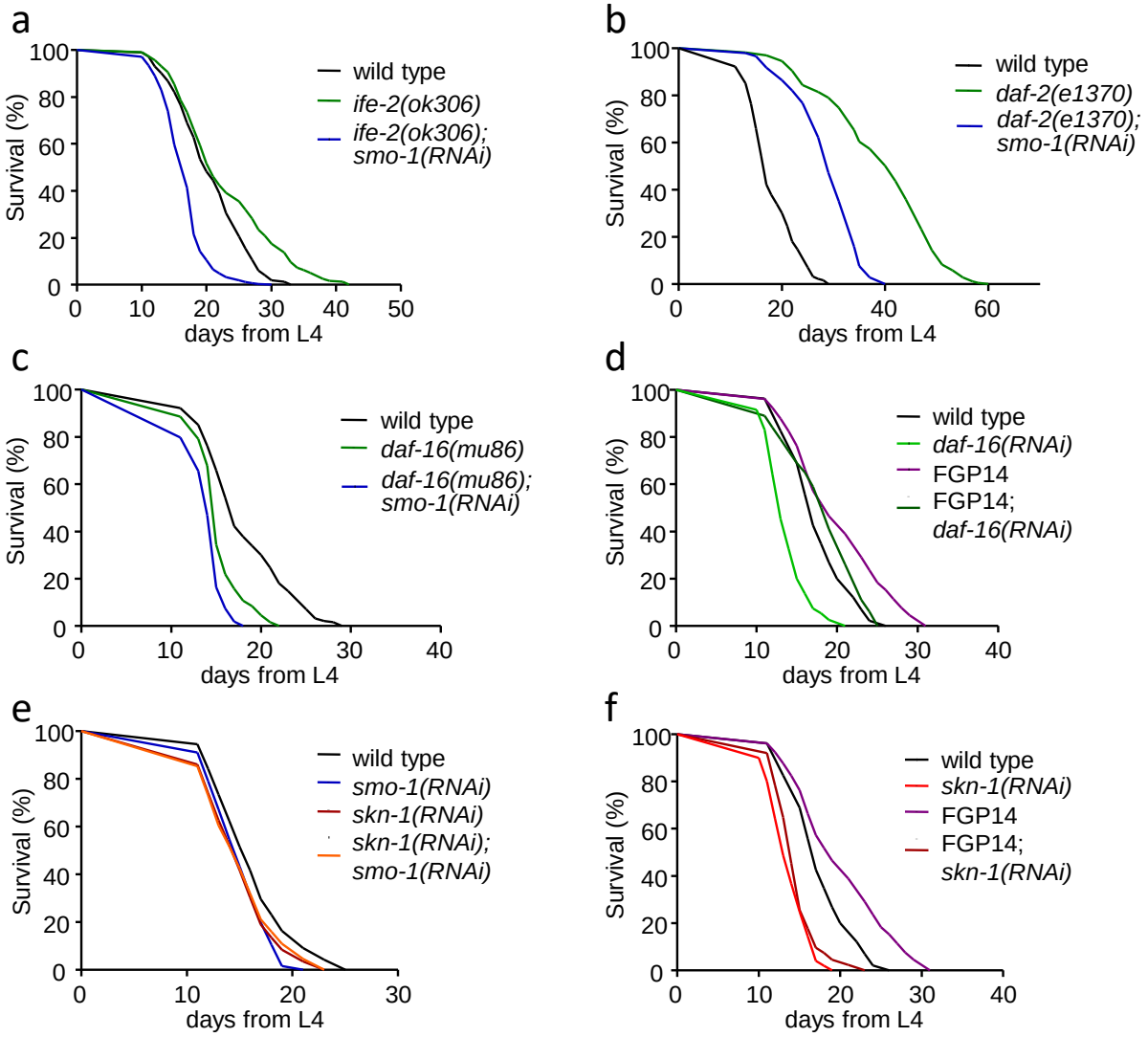

Figure 8: SUMO influences lifespan via DAF-16 and SKN-1. a) Loss of *smo-1* shortens long lifespan of *ife-2* mutant animals. b) *smo-1(RNAi)* shortens the long lifespan of *daf-2(e1370)* animals. c) Removing *smo-1* in a *daf-16* mutant background leads to lifespan shortening. d) Overexpression of SUMO (FGP14) causes lifespan extension and *daf-16(RNAi)* shortens the lifespan of these animals. e) *smo-1(RNAi)* does not further shorten the lifespan of *skn-1(RNAi)* treated animals. f) *skn-1(RNAi)* shortens the long lifespan of the SUMO overexpressing strain below wild type levels. Lifespan assays were carried out at 20°C. The percentage of animals remaining alive is plotted against age.

SKN-1 affects ageing in parallel to the insulin signaling pathway (18). Interestingly, in a *skn-1(RNAi)* background, knocking down *smo-1* did not further reduce the lifespan of animals (Figure 8e). Furthermore, *skn-1(RNAi)* shortened the lifespan of the SMO-1 overexpressing animals (FGP14) to the level seen in wild type animals on *skn-1(RNAi)* (Figure 8f). These data suggest that SUMO conveys its longevity modulating effect through SKN-1 and DAF-16.

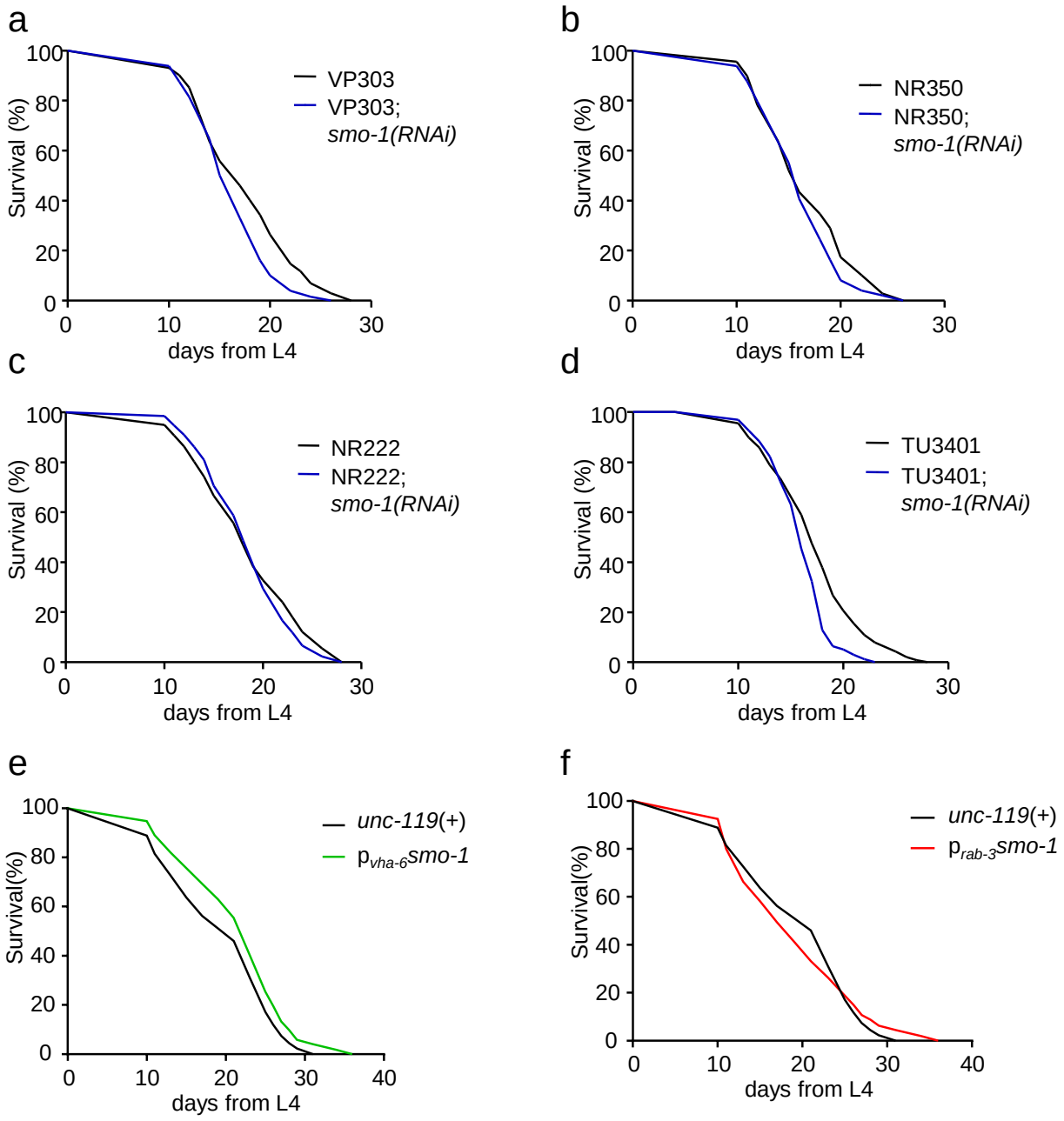

Figure 9: SUMO modulates lifespan through the intestine and nervous system. a) Intestine specific *smo-1(RNAi)* shortens lifespan. b-c) Muscle (NR350) or hypodermis (NR222) specific knock-down of *smo-1* does not have an effect on lifespan. d) Neuron specific *smo-1(RNAi)* reduces lifespan. e) Intestine specific *smo-1* overexpression extends lifespan. f) Overexpression of *smo-1* in the neurons, does not affect animal lifespan. Lifespan assays were carried out at 20°C. The percentage of animals remaining alive is plotted against age.

Next we wondered whether SUMO could influence lifespan through specific tissues. To examine this possibility, we utilized strains in which the RNAi is only effective in select tissues. These transgenic strains harbor a mutation in *rde-1* gene (RNAi defective), which encodes an Argonaute protein family

member that is required for RNA interference (128), and it is re-introduced to the animals in a tissue specific manner. We analyzed the effect of the loss of SUMO in 3 tissue specific strains: intestine (VP303), hypodermis (NR222) and muscles (NR350). Upon *smo-1(RNAi)*, only the intestine specific RNAi strain (VP303) displayed shorter lifespan, compared to their respective controls (Figure 9a-c). This is intriguing, considering the fact that DAF-16 also regulates lifespan cell-nonautonomously, through the intestine in *C. elegans* and fat body in *Drosophila* (129). The nervous system of *C. elegans* is mostly resistant to RNAi, but specific neurons (amphids and phasmids which have a connection with the environment) are susceptible (130). We wished to probe for the potential neuron specificity of the effect of SUMO on lifespan; therefore we utilized another strain, TU3401. This strain carries a mutation for *sid-1* (systemic RNA interference defective), together with a transgene of *sid-1*, driven by a pan-neuronal promoter, *unc-119* (131). SID-1 is a transmembrane channel for dsRNA, and it is required for systemic RNA interference (132). Reducing *smo-1* expression, specifically in neurons, resulted in a reduction of lifespan (Figure 9d). Importantly, overexpression of *smo-1* explicitly in the intestine ($p_{vha\text{-}6}$*smo-1*), led to an extended lifespan (Figure 9e). On the contrary, neuron-specific *smo-1* overexpression ($p_{rab\text{-}3}$*smo-1*) did not have any significant effect on the lifespan of the animals (Figure 9f). This result suggests the importance of balanced SUMO levels in the nervous system. Taken together, these findings indicate that SUMO influences *C. elegans* lifespan through the intestine and the nervous system.

The transcriptional activity of DAF-16 and SKN-1 is regulated by SUMO

Considering that DAF-16 is the terminal transcription factor of IIS and can be a target of many post-translational modifications, e.g. phosphorylation, methylation, ubiquitination (8, 133, 134); we sought to identify whether DAF-16 can also be SUMOylated. With the use of an *in silico* method, SUMOplot (http://www.abgent.com/sumoplot), we predicted 2 high-probability SUMOylation sites in DAF-16 (Figure 10a). However, as mentioned in the introduction, recently a new, more reliable prediction tool became available for SUMOylation, SUMOgo. Subjecting the sequence of DAF-16 to this method resulted in 3 different possible SUMOylation sites (Figure 10a).

To confirm the SUMOylated status of DAF-16, we conducted *in vitro* SUMOylation assays with purified, bacterially expressed and 6xHis-MBP tagged DAF-16. We detected SUMO conjugation to DAF-16 (Figure 10b, c). To increase the sensitivity of our assay, we added fluorescently labelled SUMO (SUMO-AlexaFluor^{TM} 680) (116), which facilitated detection of the SUMO-modified form of DAF-16 (Figure 10b). Therefore, DAF-16 is a *bona fide* SUMOylation target.

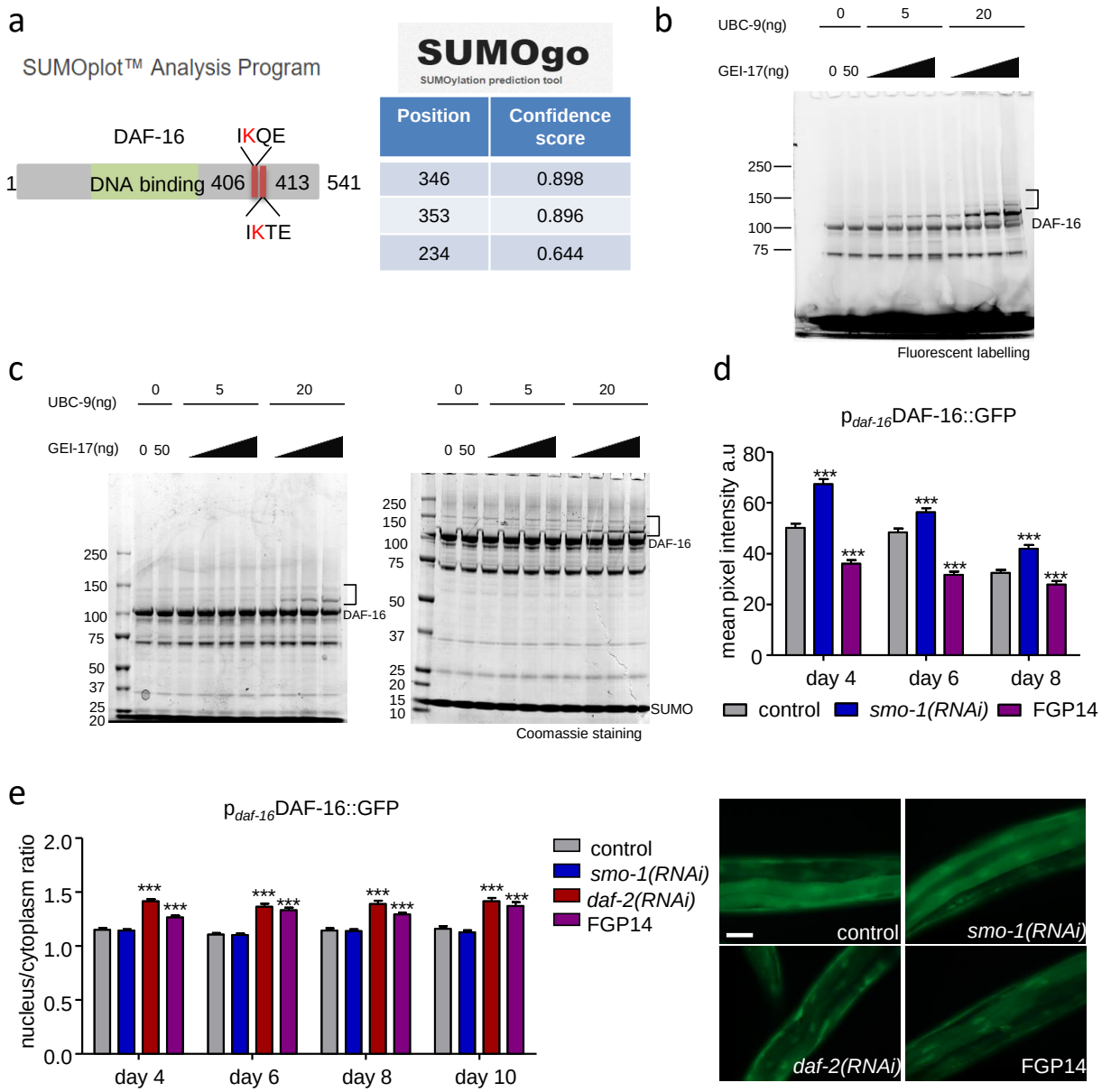

Figure 10: DAF-16 is SUMO modified and SUMOylation influences DAF-16 protein levels and nuclear localization. a) Schematic representation of the *in silico* predicted SUMOylation sites of DAF-16 with SUMOplot and position and confidence score of modification sites generated by SUMOgo for DAF-16. b) *In vitro* SUMOylation assay with fluorescent (SUMO-AlexaFluor™ 680) SUMO labelling on 3-8% Tris-Acetate gel. c) *In vitro* SUMOylation assay, visualized by Coomassie staining. Left: 3-8% Tris-Acetate gel, right: 4-12% Bis-Tris gel. Brackets indicate the SUMO modified form of DAF-16. d) Decreasing *smo-1* expression increases p_{daf-16}DAF-16::GFP expression, while overexpression of *smo-1* reduces it (n=100, ***p<0.001, unpaired t-test). e) Nuclear localization of p_{daf-16}DAF-16::GFP in control, *smo-1(RNAi)* and *smo-1* overexpressing background (FGP14), *daf-2(RNAi)* was used as a positive control, scale bar: 50 µm. Images were aquired using x40 objective lens (n=50, ***p<0.001, unpaired t-test).

Interestingly, the protein level of DAF-16, measured by GFP fluorescence of the p_{daf-16}DAF-16::GFP strain, was increased on *smo-1(RNAi)* and it showed a reduction in FGP14 background (Figure 10d). We next asked whether the change in SUMOylation levels will affect the nuclear localization of DAF-16 next to its

protein level. Reducing the expression of *smo-1* by RNAi did not influence the nuclear/cytoplasm ratio of DAF-16 at any tested age (Figure 10e). On the other hand, overexpression of SMO-1 promoted the nuclear localization of DAF-16, to a similar extent observed in the positive control, *daf-2(RNAi)* (Figure 10e). Taken together, changes in global SUMOylation levels affect the protein levels and subcellular localization of DAF-16.

However, the abundance and nuclear localization of a transcription factor do not directly indicate its activity. To determine the effect of SUMOylation on the transcriptional activity of DAF-16, we used transcriptional reporters of two DAF-16 target genes and analyzed their fluorescent intensity upon *smo-1* knock-down and overexpression during ageing. We utilized the p_{ges-1}mtGFP and p_{sod-3}GFP reporters; *ges-1* (abnormal gut esterase) is a gut specific type B carboxylesterase and it is expressed only in the intestine, and *sod-3* (superoxide dismutase) is an iron/manganese superoxide dismutase. We observed elevated expression levels for both reporters on *smo-1(RNAi)* in day 4 animals (Figure 11a, 12a), and this change was sustained in older animals as well (day 8 for p_{ges-1}mtGFP and day 6 for p_{sod-3}GFP) (Figure 11b, 12b). We used *daf-2(RNAi)* as a positive control, where DAF-16 is transcriptionally active (Figure 11a, 12a). Intriguingly, knock-down of *skn-1* also activated DAF-16 (Figure 11a, 12a). This could suggest a compensation mechanism for the loss of a stress responsive transcription factor and indicate that DAF-16 and SKN-1 could act together to regulate the expression of select target genes. Additionally, overexpression of SMO-1 resulted in a decreased expression of p_{sod-3}GFP in day 4 and day 6 animals (Figure 12a, b). However, when we knocked-down *skn-1* or *daf-2* in this genetic background we could still induce *sod-3* expression (Figure 12a, b). Notably, this induced expression was lower compared to the levels seen in wild type background. Overexpression of SMO-1 also decreased the mRNA levels of *ges-1* and *sod-3* in day 4 animals, while *smo-1(RNAi)* did not have a significant effect on the mRNA levels of these genes in day 4 animals (Figure 11c, 12c). All the aforementioned data indicate that while the protein level of DAF-16 is reduced and DAF-16 is localized mostly in the nucleus when SUMO is overexpressed, its transcriptional activity is suppressed by the conjugation of SUMO.

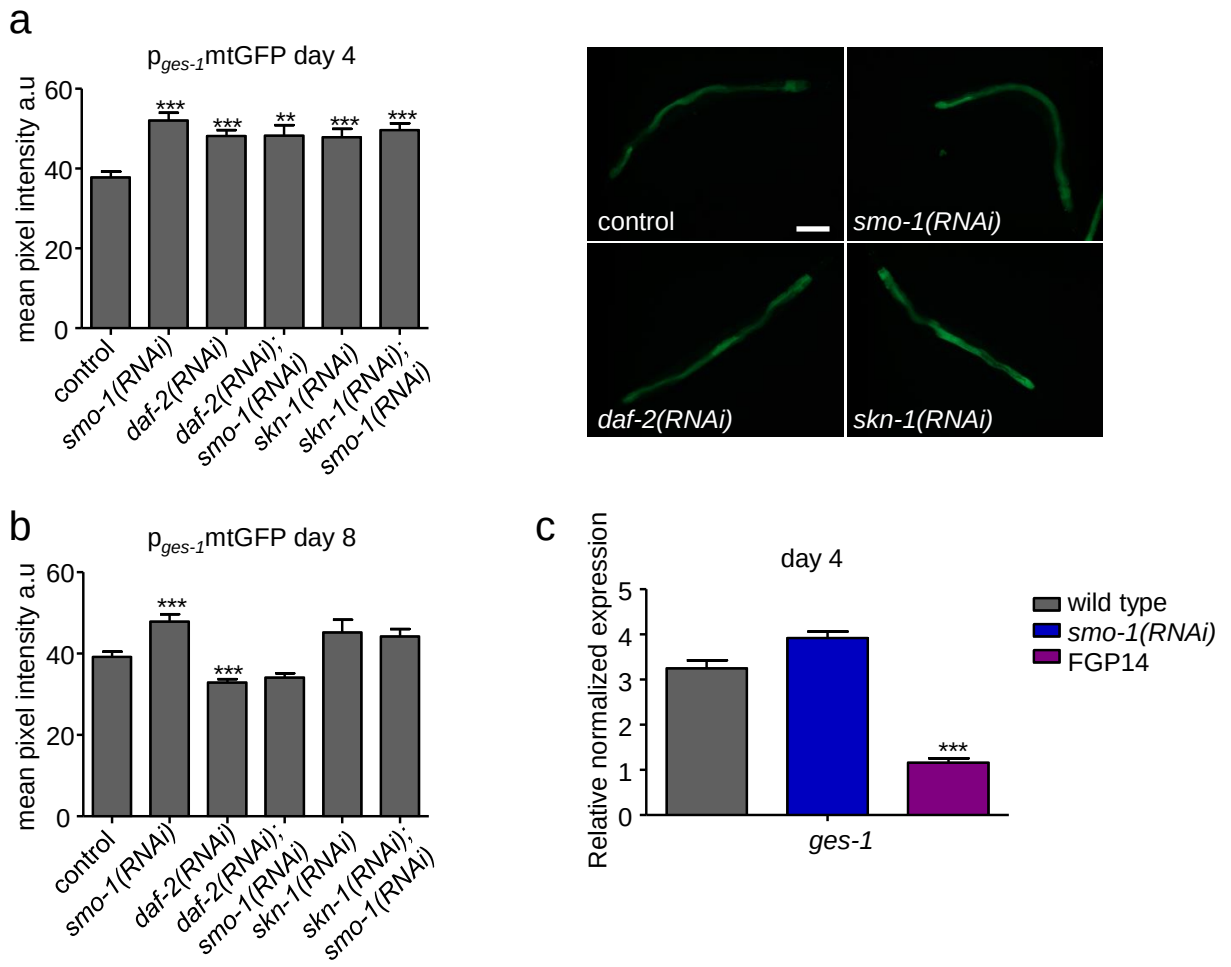

Figure 11: SUMO regulates the expression of *ges-1*, a DAF-16 target gene. a) RNAi treatment against *smo-1*, *daf-2* and *skn-1* increases the expression of p$_{ges-1}$mtGFP reporter in day 4 animals. Images were acquired using x10 objective lens, scale bar: 200 µm (n=100, ***p<0.001, unpaired t-test). b) In day 8 animals, only smo-1(RNAi) increases the expression of p$_{ges-1}$mtGFP. (n=100, ***p<0.001, unpaired t-test). c) The mRNA levels of *ges-1* are reduced in day 4 animals in the *smo-1* overexpressing strain (***p<0.001). Error bars, S.E.M.

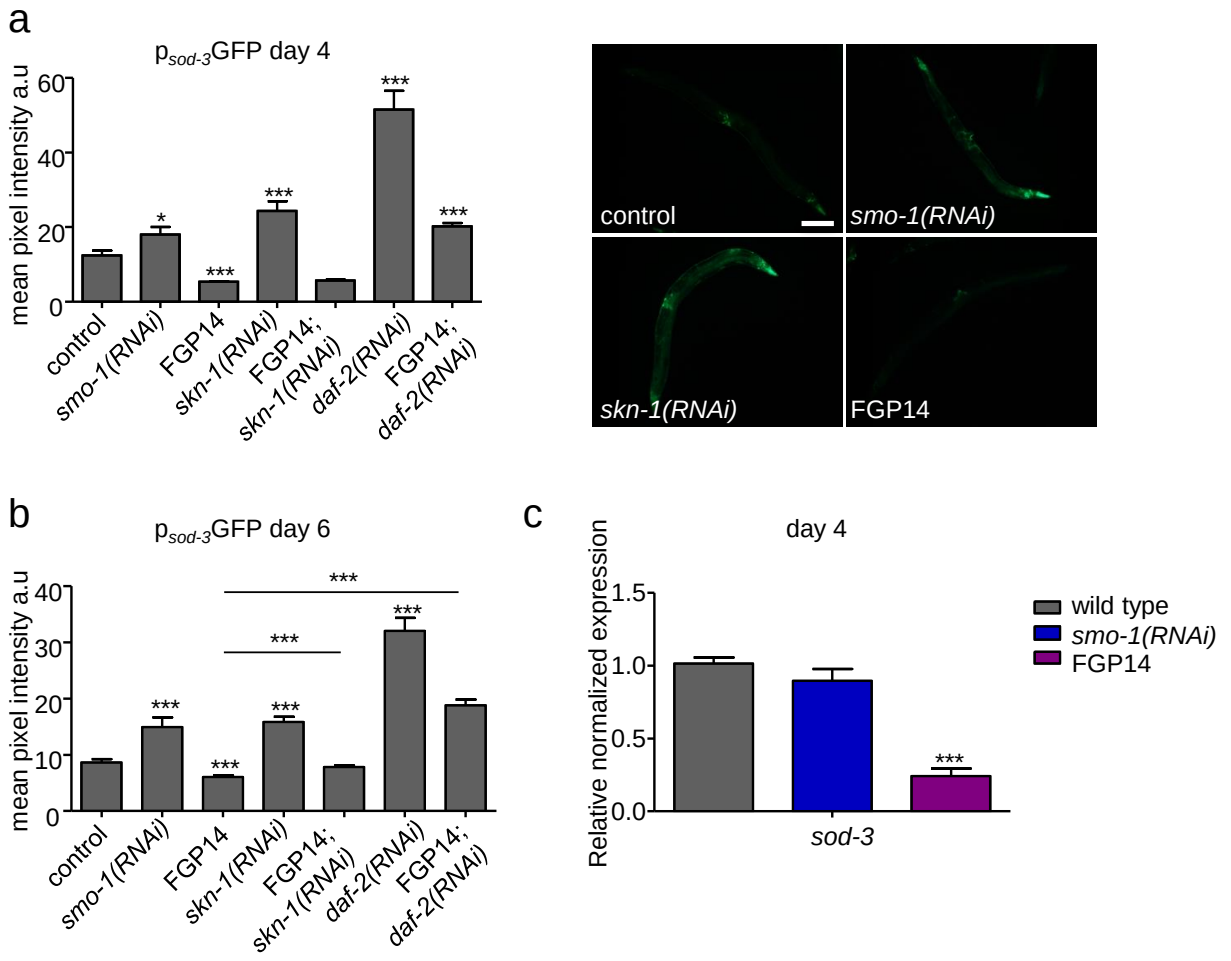

Figure 12: SUMO alters the expression of *sod-3*, a DAF-16 target gene. a) p_{sod-3}GFP is increased upon knock-down of *smo-1*, *skn-1* or *daf-2*. Overexpression of *smo-1* reduces the expression level of p_{sod-3}GFP in day 4 animals (n=100, *p<0.05, ***p<0.001, unpaired t-test). Images were acquired using x10 objective lens, scale bar: 200 µm. b) p_{sod-3}GFP expression is up-regulated upon *smo-1(RNAi)*, *skn-1(RNAi)* and *daf-2(RNAi)* in day 6 animals. The overexpression of *smo-1* decreases the expression of *sod-3* (n=75, ***p<0.001, unpaired t-test). c) The mRNA levels of *sod-3* are reduced in day 4 animals upon SMO-1 overexpression (***p<0.001). Error bars, S.E.M.

Taking into account that the lifespan shortening effect caused by loss of *smo-1* is modulated partly through SKN-1, we also tested the ability of SKN-1 to undergo SUMOylation. We found that SKN-1 is not an ideal target for SUMOylation *in vitro* (Figure 13a). Nevertheless, we analyzed the transcriptional activity of SKN-1 upon *smo-1(RNAi)* and in FGP14 background. We used p_{gst-4}GFP as a target gene of SKN-1 and observed increased fluorescent intensity of p_{gst-4}GFP upon *smo-1(RNAi)* in day 4 animals (Figure 13b). This change was not sustained in older, day 8 animals (Figure 13c). In contrast to what we detected with p_{sod-3}GFP, the expression of p_{gst-4}GFP was not downregulated in the SMO-1 overexpressing background (Figure 13b, c). The mRNA levels of *gst-4* were altered similarly to the fluorescent reporter

(Figure 13d). Intriguingly, SKN-1 also becomes more active in the absence of DAF-16 in day 4 animals in wild type and FGP14 background (Figure 13b). This increase, similar to the effect caused by *smo-1(RNAi)*, is also lost in day 8 animals, and in a higher degree in FGP14 animals (Figure 13c). This data also suggest a compensation mechanism (similar to the activation of DAF-16 on *skn-1(RNAi)*) and the common regulation of stress response genes. Here, we find that while reducing SMO-1 levels in the animal triggers the transcriptional activity of SKN-1, the over-abundance of SMO-1 does not change the activity of SKN-1 under normal conditions.

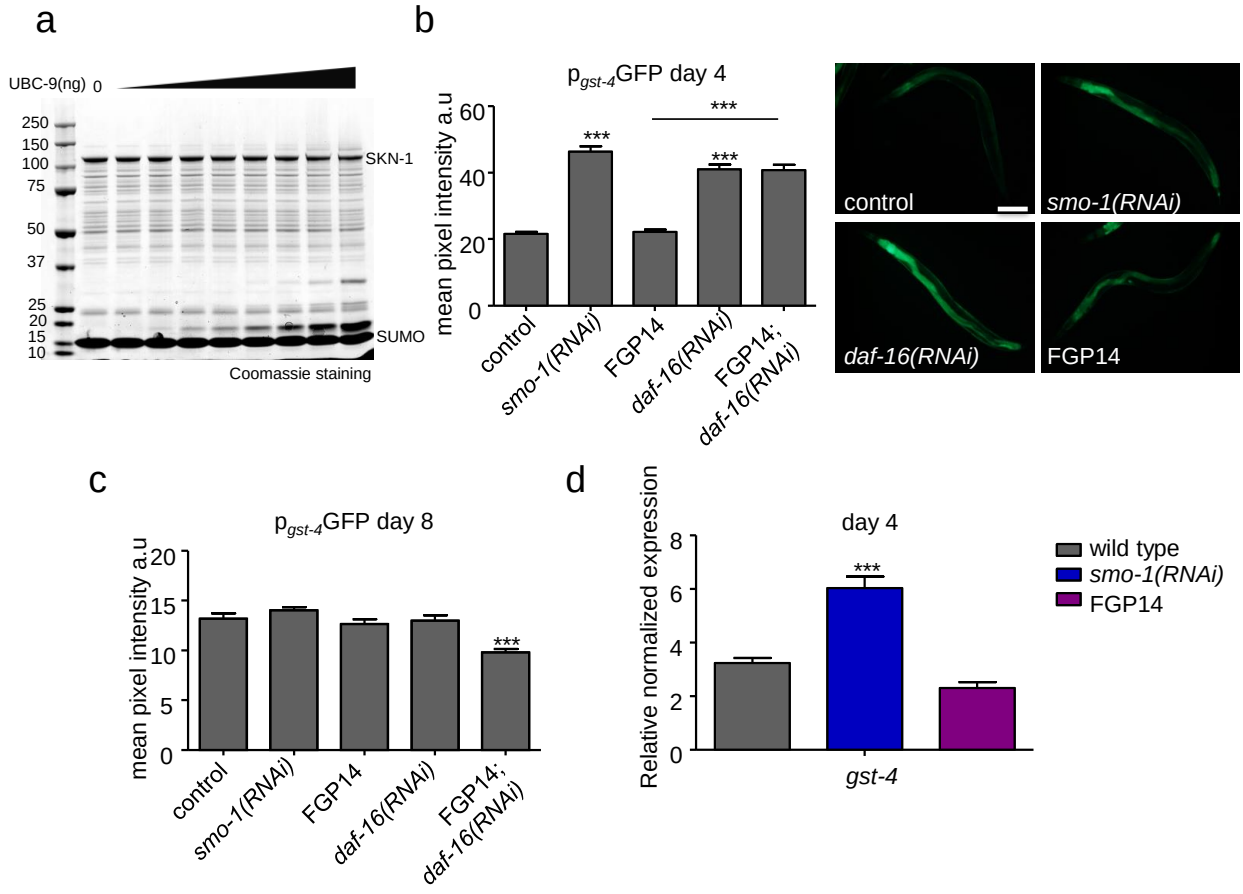

Figure 13: SUMO modulates the transcriptional acitivity of SKN-1. a) *In vitro* SUMOylation assay with SKN-1, visualized by Coomassie staining on a 4-12% Bis-Tris gel. b-c) p_{gst-4}GFP expression is increased upon *smo-1(RNAi)* and *daf-16(RNAi)* but does not change when *smo-1* is overexpressed in day 4 animals and this change is not detectable in day 8 animals (n=100, ***p<0.001, unpaired t-test). Images were acquired using x10 objective lens, scale bar: 200 µm. d) The mRNA levels of *gst-4* are increased when we knock-down *smo-1*, but there is no change upon *smo-1* overexpression in day 4 animals (***p<0.001). Error bars, S.E.M.

Since both DAF-16 and SKN-1 are transcription factors which govern stress responses in the cell, we were curious to examine the survival of animals under heat and oxidative stress conditions when we interfere with protein SUMOylation levels. We exposed 6 days old wild type, FGP14 and *smo-1(RNAi)*

treated animals to 2mM paraquat in order to induce oxidative stress and recorded their survival. Unexpectedly, the SMO-1 overexpressing animals were resistant to oxidative stress, while the reduction in *smo-1* expression did not influence the survival on paraquat (Figure 14a). Here we used *skn-1(RNAi)* as control, and observed reduced survival rates, as expected, since SKN-1 is a master regulator of oxidative stress response (17). These results indicate that under oxidative stress conditions, having higher basal SUMO concentration in the cell is beneficial. Upon oxidative stress, the SUMO conjugation pathway is inhibited; H_2O_2 is capable of the inactivation of SUMO E1 and E2 enzymes (135). H_2O_2 is catalyzing the formation of a disulfide bond between the catalytic sites of the two SUMO enzymes; however, this modification is reversible and serves as a redox sensor in the cell (136). This is in agreement with a recent report which shows that several stress conditions (heat shock, osmotic stress, UV irradiation) are able to elevate the amount of SUMOylated proteins in *C. elegans*, but not oxidative stress (9). Exposing the animals to acute (2 hours) heat shock at 37°C and then scoring their survival at 20°C produced similar results. The FGP14 strain survived longer after heat shock, and animals subjected to *smo-1* RNAi did not show a significant difference compared to wild type (Figure 14b). In order to gain insight as to why the SMO-1 overexpressing strain displayed stress resistance, we measured p_{gst-4}GFP levels in day 2 animals on 2 mM paraquat. We chose this time point because stress responses are declining later in life (137). We found that unlike under normal conditions, *smo-1(RNAi)* reduced the expression of *gst-4* and overexpression of SMO-1 further increased *gst-4* expression (Figure 14c). We conclude that under stress conditions an excess amount of SUMO protein enables the animals to mount a more successful stress response, while *smo-1(RNAi)* tends to reduce this capacity.

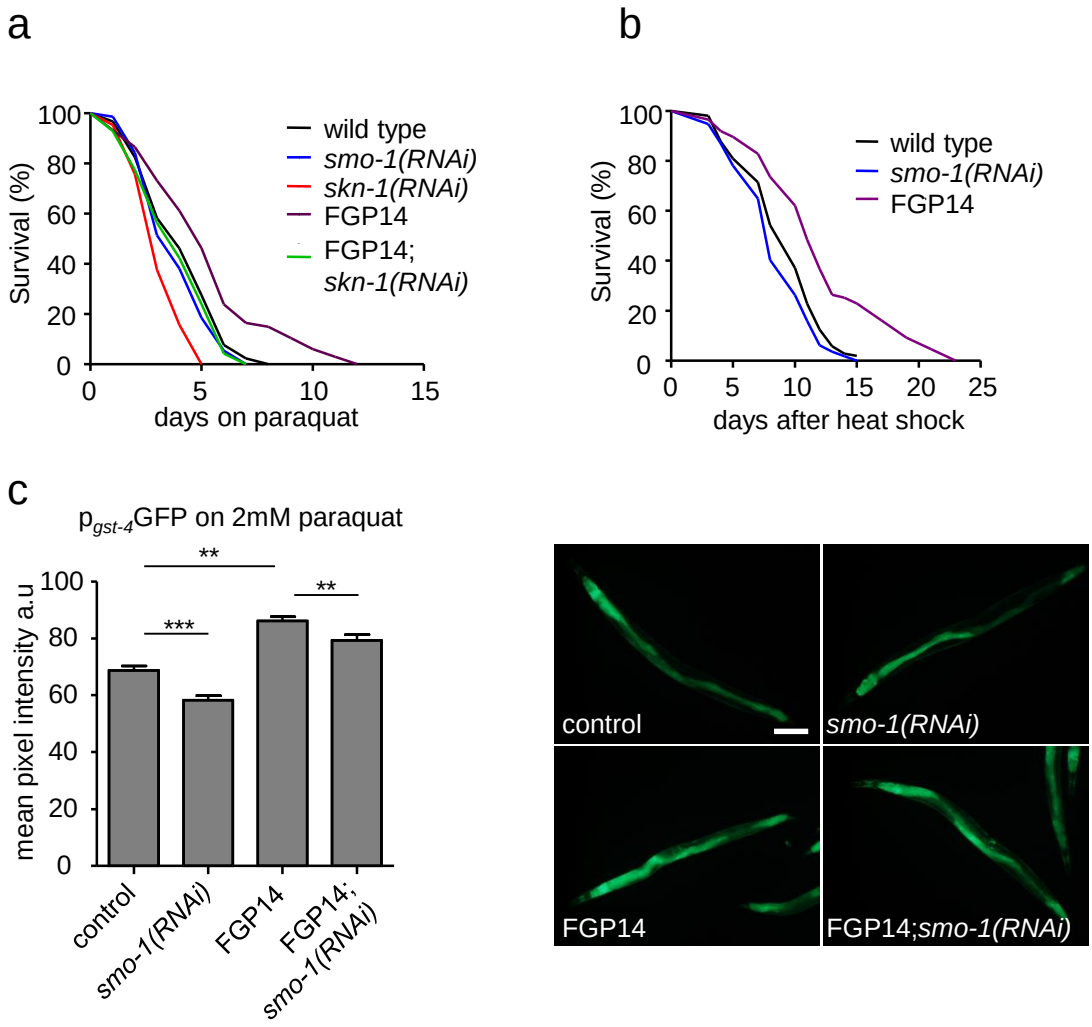

Figure 14: Overexpression of SMO-1 confers stress resistance. a) SMO-1 overexpressing animals survive longer on 2mM paraquat, while loss of *smo-1* does not change the survival compared to wild type animals. *skn-1(RNAi)* treated animals have a reduced survival rate on paraquat. b) Heat shock did not change the survival of *smo-1(RNAi)* fed animals while worms overexpressing SMO-1 displayed increased survival rates. The percentage of animals remaining alive is plotted against age. c) FGP14 animals are mounting a stronger oxidative stress response in day 2 animals compared to control, measured by p_{gst-4}GFP expression. *smo-1(RNAi)* reduced the responsiveness of animals to paraquat. Images were acquired using x10 lens, scale bar: 200 µm. (n=40, ***p<0.001, **p<0.01 unpaired t-test). Error bars, S.E.M.

SUMO facilitates mitochondrial homeostasis

Mitochondrial metabolism is an important determinant of ageing across diverse organisms. In addition to regulating the lifespan and stress response pathways of *C. elegans*, DAF-16 and SKN-1 are major regulators of the mitochondrial homeostasis (113, 138). We found that SUMOylation levels increase not just in whole worm lysates (Figure 5a), but also in the mitochondrial fraction (Figure 15a). Hence, we tested whether knocking down *smo-1*, would have any consequences on mitochondrial function. Active mitochondria can be stained by feeding the animals with the dye TMRE (tetramethylrhodamine, ethyl

ester), which enters mitochondria according to their membrane potential. Wild type animals display reduced mitochondrial membrane potential during ageing (73), however, in *smo-1(RNAi)* treated animals we could not detect this functional decline (Figure 15b, c). Interestingly, overexpression of *smo-1* led to more active mitochondria in young animals (Figure 15b), but this effect did not persist in older, day 8 worms (Figure 15c). Testing various conditions in which DAF-16 is activated (*isp-1(qm150)*, *skn-1(RNAi)*, *daf-2(e1370)*) we could observe that *smo-1(RNAi)* caused an additional effect (Figure 15b, c). However, exposing *daf-16(-)* animals to *smo-1(RNAi)*, did not exacerbate the already higher mitochondrial membrane potential (Figure 15b, c). Furthermore, we also measured mitochondrial ROS production, using the MitoTracker ROS dye. These results were in agreement with the TMRE data; showing altered ROS production upon *smo-1(RNAi)* in all conditions tested, except in *daf-16(mu86)* mutant animals (Figure 15d, e). Additionally, we utilized the $p_{rpl\text{-}17}$HyPer strain (139)to determine H_2O_2 levels in animals treated with RNAi against *smo-1*. Congruent to our MitoTracker ROS staining, aged (8-day old) *smo-1* depleted animals exhibited higher H_2O_2 levels compared to control (Figure 15f). Interestingly, SMO-1 overexpressing animals showed increased ROS production during ageing (Figure 15e). Treatment with the antioxidant NAC (N-acetyl cysteine), diminished the extended lifespan of *smo-1* overexpressing animals (Figure 15g). Together, these findings suggest that SUMO represses mitochondrial activity during ageing via DAF-16.

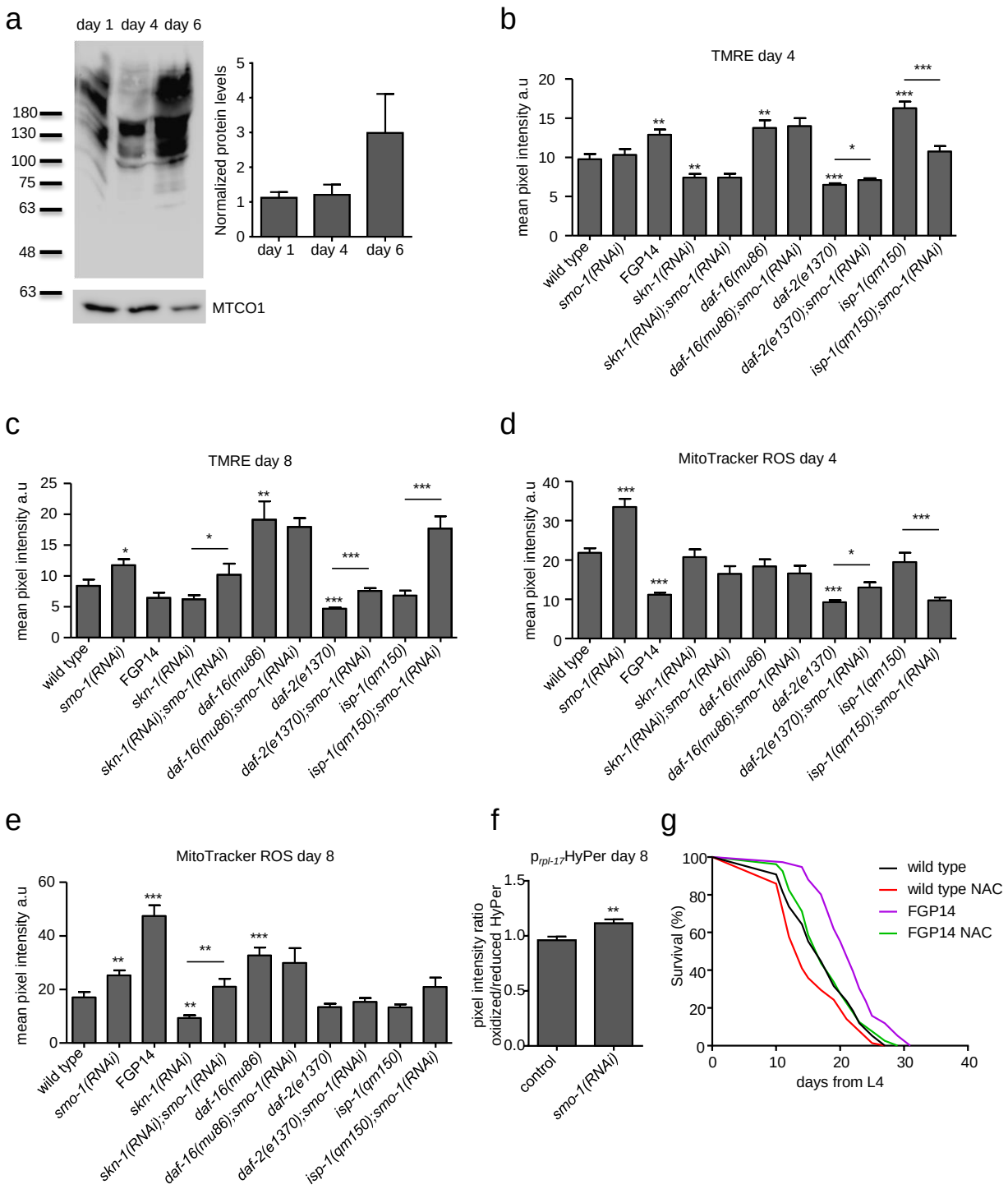

Figure 15: SUMO levels increase in the mitochondrial fraction and SUMO alters mitochondrial function. a) Western blot analysis of SUMOylated proteins in the mitochondrial fraction in day 1, 4 and 6 wild type animals (N=4). Protein levels were normalized to MTCO1. b-c) TMRE staining declines during ageing in wild type but not *smo-1(RNAi)* treated animals, and this change is DAF-16 dependent (n=100, *p<0.05, **p<0.01, ***p<0.001, one-way ANOVA). d-e) Mitochondrial ROS production, measured by MitoTracker ROS, is increased when we knockdown *smo-1* and this effect is also DAF-16 dependent (n=75, *p<0.05, **p<0.01, ***p<0.001, one-way ANOVA). f) H_2O_2 levels are increased in aged (day 8) animals upon *smo-1(RNAi)*, measured by the HyPer biosensor (n=30, **p<0.01, unpaired t-test). Error bars, S.E.M. g) Treatment with the antioxidant NAC (N-acetyl cyteine)

abrogates the long lifespan of *smo-1* overexpressing animals. Lifespan assays were carried out at 20°C. The percentage of animals remaining alive is plotted against age.

As readouts of mitochondrial function, we measured production of ATP and oxygen consumption rates in 4-day old animals. We did not detect any significant change upon *smo-1(RNAi)* in wild type or *daf-16(-)* genetic background (Figure 16a, b). *daf-2(e1370)* animals displayed lower oxygen consumption rates, and *smo-1(RNAi)* did not significantly alter this rate (Figure 16b). On the contrary, knockdown of *smo-1* resulted in higher ATP production in day 6 wild type animals (Figure 16c), consistent with the TMRE and MitoTracker ROS staining results (Figure 15b-e). Intriguingly, SMO-1 depletion reduced ATP levels in *daf-2(e1370)* and *daf-16(mu86)* animals (Figure 16c), indicating that mitochondrial ROS and ATP production are uncoupled in these genetic backgrounds. To assay mitochondrial content, we used two methods: paraquat (4mM) treatment followed by TMRE staining and mitochondrial DNA copy number measurement. Administration of paraquat leads to mitochondrial membrane potential dissipation, therefore the accumulation of TMRE will reflect the number of mitochondria. Interestingly, downregulation of *smo-1* increased the number of mitochondria during ageing in a DAF-16 dependent manner (Figure 16d, e); but not the mitochondrial DNA copy number (Figure 16f, g). Thus, mitochondrial function and mass are upregulated upon *smo-1* knockdown during ageing.

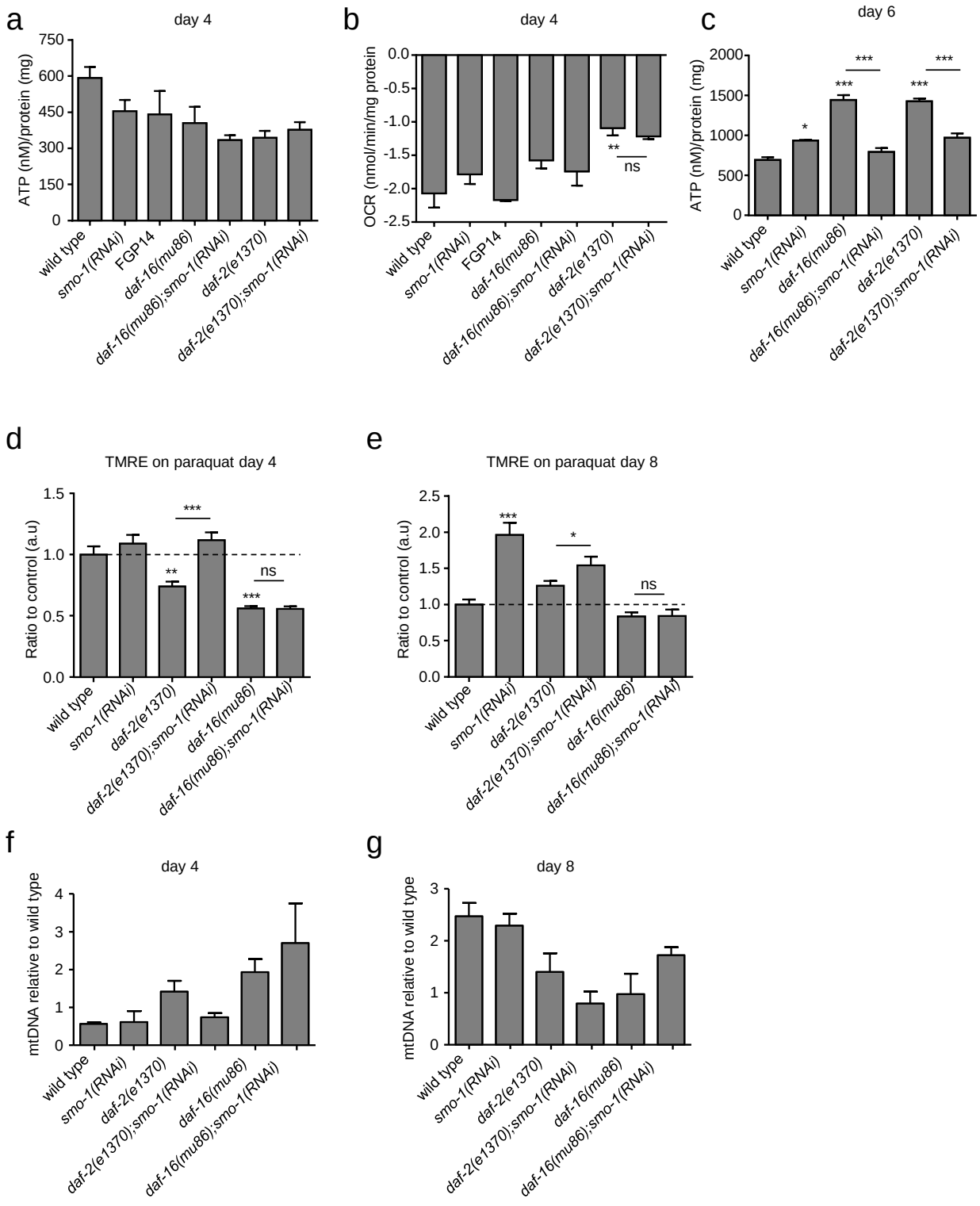

Figure 16: SUMO regulates mitochondrial content during ageing. a) ATP levels do not change in 4-day old animals upon *smo-1* knockdown. b) Oxygen consumption rates are not affected by *smo-1* depletion at day 4, while *daf-2(e1370)* animals exhibit lower oxygen consumption (**p<0.01, unpaired t-test). c) ATP production is increased upon knockdown of *smo-1* in day 6 wild type animals, but not in *daf-16(-)* or *daf-2(-)* background (*p<0.05, ***p<0.001, unpaired t-test). d-e) Mitochondrial content is increased during ageing upon *smo-1(RNAi)* in a DAF-16 dependent manner, measured by subsequent paraquat treatment and TMRE staining (n=50, *p<0.05, **p<0.01,

***p<0.001, one-way ANOVA). f-g) Mitochondrial DNA copy number, normalized to genomic DNA. *smo-1(RNAi)* treatment does not affect the mitochondrial DNA copy number in wild type, *daf-2(e1370)* and *daf-16(mu86)* background in day 4 or day 8 animals. Error bars, S.E.M.

During ageing, the activity of mitochondria declines and they are undergoing morphological changes as well. The interconnected, tubular mitochondrial network of a young organism becomes fragmented as the animal ages (113, 140). We screened the morphology of intestinal mitochondria with the use of $p_{ges\text{-}1}$mtGFP reporter and observed an interconnected network in day 4 animals, in every genetic background tested (Figure 17a, b). This network displayed fragmentation by day 8 of adulthood in wild type *C. elegans*, but not in *smo-1(RNAi)* treated animals (Figure 17c). Mitochondrial morphology is regulated by DAF-16 (113); knocking down *daf-16* by RNAi also leads to a fragmented network and depleting *smo-1* in a *daf-16(RNAi)* background is unable to rescue the fragmented morphology (Figure 17c). An indirect target gene of DAF-16, which regulates mitochondrial morphology, is *eat-3*/OPA1 (141). EAT-3 (eating: abnormal pharyngeal pumping) is required for the fusion of inner mitochondrial membrane (142); *eat-3(RNAi)* animals displayed a fragile, fragmented intestinal mitochondrial network. Moreover we found that EAT-3 was epistatic over SMO-1, since *smo-1(RNAi)* could not restore the mitochondrial network defect caused by *eat-3(RNAi)* (Figure 17b, c). Mitochondrial network remodeling is also regulated by DRP-1 (dynamin related protein-1) and FZO-1 (Fzo mitochondrial fusion protein related). The SUMOylated status of DRP1 has been reported during mitosis, cell death and ischemia (143-146). In *C. elegans*, reducing the expression of *drp-1* or *fzo-1* by RNAi leads to the fragmentation of mitochondrial network (113) (Figure 17d). Interestingly, when we knock-down simultaneously *smo-1* and *drp-1* or *smo-1* and *fzo-1*, the intestinal mitochondrial network remains more connected; the loss of *smo-1* partially ameliorates the detrimental effects of *drp-1(RNAi)* and *fzo-1(RNAi)* (Figure 17d). This indicates that SUMO is required for the sufficient fission of mitochondria. These data delineate the effect of SUMO on the mitochondrial network morphology via DAF-16 and the mitochondrial fusion/fission machinery.

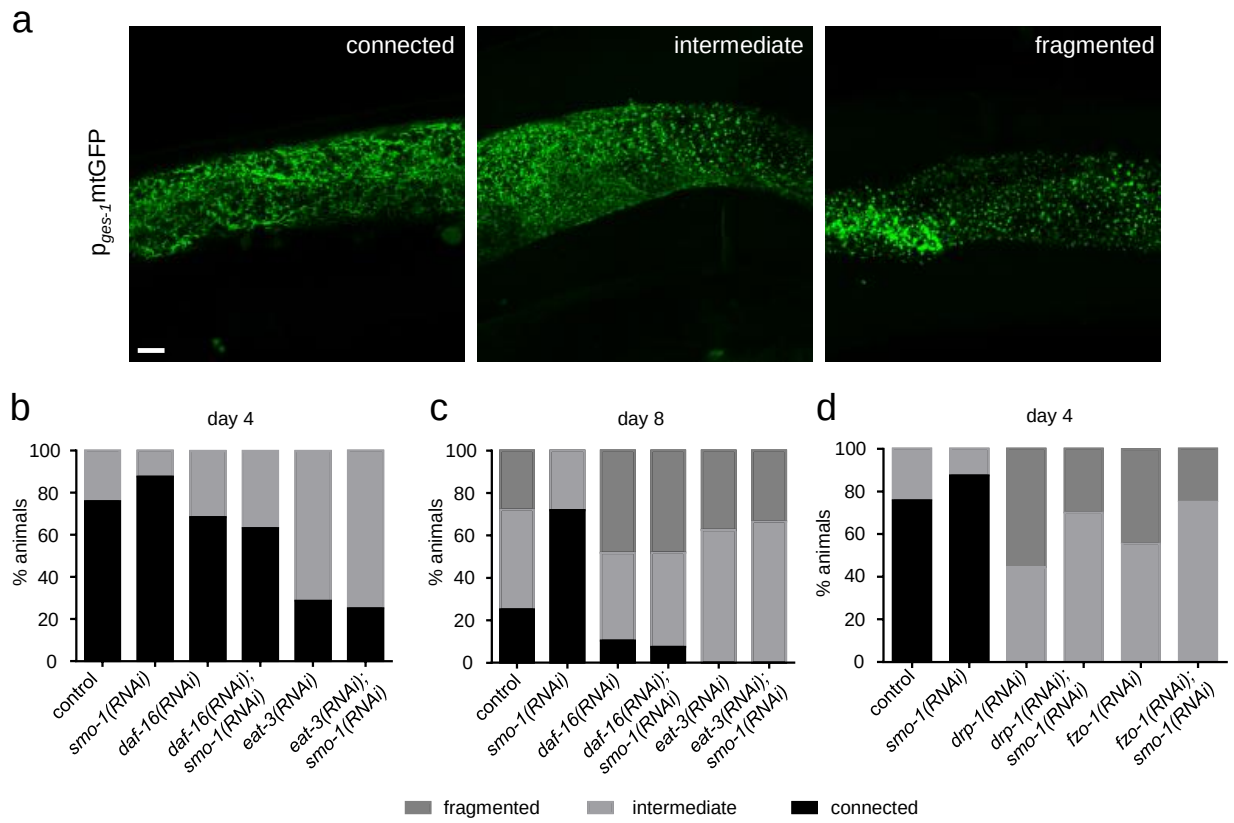

Figure 17: SUMO is required for efficient mitochondrial fission. a) Representative images, showing the basis for scoring of the intestinal mitochondrial network, visualized by p_{ges-1}mtGFP reporter, scale bar: 10 µm. Images were acquired, using x63 objective lens. b-c) The intestinal mitochondrial network becomes fragmented during ageing in a DAF-16 and EAT-3 dependent manner (n=40). d) Depletion of *smo-1* partially recues the fragmented network phenotype of *drp-1(RNAi)* and *fzo-1(RNAi)* treated animals (n=15).

It is a widely accepted notion that mitochondrial fission precedes the process of mitophagy (74). Since SUMO alters mitochondrial dynamics, we tested whether mitophagy is also affected upon reduced *smo-1* expression. We utilized the previously reported mitochondria targeted Rosella biosensor in body wall muscle cells (113), with a minor change: we generated a new transgenic line with biolistic transformation in order to achieve a healthier line through the reduction of transgene copy number and expression level. Indeed, these new transgenic animals are phenotypically wild types and display weaker, yet well detectable expression compared to the original line. Induction of mitophagy is represented by the reduction of pH sensitive GFP and pH insensitive DsRed ratio, as demonstrated upon *daf-2(RNAi)* condition (Figure 18a). Targeting *smo-1* by RNAi led to the increase in the GFP/DsRed ratio, indicating that mitophagy is blocked in the absence of SUMO (Figure 18a). This agrees with the observation that *smo-1(RNAi)* blocks mitochondrial fission (Figure 17). Additionally, we also assayed mitophagy in the nervous system (147), in the RNAi sensitive, *rrf-3(pk1426)* mutant background.

Surprisingly, reduced *smo-1* expression resulted in the induction of mitophagy in neurons (Figure 18b). Thus, SUMO is required to perform mitochondrial fission and mitophagy in a tissue specific manner.

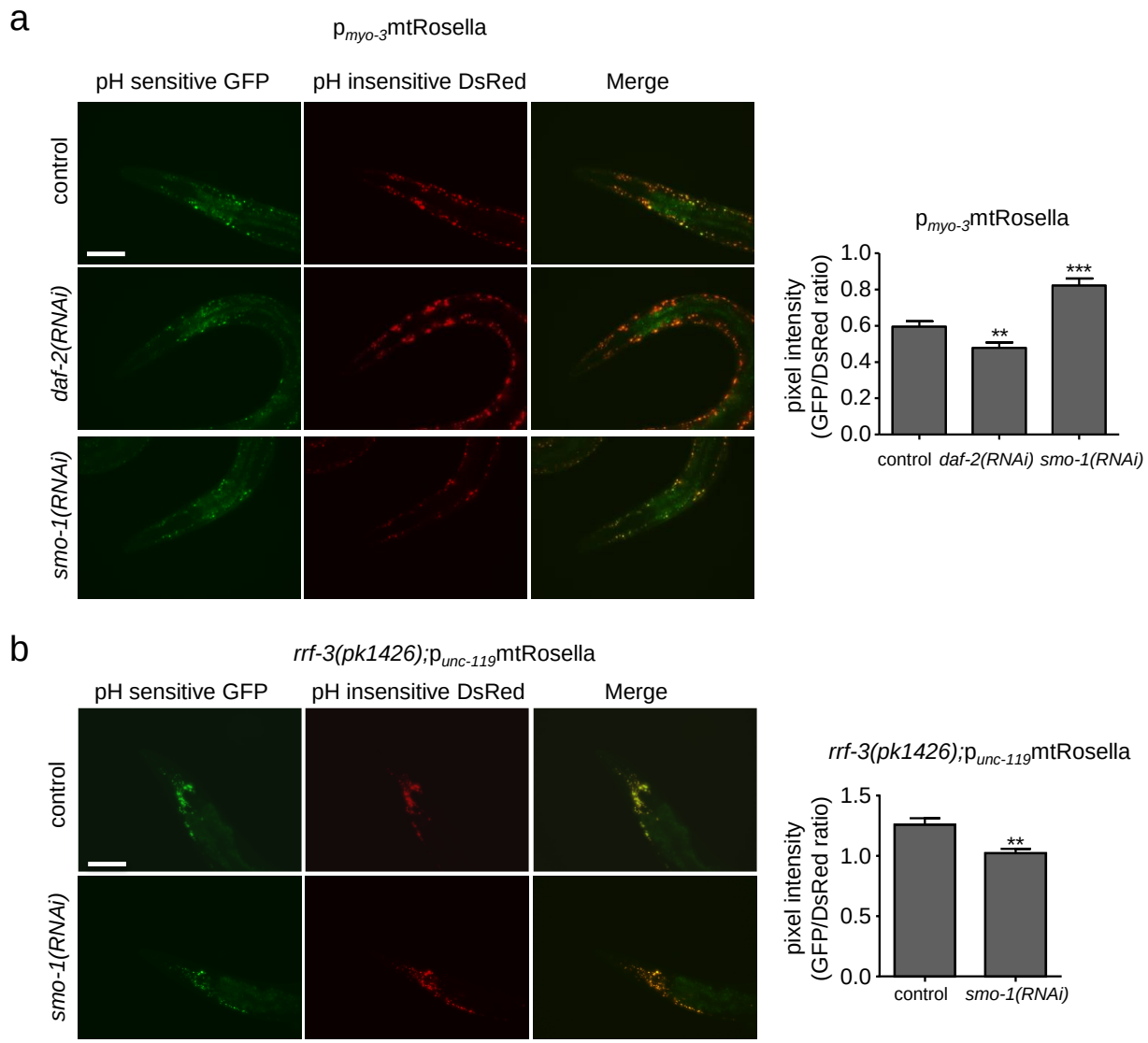

Figure 18: SUMO influences mitophagy in muscles and neurons. a) Animals expressing mitochondria targeted Rosella biosensor in body wall muscle cells. *daf-2(RNAi)* increases, while *smo-1(RNAi)* inhibits mitophagy, scale bar: 100 µm (n=40, **p<0.01, ***p<0.001, unpaired t-test). Images were aquired using x20 objective lens. b) Mitochondria targeted Rosella biosensor, expressed in neurons. Knockdown of *smo-1* induces neuronal mitophagy, scale bar: 100 µm. Images were aquired using x20 objective lens (n=20, **p<0.01, unpaired t-test). Error bars, S.E.M.

To resolve the impact of SUMO on the lifespan of mitochondrial mutants, we examined 3 long-lived mitochondrial mutants under the circumstances of SUMO shortage in the cell. First, we tested *isp-1*

(iron-sulphur protein) mutant animals; *isp-1* encodes a Rieske iron sulphur protein, which is a part of complex III of mitochondrial electron transport chain (ETC). Surprisingly, the loss of *smo-1* in *isp-1(qm150)* background caused a significant lifespan extension (Figure 19a). The same effect could not be observed when we knocked down *smo-1* in *nuo-6(qm200*) or *clk-1(e2519)* animals; in these mutants *smo-1(RNAi)* led to a shortened lifespan (Figure 19b, c). *nuo-6* (NADH ubiquinone oxidoreductase) is a subunit of NADH dehydrogenase complex and part of complex I of the ETC, while *clk-1* (clock abnormality) encodes the enzyme demethoxyubiquinone hydroxylase, required for the biosynthesis of ubiquinone. Our data indicate that depending on which mitochondrial complex we interfere with, SUMOylation can have a beneficial or detrimental effect on animal lifespan.

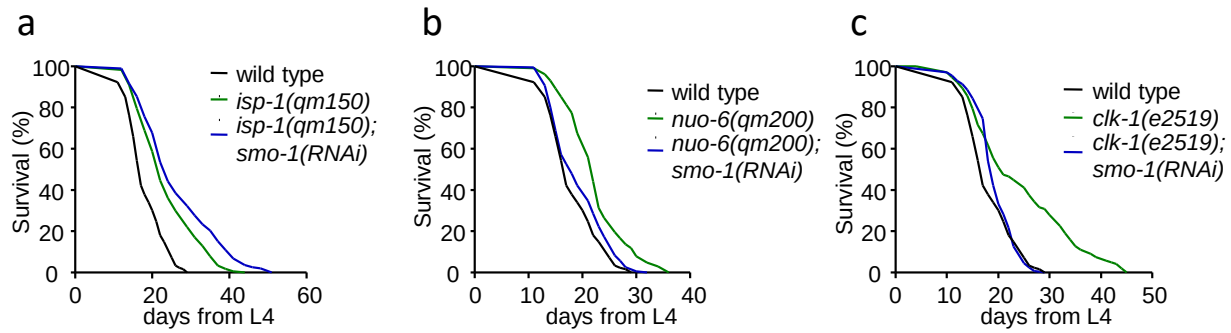

Figure 19: SUMOylation alters the lifespan of mitochondrial mutants. a) Knocking-down *smo-1* in *isp-1(qm150)* background extends the lifespan of animals. b-c) *smo-1(RNAi)* shortens the long lifespan of *nuo-6(qm200)* and *clk-1(e2519).* Lifespan assays were carried out at 20°C. The percentage of animals remaining alive is plotted against age.

Discussion

Here, we present data supporting the notion that SUMOylated proteins are accumulating over the course of *C. elegans*' lifespan. In accordance with this observation, it has been reported that in mouse brain and plasma, SUMOylation of proteins increases until 6 months of age (122). There has been extensive research linking neuronal function and diseases to the process of SUMOylation (148-150). We also found that the lifespan modulating effect of SUMOylation is partly neuron specific, further strengthening the important role of SUMO in neuronal function.

Recently, a connection between insulin and germline signaling via SUMOylation of CAR-1 (cytokinesis, apoptosis, RNA-associated), an RNA binding protein has been demonstrated. Under reduced insulin signaling conditions (e.g. *daf-2* mutation), CAR-1 is less likely to be SUMO modified and it can inhibit *glp-1* levels more efficiently (95). The study establishes a link between SUMOylation in the germline and organismal ageing. We report that DAF-16 and SKN-1 are mediating the lifespan influencing effect of SUMOylation in the soma. More specifically, we report for the first time the SUMOylated status of DAF-16 and its inhibitory consequence on transcriptional activity (Figure 20). SUMOylation of transcription factors are most frequently coupled with transcriptional repression (151). Interestingly, removing SUMO from the animals led to the upregulation of stress responsive genes, controlled by DAF-16 and SKN-1, and even the protein levels of DAF-16 were elevated. This could be explained by three, not mutually exclusive way. First, one of the major functions of SUMOylation is the regulation of cellular stress responses (e.g. DNA damage response, ER stress, heat shock) where SUMO is indispensable for cellular survival (79). Based on this, it is likely that removing SUMO from the cell triggers a general stress response and the prolonged stress eventually exhausts the cell and leads to early death. Second, SUMOylation has also been associated with mRNA translation; however, studies showed a positive correlation between SUMOylation and translation (152). In our case, we saw that the absence of SUMO could lead to increased expression of transcriptional and translational reporters, which indicates that in *C. elegans* SUMOylation decreases translation of at least some selected, stress response genes. The exact, mechanistic connection between translational rates and SUMOylation in *C. elegans* is a subject for future research. Third, SUMOylation of proteins and DNA affect chromatin organization. Most studies showed a repressive connection between chromatin and SUMO, although recent research indicates that SUMO can be associated with active chromatin (153). Moreover, SUMO also regulates the pluripotent state of a cell by acting on the chromatin. Hyposumoylation is associated with pluripotency reprogramming and enhanced lineage transdifferentiation (154). Taking this into account, it could be possible that the observed changes in transgene expression are only an indirect consequence of an

altered chromatin structure, instead of a result of direct regulation by specific transcription factors. However, in the case of SUMO overexpression, *daf-2(RNAi)* can efficiently increase the expression of *sod-3*, which is significantly reduced under control condition. Furthermore, the expression of *gst-4* is not affected upon SUMO overexpression under normal conditions and it is even further increased following paraquat treatment, compared to control. In conclusion, the most possible way of action is the first scenario; loss of SUMOylation imposes constant stress on the animals.

SUMOylation has been linked to mitochondrial biogenesis and network remodeling through PGC-1α and Drp1 in mammals (146, 155, 156). Here, we sought to determine whether SUMOylation have an effect on mitochondrial homeostasis in *C. elegans*. Our data suggest that the amount of mitochondria increases, without a change in mitochondrial DNA copy number upon loss of *smo-1*. Furthermore, during ageing we observed increased ATP and ROS production in a *smo-1* deficient background. This excess energy can be used to fuel the enhanced expression of stress response genes. Considering the importance of mitochondrial dynamics in their function, we wished to resolve the effect of SUMOylation on the morphology and turnover of this organelle. We show that SUMOylation promotes mitochondrial fragmentation during ageing and it is also required for the turnover of the organelle by mitophagy in muscle cells but not in neurons. Admittedly, it has been reported that in long lived mutants mitochondria display an elongated morphology. This allows for their longevity and reduces ROS production (141). In this study we find that our short-lived *smo-1(RNAi)* treated animals feature an elongated mitochondrial network and increased ROS levels (Figure 20). This contradiction can be explained by the fact that long lived mutants not only present interconnected mitochondrial network, but also their turnover is increased, thereby maintaining their health and keeping ROS production at lower levels (113, 157). In a reduced SMO-1 paradigm, the dynamics of mitochondria is blocked, mitophagy is inhibited and as a consequence, the damage cannot be eliminated, ROS levels are increased which results in a shorter lifespan. Our results are in accordance with the recently proposed model which hypothesizes that during ageing the impairment of mitochondrial dynamics negatively affects mitochondrial function and can be the cause of age-related diseases (76). Additionally, changes in SUMOylation levels affect the lifespan of mitochondrial mutants. Here, we tested three different strains that carry mutations in distinct ETC complexes. The long lifespan of *isp-1*, *nuo-6* and *clk-1* mutants has been reported to be dependent on DAF-16 (158). Notably, these strains are only partial loss-of-function mutants, harboring a missense mutation in their gene, resulting in the impairment of ETC and elevated ROS production. Another study showed that the origin of ROS has distinct effect on organismal lifespan. While increase in mitochondrial ROS levels can extend lifespan, elevated cytoplasmic ROS levels decrease lifespan (159). Recently it was demonstrated that *isp-1* mutants require

two specific superoxide dismutases (*sod-3* and *sod-5*) for their longer lifespan (160). It is compelling to hypothesize that the even longer lifespan displayed by *isp-1* mutants on *smo-1(RNAi)* could be a result of activated *sod-3* expression under this condition. All the aforementioned findings point to the conclusion that SUMOylation decreases mitochondrial function and promotes the fission of mitochondria during ageing in *C. elegans*.

In this study, we establish a direct, regulatory role for SUMOylation in the process of ageing on an organismal level (Figure 20). *C. elegans* possesses a sole SUMO protein that we can specifically deplete from the animals after they reach adulthood. This unique feature of *C. elegans* allowed us to examine the consequences of SUMOylation explicitly on ageing and to exclude any non-specific, pleiotropic effects caused by developmental defects. We find that SUMOylation exerts its control over lifespan mainly through DAF-16 and SKN-1 in a tissue specific manner; the intestine and nervous system of the animals convey the lifespan influencing effect of SUMOylation. The transcriptional activity of SUMO modified DAF-16 is repressed. SUMOylation also alters the function and dynamics of mitochondria. In conclusion, our data indicate that a balanced SUMOylation rate of proteins is a prerequisite for the healthy ageing of the animals (Figure 20). This is in concert with recent research implicating SUMOylation in senescent decline. The main senescent regulator, p53 can be modified by SUMO1, leading to cellular senescence (161). Another study showed that deSUMOylation of Bmi1, a polycomb repressive complex member, is crucial for senescence (162). More recently, the SUMO E2 enzyme itself, Ubc9 was linked to the regulation of senescence, by relocating the SUMOylated proteins to PML nuclear bodies (163). These results, together with our findings demonstrate the requirement for a balance between SUMOylated/deSUMOylated protein pools during normal ageing.

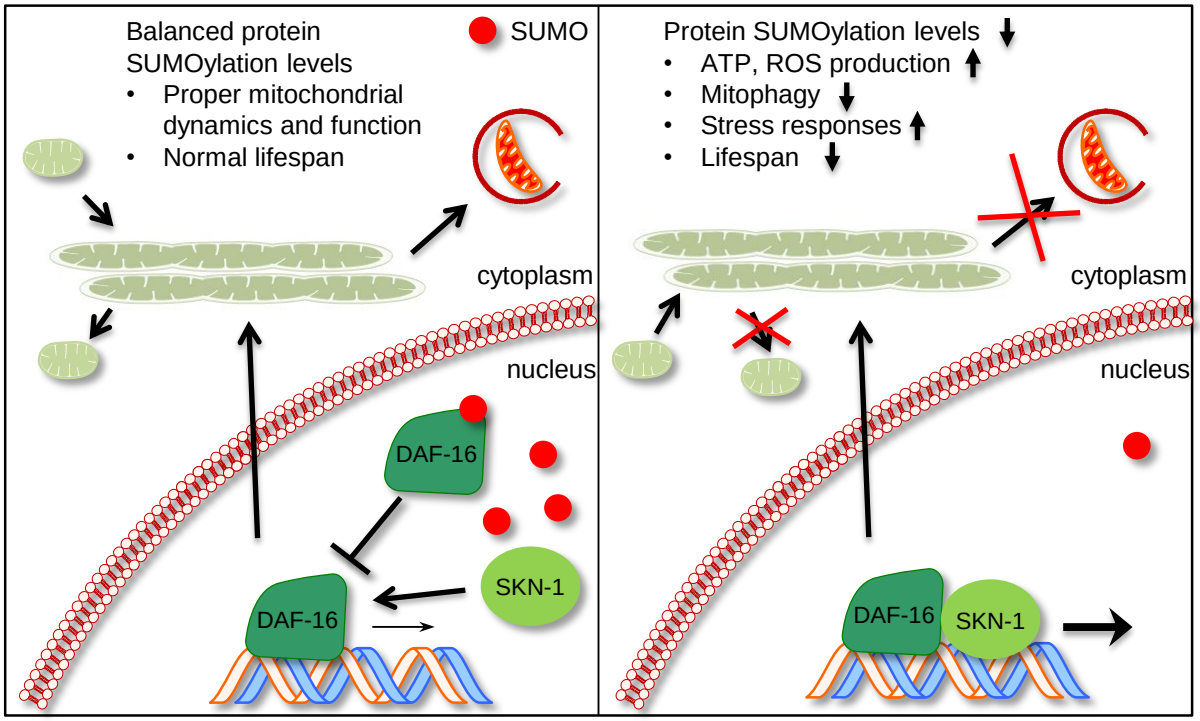

Figure 20: Proposed model. Under normal conditions protein SUMOylation levels are balanced through conjugation and cleavage events. This ensures the tight control of mitochondrial function and dynamics, allowing for a normal lifespan. Reducing protein SUMOylation levels in cell leads to the activation of stress responses, impairment of mitochondrial function and mitophagy which results in a shorter lifespan. Our results also implicate a possible complex formation of DAF-16 and SKN-1 in order to regulate the expression of their target genes. The size of the arrows pointing from DAF-16 and DAF-16/SKN-1 indicate the intensity of transcription activation.

Part 2: Investigating the role of eIF4E beyond translation initiation

Introduction

The eukaryotic translation initiation factor eIF4E has been implicated in the control of protein translation, the formation of stress induced cytoplasmic granules and the export of specific mRNAs from the nucleus. Originally it was described as a translation initiation factor, which binds to the 5' end of mRNAs and promotes translation (164). In order to be regulated by eIF4E, an mRNA has to possess a highly structured 5' UTR (untranslated region) and a 7-methyl guanosine dinucleotide "cap" structure (m^7Gcap). Housekeeping genes and mRNAs with short, unstructured 5' UTR are not affected by the availability of eIF4E (164, 165). Under cellular stress conditions (oxidative stress, heat shock, ageing, etc.), the mRNAs bound to various translation initiation factors assemble into membrane-less messenger ribonucleotide protein complexes (mRNP) called stress granules. These granules can store mRNAs and protect them from degradation and in some cases can even be a site of active translation (157). In contrast, P bodies (processing bodies) are generally formed in all cell types even under normal conditions. Initially P bodies were associated with the degradation of mRNAs (166) however; recent studies demonstrate a storage role for these granules (167). eIF4E can be a component of both stress granules and P bodies (168-170). Surprisingly, eIF4E can also be found in the nucleus, diffused or in nuclear bodies (171, 172). Nuclear eIF4E plays a role in the export of selected mRNAs from the nucleus (173). This process depends on the binding to the m^7Gcap structure and on the presence of the eIF4E sensitivity element (4E-SE) in the 3' UTR (174). 4E-SE is an approximately 50 nucleotide long region and it associates with the leucine-rich pentatricopeptide repeat protein (LRPPRC) which also binds to eIF4E (175). The nuclear export of this complex is achieved via CRM1 (chromosomal maintenance 1) association (175) and this process is distinct from the bulk mRNA export pathway (176). The mRNA export function of eIF4E is associated with its oncogenic potential; in many cancer types eIF4E levels are upregulated (177, 178). The common denominator in all 3 aforementioned functions of eIF4E is its m^7Gcap binding. Through this connection, eIF4E can regulate an mRNA's export, translation and stability (179). Recently, it has been shown that eIF4E is transported to the nucleus via Importin 8 through the cap binding site of eIF4E; therefore Importin 8 competes with mRNAs for the binding of eIF4E (180). Another competition for the binding of eIF4E happens in the nucleus where LRPPRC and PML promote mRNA export and sequestration of eIF4E in an RNA-free state respectively (181, 182) (Figure 21).

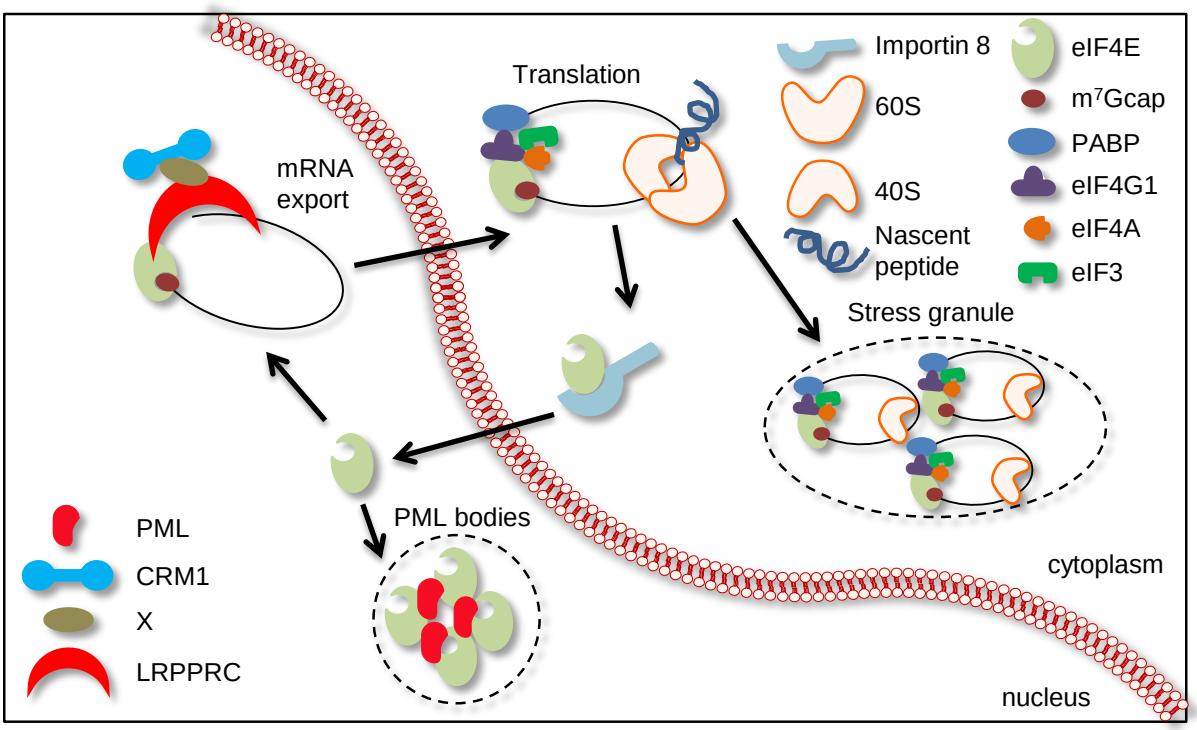

Figure 21: Diverse functions of eIF4E in the cell. In the cytoplasm eIF4E can promote translation or the storage of mRNAs depending on the demands of the cell and environmental conditions. In the nucleus the cap-bound eIF4E facilitates the export of specific mRNAs, while the cap-free eIF4E accumulates in PML nuclear bodies. X indicates yet unknown protein/proteins bringing together the CRM1 export factor and LRPPRC bound to mRNA and eIF4E.

5 isoforms of eIF4E has been characterized in *C. elegans* (*ife-1 – 5*) (183, 184). 3 isoforms (*ife-1, -3, -5*) are expressed in the germline, taking part in development and in the maintenance of germ cells (185-187). IFE-4 is a somatic isoform expressed in a subset of neurons, muscles and it controls the translation of a small subset of mRNAs (188). The most widely expressed isoform is IFE-2; it can be found in all somatic tissues but not in the germline and reducing its expression extends the lifespan of *C. elegans* (111). Here we uncover a peculiar relationship between IFE-2 and the heat shock transcription factor, HSF-1 during ageing. The function of HSF-1 is required for the reduced *ife-2* expression during ageing and for the proper subcellular localization of IFE-2. Furthermore, the lack of an exportin gene, *xpo-1*, led to a shortened lifespan. However, up until now *xpo-1(RNAi)* failed to entrap IFE-2 in the nucleus.

Results

HSF-1 promotes the degradation and prevents the nuclear accumulation of IFE-2

We previously demonstrated that the level of $p_{ife\text{-}2}$IFE-2::GFP gradually declines during ageing (Figure 22a). Moreover, we found that knocking down *daf-16* and *skn-1* did not change $p_{ife\text{-}2}$IFE-2::GFP levels, while reducing the expression of *hsf-1* prevented the age-related decline of the protein (Figure 22b) (114). This indicates that the upregulation of $p_{ife\text{-}2}$IFE-2::GFP is not a general response employed by the cell when a stress responsive transcription factor is missing, but it is specific to the loss of HSF-1. We showed that the differences observed in the level of $p_{ife\text{-}2}$IFE-2::GFP are a result of changes in translational rates. Notably, the expression of $p_{ife\text{-}2}$GFP transcriptional reporter was increased upon *hsf-1(RNAi)* during ageing, although the mRNA levels of *ife-2* remained unaffected by ageing and by removal or overexpression of *hsf-1* (Figure 22c) (114). Intriguingly, $p_{ife\text{-}2}$IFE-2::GFP displayed a peculiar subcellular distribution in day 8 old animals on *hsf-1(RNAi)*; we observed a nuclear and stress granule-like localization and accumulation of IFE-2 in various cell types (e.g. muscle, intestine and seam cells) (Figure 23a). In order to confirm the nuclear localization of $p_{ife\text{-}2}$IFE-2::GFP, we performed DAPI staining and saw that IFE-2 is indeed nuclear under these conditions (Figure 23b). Moreover, we used an *in silico* method, NLS mapper (http://nls-mapper.iab.keio.ac.jp/cgi-bin/NLS_Mapper_form.cgi) (189) , to determine whether the protein sequence of IFE-2 contains nuclear localization signal and identified a strong NLS at the N terminal of the protein (Figure 23c).

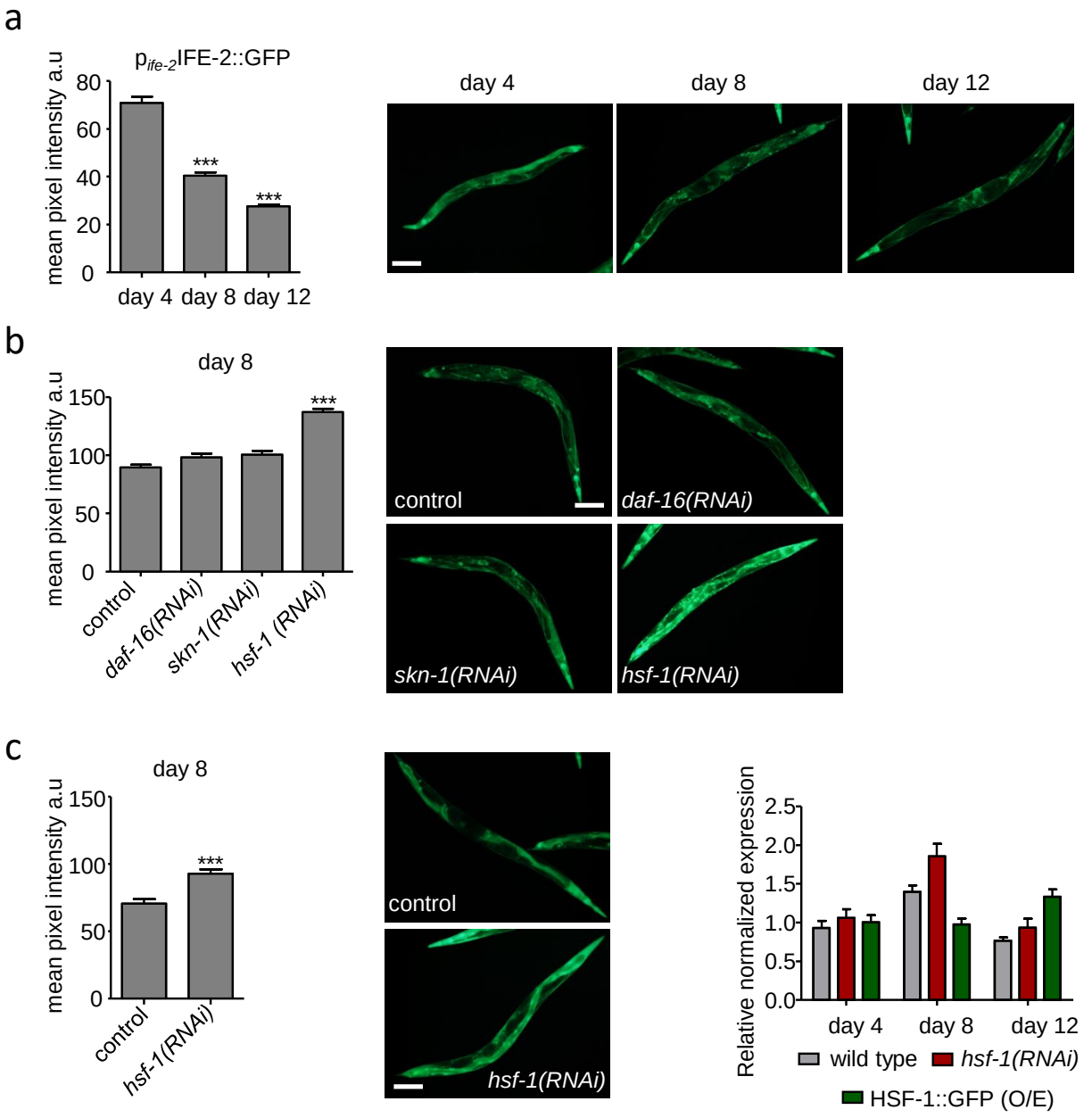

Figure 22: The levels of IFE-2 are specifically affected by HSF-1 during ageing. a) The levels of IFE-2, visualized by the fluorescent reporter p$_{ife-2}$IFE-2::GFP, are decreasing during ageing (n=100,***p<0.001, unpaired t-test). b) p$_{ife-2}$IFE-2::GFP levels are maintained specifically upon *hsf-1(RNAi)* in day 8 old animals (n=100,***p<0.001, unpaired t-test). c) p*ife-2*GFP levels are increased on *hsf-1(RNAi)* at day 8 of adulthood. The mRNA levels of ife-2 is not subject to change during ageing or under hsf-1(RNAi) and HSF-1 overexpressing conditions. Images were acquired using x10 objective lens, scale bar: 200 µm (n=100,***p<0.001, unpaired t-test). Error bars, S.E.M.

a

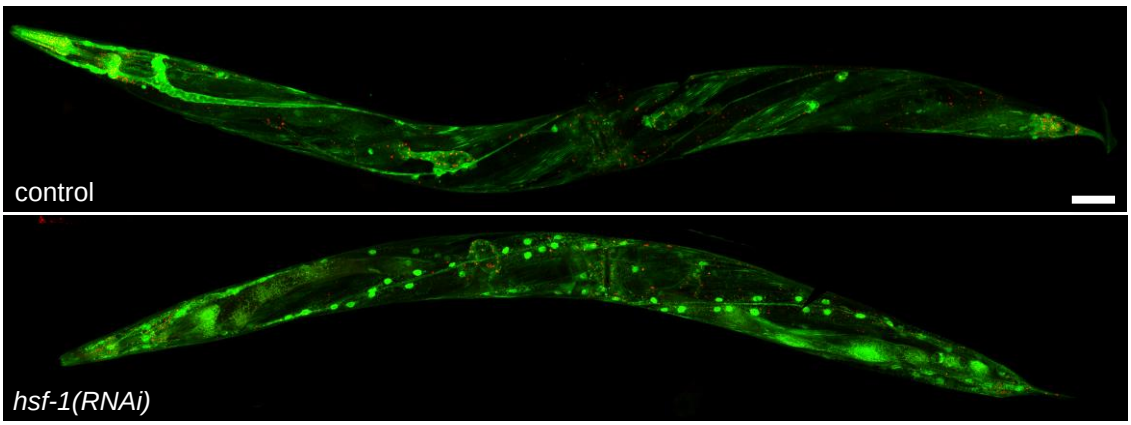

b

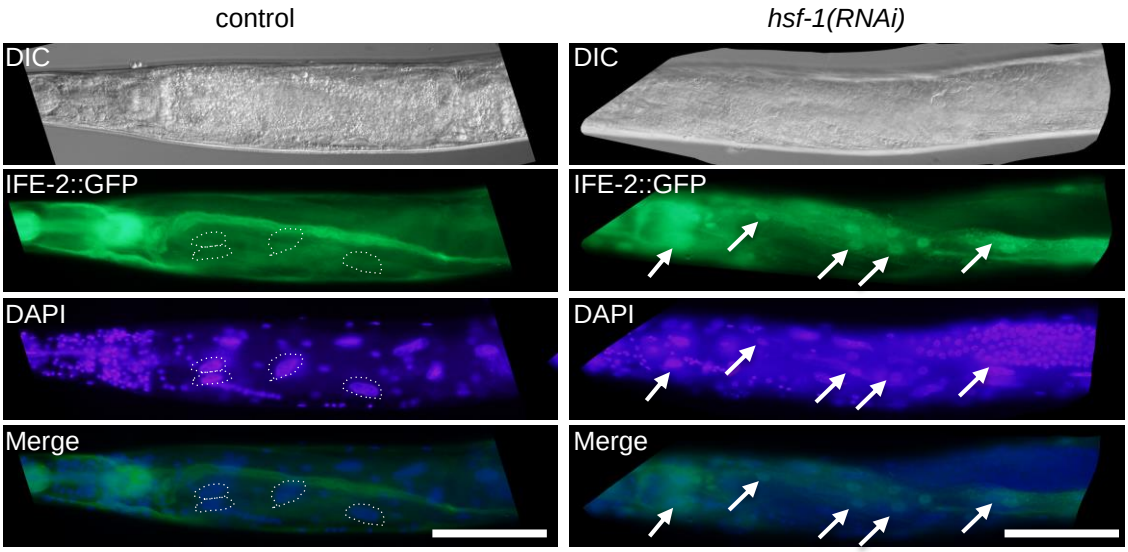

c

Position	Sequence	Score
19	LKRNWTWWYLNDERNKSWEERLKNVKT	9.1

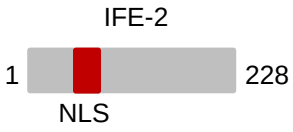

Figure 23: IFE-2 localizes to the nucleus during ageing in the absence of HSF-1. a) Confocal images illustrating the subcellular localization of p_{ife-2}IFE-2::GFP in control and *hsf-1(RNAi)* animals at day 8 of adulthood. Images were acquired using x20 objective lens, scale bar: 100 µm. b) DAPI staining confirms the nuclear localization of p_{ife-2}IFE-2::GFP in day 8 old animals treated with *hsf-1(RNAi)*. Arrows point nuclei detectable as GFP and DAPI signal. Images were acquired using x40 objective lens, scale bar: 100 µm. c) *In silico* NLS mapper analysis identified a strong nuclear localization signal in the sequence of IFE-2.

XPO-1 influences lifespan but not the nuclear localization of IFE-2

Next, we wished to determine the mechanism by which IFE-2 becomes predominantly nuclear in the absence of HSF-1. In mammalian cells, Importin-8 and CRM-1 are responsible for the nuclear-cytoplasmic trafficking of eIF4E (175, 180). In *C. elegans* there are 3 importin beta family protein encoding genes: *imb-1-3* and we have RNAi against *imb-1* and *imb-2* in the lab (generated by Nikolaos Charmpilas). We hypothesized that combining *imb-1(RNAi)* with *hsf-1(RNAi)* and *imb-2* with *hsf-1(RNAi)* would result in the exclusion of IFE-2 from the nucleus if the nuclear import of the protein is facilitated by one of these importers. However, this was not the case, IFE-2 still accumulated in the nucleus of day 8 old animals upon *imb-1(RNAI);hsf-1(RNAi)* and *imb-2(RNAi);hsf-1(RNAi)* (Figure 24a). The orthologue of CRM1 is XPO-1 (exportin) in the worm. We expected to see nuclear accumulation of IFE-2 during ageing under control conditions when we knock down *xpo-1*. On the contrary, we found no difference in the subcellular localization of IFE-2 between control and *xpo-1(RNAi)* treated animals (Figure 24a).

We wondered whether knocking down *xpo-1* would have any effect on lifespan in wild type or different long-lived mutants. Our data show a reduced lifespan for *xpo-1(RNAi)* treated animals in all conditions tested (Figure 24b-e). This is in contrast to what a recent study found: it was demonstrated that *xpo-1(RNAi)* causes lifespan extension via HLH-30 entrapment in the nucleus and activation of autophagy genes (37). To resolve this contradiction, first of all we have to test whether autophagy is activated upon our *xpo-1(RNAi)* in the future.

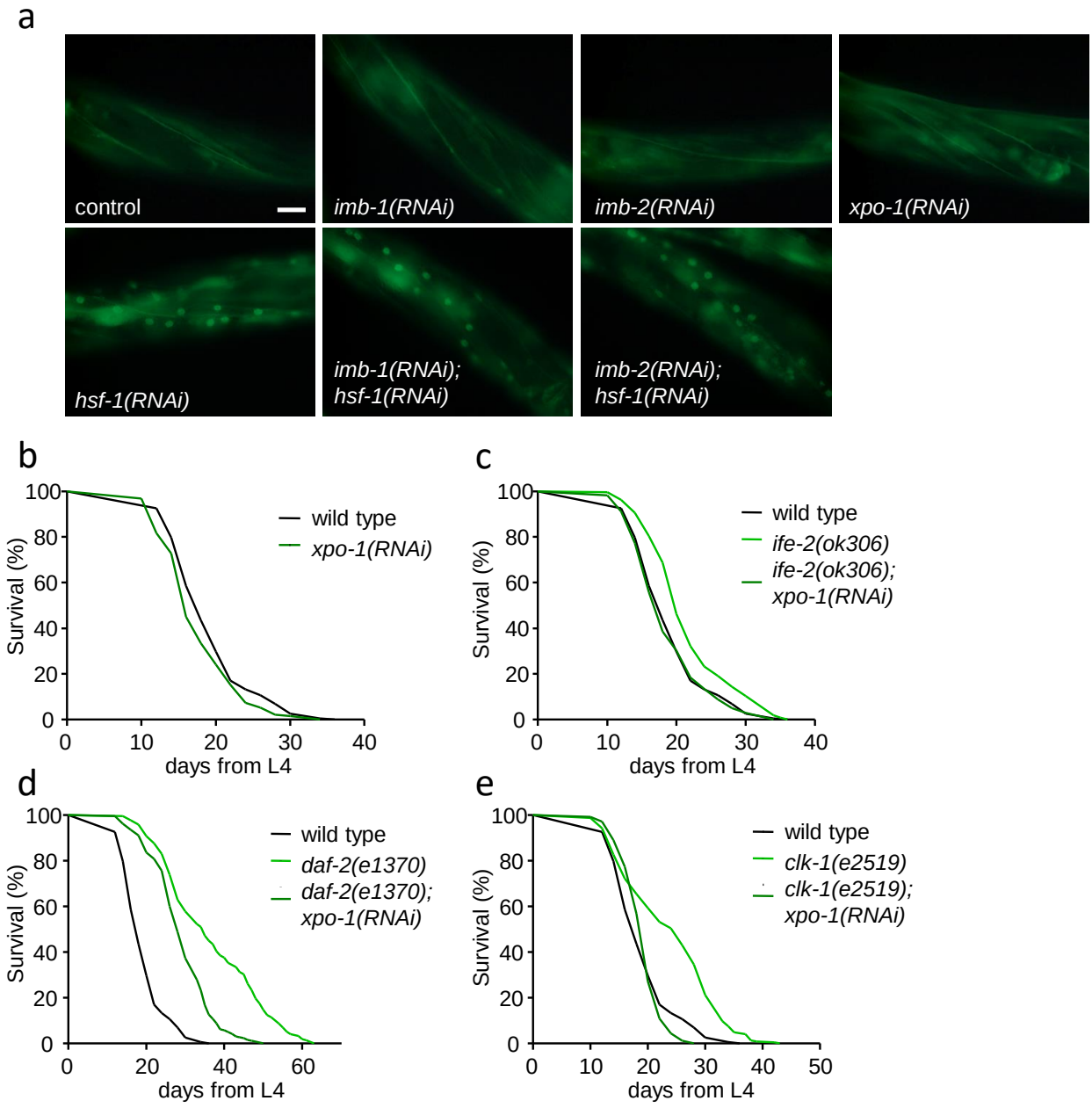

Figure 24: XPO-1 does not change the subcellular localization of IFE-2; it affects organismal lifespan. a) Knock-down of *imb-1*, *imb-2* or *xpo-1* did not alter the subcellular distribution of IFE-2 in control or *hsf-1(RNAi)* background. Images were acquired using x40 objective lens, scale bar: 50 µm. b-e) Reduced expression of *xpo-1* results in a shorter lifespan in wild type and long-lived mutants. Lifespan assays were carried out at 20°C. The percentage of animals remaining alive is plotted against age.

Heat stress sequesters IFE-2 in stress granules but not in the nucleus

Taking into account the specificity of HSF-1 to alter IFE-2 localization and stability, and the main function of HSF-1 in the heat shock response, we probed for the subcellular localization of $p_{ife\text{-}2}$IFE-2::GFP at 25°C. Animals subjected to *hsf-1* RNAi displayed stress granule formation and increased IFE-2::GFP levels at

day 6 of adulthood compared to control (Figure 25a). Interestingly, we could not observe any obvious nuclear localization. Additionally, we exposed 2 days old worms to extreme heat stress (37°C) for 8 hours and detected accumulation of IFE-2 in stress granules and also in the nucleus (Figure 25b). However, this nuclear localization was more subtle compared to day 8 *hsf-1(RNAi)* treated animals, most likely because during 8 hours there is not enough time to sequester a bigger amount of IFE-2 to the nucleus compared to day 8 animals. Alternatively, another explanation can be true as well: extreme heat shock induced stress granule formation of p_{ife-2}IFE-2::GFP; it is possible that under heat stress IFE-2 is preferentially sequestered in stress granules and not in the nucleus as in the case of ageing. This data indicate that HSF-1 functions separately from its role in heat shock response under normal conditions to maintain the proper circulation of IFE-2 between the cytoplasm and the nucleus.

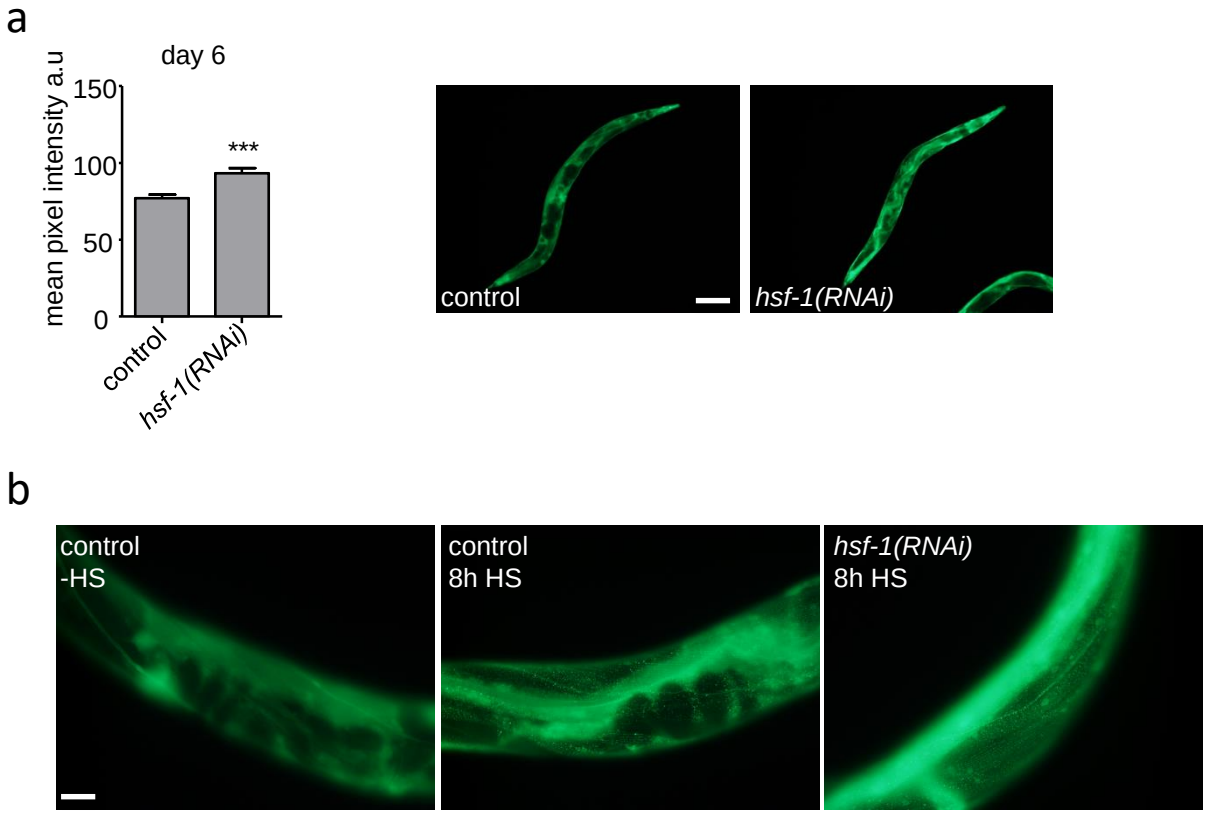

Figure 25: Heat shock induces p_{ife-2}IFE-2::GFP expression and stress granule formation. a) Animals grown at 25°C exhibit higher p_{ife-2}IFE-2::GFP levels at day 6 of adulthood. Images were acquired using x10 objective lens, scale bar: 200 µm (n=100,***p<0.001, unpaired t-test). Error bars, S.E.M. b) Day 2 old animals exposed to 37°C for 8 hours exhibit increased stress granule formation and nuclear localization upon hsf-1(RNAi). Images were acquired using x40 objective lens, scale bar: 50 µm.

Outlook

Here we found that the *C. elegans* orthologue of eIF4E, IFE-2 is controlled by HSF-1 on multiple levels. First, the age-associated decline in the translation of *ife-2* is *hsf-1* dependent. It would be a valuable experiment to perform FRAP (fluorescent recovery after photobleaching) in order to determine the translational rates in *hsf-1(RNAi)* treated animals. Second, the formation of stress granules is increased in the absence of *hsf-1* during ageing and under heat stress conditions. In the future we are planning to subject p_{ife-2}IFE-2::GFP transgenic animals to other types of stresses as well, like oxidative stress, starvation, and see how stress granule formation is affected, if all. Third, HSF-1, through a yet unknown mechanism, inhibits the nuclear localization of IFE-2 later in life. In mammalian cells CRM-1/XPO-1 can be inhibited by the chemical Leptomycin B. We will expose p_{ife-2}IFE-2::GFP animals to Leptomycin B in a hope to capture IFE-2 in the nucleus under control conditions. This could give us indication about the dynamics and mechanism of IFE-2 shuttling between the nucleus and cytoplasm. Furthermore, it is possible that we can get more information about the involvement of *imb-1*, *imb-2* and *xpo-1* in the regulation ofIFE-2 subcellular localization by checking later time-points during ageing (day 12, 17). Additionally, the creation of a p_{ife-2}IFE-2::DsRed transgenic line and its cross with p_{hsf-1}HSF-1::GFP would illustrate whether the two protein is physically interacting. Furthermore, introducing p_{ife-2}IFE-2::GFP to a genetic background where HSF-1 is more active under normal conditions, e.g. *hsb-1(cg116)* mutant, is in our immediate plans. Monitoring the expression level and pattern in these animals will also be informative regarding the functional interaction of IFE-2 and HSF-1. Recently, it has been shown that the developmental arrest of an *hsf-1* partial loss-of function mutant caused by exposure to heat stress can be rescued via *rsks-1* mutation. Interestingly, this effect is not mediated through reduced translational rates or activation of stress responses (190). Although in this study the focus was placed on development, but it would be exciting to see if the combined knock-down of *rsks-1* and *hsf-1* will have any effect on IFE-2 localization/function.

References

1. Corsi AK, Wightman B, Chalfie M. A Transparent Window into Biology: A Primer on Caenorhabditis elegans. Genetics. 2015;200(2):387-407. Epub 2015/06/20.
2. Mello CC, Conte D, Jr. Revealing the world of RNA interference. Nature. 2004;431(7006):338-42. Epub 2004/09/17.
3. Rieckher M, Kourtis N, Pasparaki A, Tavernarakis N. Transgenesis in Caenorhabditis elegans. Methods Mol Biol. 2009;561:21-39. Epub 2009/06/09.
4. Denzel MS, Lapierre LR, Mack HID. Emerging Topics in C. elegans aging research: Transcriptional regulation, stress response and epigenetics. Mechanisms of ageing and development. 2018. Epub 2018/08/23.
5. Murphy CT, Hu PJ. Insulin/insulin-like growth factor signaling in C. elegans. WormBook : the online review of C elegans biology. 2013:1-43. Epub 2014/01/08.
6. Chiang WC, Tishkoff DX, Yang B, Wilson-Grady J, Yu X, Mazer T, et al. C. elegans SIRT6/7 homolog SIR-2.4 promotes DAF-16 relocalization and function during stress. PLoS genetics. 2012;8(9):e1002948. Epub 2012/10/03.
7. Ogg S, Ruvkun G. The C. elegans PTEN homolog, DAF-18, acts in the insulin receptor-like metabolic signaling pathway. Molecular cell. 1998;2(6):887-93. Epub 1999/01/14.
8. Takahashi Y, Daitoku H, Hirota K, Tamiya H, Yokoyama A, Kako K, et al. Asymmetric arginine dimethylation determines life span in C. elegans by regulating forkhead transcription factor DAF-16. Cell metabolism. 2011;13(5):505-16. Epub 2011/05/03.
9. Drabikowski K, Ferralli J, Kistowski M, Oledzki J, Dadlez M, Chiquet-Ehrismann R. Comprehensive list of SUMO targets in Caenorhabditis elegans and its implication for evolutionary conservation of SUMO signaling. Scientific reports. 2018;8(1):1139. Epub 2018/01/20.
10. Heimbucher T, Liu Z, Bossard C, McCloskey R, Carrano AC, Riedel CG, et al. The Deubiquitylase MATH-33 Controls DAF-16 Stability and Function in Metabolism and Longevity. Cell metabolism. 2015;22(1):151-63. Epub 2015/07/15.
11. Libina N, Berman JR, Kenyon C. Tissue-specific activities of C. elegans DAF-16 in the regulation of lifespan. Cell. 2003;115(4):489-502. Epub 2003/11/19.
12. Honjoh S, Yamamoto T, Uno M, Nishida E. Signalling through RHEB-1 mediates intermittent fasting-induced longevity in C. elegans. Nature. 2009;457(7230):726-30. Epub 2008/12/17.
13. Greer EL, Dowlatshahi D, Banko MR, Villen J, Hoang K, Blanchard D, et al. An AMPK-FOXO pathway mediates longevity induced by a novel method of dietary restriction in C. elegans. Current biology : CB. 2007;17(19):1646-56. Epub 2007/09/29.
14. Apfeld J, O'Connor G, McDonagh T, DiStefano PS, Curtis R. The AMP-activated protein kinase AAK-2 links energy levels and insulin-like signals to lifespan in C. elegans. Genes & development. 2004;18(24):3004-9. Epub 2004/12/03.
15. Kaeberlein TL, Smith ED, Tsuchiya M, Welton KL, Thomas JH, Fields S, et al. Lifespan extension in Caenorhabditis elegans by complete removal of food. Aging cell. 2006;5(6):487-94. Epub 2006/11/04.
16. Lee GD, Wilson MA, Zhu M, Wolkow CA, de Cabo R, Ingram DK, et al. Dietary deprivation extends lifespan in Caenorhabditis elegans. Aging cell. 2006;5(6):515-24. Epub 2006/11/14.
17. Blackwell TK, Steinbaugh MJ, Hourihan JM, Ewald CY, Isik M. SKN-1/Nrf, stress responses, and aging in Caenorhabditis elegans. Free radical biology & medicine. 2015;88(Pt B):290-301. Epub 2015/08/02.
18. Tullet JM, Hertweck M, An JH, Baker J, Hwang JY, Liu S, et al. Direct inhibition of the longevity-promoting factor SKN-1 by insulin-like signaling in C. elegans. Cell. 2008;132(6):1025-38. Epub 2008/03/25.
19. An JH, Vranas K, Lucke M, Inoue H, Hisamoto N, Matsumoto K, et al. Regulation of the Caenorhabditis elegans oxidative stress defense protein SKN-1 by glycogen synthase kinase-3.

Proceedings of the National Academy of Sciences of the United States of America. 2005;102(45):16275-80. Epub 2005/10/28.
20. Inoue H, Hisamoto N, An JH, Oliveira RP, Nishida E, Blackwell TK, et al. The C. elegans p38 MAPK pathway regulates nuclear localization of the transcription factor SKN-1 in oxidative stress response. Genes & development. 2005;19(19):2278-83. Epub 2005/09/17.
21. Okuyama T, Inoue H, Ookuma S, Satoh T, Kano K, Honjoh S, et al. The ERK-MAPK pathway regulates longevity through SKN-1 and insulin-like signaling in Caenorhabditis elegans. The Journal of biological chemistry. 2010;285(39):30274-81. Epub 2010/07/14.
22. Tullet JMA, Green JW, Au C, Benedetto A, Thompson MA, Clark E, et al. The SKN-1/Nrf2 transcription factor can protect against oxidative stress and increase lifespan in C. elegans by distinct mechanisms. Aging cell. 2017;16(5):1191-4. Epub 2017/06/15.
23. Anckar J, Sistonen L. Regulation of HSF1 function in the heat stress response: implications in aging and disease. Annual review of biochemistry. 2011;80:1089-115. Epub 2011/03/23.
24. Akerfelt M, Morimoto RI, Sistonen L. Heat shock factors: integrators of cell stress, development and lifespan. Nature reviews Molecular cell biology. 2010;11(8):545-55. Epub 2010/07/16.
25. Brunquell J, Morris S, Lu Y, Cheng F, Westerheide SD. The genome-wide role of HSF-1 in the regulation of gene expression in Caenorhabditis elegans. BMC genomics. 2016;17:559. Epub 2016/08/09.
26. Barna J, Princz A, Kosztelnik M, Hargitai B, Takacs-Vellai K, Vellai T. Heat shock factor-1 intertwines insulin/IGF-1, TGF-beta and cGMP signaling to control development and aging. BMC developmental biology. 2012;12:32. Epub 2012/11/03.
27. Chiang WC, Ching TT, Lee HC, Mousigian C, Hsu AL. HSF-1 regulators DDL-1/2 link insulin-like signaling to heat-shock responses and modulation of longevity. Cell. 2012;148(1-2):322-34. Epub 2012/01/24.
28. Das R, Melo JA, Thondamal M, Morton EA, Cornwell AB, Crick B, et al. The homeodomain-interacting protein kinase HPK-1 preserves protein homeostasis and longevity through master regulatory control of the HSF-1 chaperone network and TORC1-restricted autophagy in Caenorhabditis elegans. PLoS genetics. 2017;13(10):e1007038. Epub 2017/10/17.
29. Baird NA, Douglas PM, Simic MS, Grant AR, Moresco JJ, Wolff SC, et al. HSF-1-mediated cytoskeletal integrity determines thermotolerance and life span. Science. 2014;346(6207):360-3. Epub 2014/10/18.
30. Higuchi-Sanabria R, Paul JW, Durieux J, Benitez C, Frankino PA, Tronnes SU, et al. Spatial regulation of the actin cytoskeleton by HSF-1 during aging. Molecular biology of the cell. 2018:mbcE18060362. Epub 2018/08/23.
31. Hsu AL, Murphy CT, Kenyon C. Regulation of aging and age-related disease by DAF-16 and heat-shock factor. Science. 2003;300(5622):1142-5. Epub 2003/05/17.
32. Kumsta C, Chang JT, Schmalz J, Hansen M. Hormetic heat stress and HSF-1 induce autophagy to improve survival and proteostasis in C. elegans. Nature communications. 2017;8:14337. Epub 2017/02/16.
33. O'Rourke EJ, Ruvkun G. MXL-3 and HLH-30 transcriptionally link lipolysis and autophagy to nutrient availability. Nature cell biology. 2013;15(6):668-76. Epub 2013/04/23.
34. Visvikis O, Ihuegbu N, Labed SA, Luhachack LG, Alves AF, Wollenberg AC, et al. Innate host defense requires TFEB-mediated transcription of cytoprotective and antimicrobial genes. Immunity. 2014;40(6):896-909. Epub 2014/06/03.
35. Lapierre LR, De Magalhaes Filho CD, McQuary PR, Chu CC, Visvikis O, Chang JT, et al. The TFEB orthologue HLH-30 regulates autophagy and modulates longevity in Caenorhabditis elegans. Nature communications. 2013;4:2267. Epub 2013/08/09.

36. Roczniak-Ferguson A, Petit CS, Froehlich F, Qian S, Ky J, Angarola B, et al. The transcription factor TFEB links mTORC1 signaling to transcriptional control of lysosome homeostasis. Science signaling. 2012;5(228):ra42. Epub 2012/06/14.
37. Silvestrini MJ, Johnson JR, Kumar AV, Thakurta TG, Blais K, Neill ZA, et al. Nuclear Export Inhibition Enhances HLH-30/TFEB Activity, Autophagy, and Lifespan. Cell reports. 2018;23(7):1915-21. Epub 2018/05/17.
38. Seah NE, de Magalhaes Filho CD, Petrashen AP, Henderson HR, Laguer J, Gonzalez J, et al. Autophagy-mediated longevity is modulated by lipoprotein biogenesis. Autophagy. 2016;12(2):261-72. Epub 2015/12/17.
39. Lin XX, Sen I, Janssens GE, Zhou X, Fonslow BR, Edgar D, et al. DAF-16/FOXO and HLH-30/TFEB function as combinatorial transcription factors to promote stress resistance and longevity. Nature communications. 2018;9(1):4400. Epub 2018/10/26.
40. Panowski SH, Wolff S, Aguilaniu H, Durieux J, Dillin A. PHA-4/Foxa mediates diet-restriction-induced longevity of C. elegans. Nature. 2007;447(7144):550-5. Epub 2007/05/04.
41. Kalb JM, Lau KK, Goszczynski B, Fukushige T, Moons D, Okkema PG, et al. pha-4 is Ce-fkh-1, a fork head/HNF-3alpha,beta,gamma homolog that functions in organogenesis of the C. elegans pharynx. Development. 1998;125(12):2171-80. Epub 1998/05/19.
42. Lapierre LR, Gelino S, Melendez A, Hansen M. Autophagy and lipid metabolism coordinately modulate life span in germline-less C. elegans. Current biology : CB. 2011;21(18):1507-14. Epub 2011/09/13.
43. Hwang AB, Lee SJ. Regulation of life span by mitochondrial respiration: the HIF-1 and ROS connection. Aging. 2011;3(3):304-10. Epub 2011/03/11.
44. Zhang Y, Shao Z, Zhai Z, Shen C, Powell-Coffman JA. The HIF-1 hypoxia-inducible factor modulates lifespan in C. elegans. PloS one. 2009;4(7):e6348. Epub 2009/07/28.
45. Lee SJ, Hwang AB, Kenyon C. Inhibition of respiration extends C. elegans life span via reactive oxygen species that increase HIF-1 activity. Current biology : CB. 2010;20(23):2131-6. Epub 2010/11/26.
46. Schiavi A, Maglioni S, Palikaras K, Shaik A, Strappazzon F, Brinkmann V, et al. Iron-Starvation-Induced Mitophagy Mediates Lifespan Extension upon Mitochondrial Stress in C. elegans. Current biology : CB. 2015;25(14):1810-22. Epub 2015/07/07.
47. Leiser SF, Miller H, Rossner R, Fletcher M, Leonard A, Primitivo M, et al. Cell nonautonomous activation of flavin-containing monooxygenase promotes longevity and health span. Science. 2015;350(6266):1375-8. Epub 2015/11/21.
48. Mahanti P, Bose N, Bethke A, Judkins JC, Wollam J, Dumas KJ, et al. Comparative metabolomics reveals endogenous ligands of DAF-12, a nuclear hormone receptor, regulating C. elegans development and lifespan. Cell metabolism. 2014;19(1):73-83. Epub 2014/01/15.
49. Motola DL, Cummins CL, Rottiers V, Sharma KK, Li T, Li Y, et al. Identification of ligands for DAF-12 that govern dauer formation and reproduction in C. elegans. Cell. 2006;124(6):1209-23. Epub 2006/03/15.
50. Goudeau J, Bellemin S, Toselli-Mollereau E, Shamalnasab M, Chen Y, Aguilaniu H. Fatty acid desaturation links germ cell loss to longevity through NHR-80/HNF4 in C. elegans. PLoS biology. 2011;9(3):e1000599. Epub 2011/03/23.
51. Pathare PP, Lin A, Bornfeldt KE, Taubert S, Van Gilst MR. Coordinate regulation of lipid metabolism by novel nuclear receptor partnerships. PLoS genetics. 2012;8(4):e1002645. Epub 2012/04/19.
52. Van Gilst MR, Hadjivassiliou H, Jolly A, Yamamoto KR. Nuclear hormone receptor NHR-49 controls fat consumption and fatty acid composition in C. elegans. PLoS biology. 2005;3(2):e53. Epub 2005/02/19.

53. Goh GYS, Winter JJ, Bhanshali F, Doering KRS, Lai R, Lee K, et al. NHR-49/HNF4 integrates regulation of fatty acid metabolism with a protective transcriptional response to oxidative stress and fasting. Aging cell. 2018;17(3):e12743. Epub 2018/03/07.
54. Wullschleger S, Loewith R, Hall MN. TOR signaling in growth and metabolism. Cell. 2006;124(3):471-84. Epub 2006/02/14.
55. Vellai T, Takacs-Vellai K, Zhang Y, Kovacs AL, Orosz L, Muller F. Genetics: influence of TOR kinase on lifespan in C. elegans. Nature. 2003;426(6967):620. Epub 2003/12/12.
56. Jia K, Chen D, Riddle DL. The TOR pathway interacts with the insulin signaling pathway to regulate C. elegans larval development, metabolism and life span. Development. 2004;131(16):3897-906. Epub 2004/07/16.
57. Sheaffer KL, Updike DL, Mango SE. The Target of Rapamycin pathway antagonizes pha-4/FoxA to control development and aging. Current biology : CB. 2008;18(18):1355-64. Epub 2008/09/23.
58. Chen D, Li PW, Goldstein BA, Cai W, Thomas EL, Chen F, et al. Germline signaling mediates the synergistically prolonged longevity produced by double mutations in daf-2 and rsks-1 in C. elegans. Cell reports. 2013;5(6):1600-10. Epub 2013/12/18.
59. Tissenbaum HA, Guarente L. Increased dosage of a sir-2 gene extends lifespan in Caenorhabditis elegans. Nature. 2001;410(6825):227-30. Epub 2001/03/10.
60. Berdichevsky A, Viswanathan M, Horvitz HR, Guarente L. C. elegans SIR-2.1 interacts with 14-3-3 proteins to activate DAF-16 and extend life span. Cell. 2006;125(6):1165-77. Epub 2006/06/17.
61. Wang Y, Tissenbaum HA. Overlapping and distinct functions for a Caenorhabditis elegans SIR2 and DAF-16/FOXO. Mechanisms of ageing and development. 2006;127(1):48-56. Epub 2005/11/11.
62. Greer EL, Brunet A. Different dietary restriction regimens extend lifespan by both independent and overlapping genetic pathways in C. elegans. Aging cell. 2009;8(2):113-27. Epub 2009/02/26.
63. Nguyen MT, Somogyvari M, Soti C. Hsp90 Stabilizes SIRT1 Orthologs in Mammalian Cells and C. elegans. International journal of molecular sciences. 2018;19(11). Epub 2018/11/23.
64. Finkel T. Signal transduction by reactive oxygen species. The Journal of cell biology. 2011;194(1):7-15. Epub 2011/07/13.
65. Yang W, Hekimi S. A mitochondrial superoxide signal triggers increased longevity in Caenorhabditis elegans. PLoS biology. 2010;8(12):e1000556. Epub 2010/12/15.
66. Wei Y, Kenyon C. Roles for ROS and hydrogen sulfide in the longevity response to germline loss in Caenorhabditis elegans. Proceedings of the National Academy of Sciences of the United States of America. 2016;113(20):E2832-41. Epub 2016/05/04.
67. Hourihan JM, Moronetti Mazzeo LE, Fernandez-Cardenas LP, Blackwell TK. Cysteine Sulfenylation Directs IRE-1 to Activate the SKN-1/Nrf2 Antioxidant Response. Molecular cell. 2016;63(4):553-66. Epub 2016/08/20.
68. Dikic I, Elazar Z. Mechanism and medical implications of mammalian autophagy. Nature reviews Molecular cell biology. 2018;19(6):349-64. Epub 2018/04/06.
69. Melendez A, Talloczy Z, Seaman M, Eskelinen EL, Hall DH, Levine B. Autophagy genes are essential for dauer development and life-span extension in C. elegans. Science. 2003;301(5638):1387-91. Epub 2003/09/06.
70. Hansen M, Chandra A, Mitic LL, Onken B, Driscoll M, Kenyon C. A role for autophagy in the extension of lifespan by dietary restriction in C. elegans. PLoS genetics. 2008;4(2):e24. Epub 2008/02/20.
71. Toth ML, Sigmond T, Borsos E, Barna J, Erdelyi P, Takacs-Vellai K, et al. Longevity pathways converge on autophagy genes to regulate life span in Caenorhabditis elegans. Autophagy. 2008;4(3):330-8. Epub 2008/01/26.
72. Tissenbaum HA. Genetics, life span, health span, and the aging process in Caenorhabditis elegans. The journals of gerontology Series A, Biological sciences and medical sciences. 2012;67(5):503-10. Epub 2012/04/14.

73. Lopez-Otin C, Blasco MA, Partridge L, Serrano M, Kroemer G. The hallmarks of aging. Cell. 2013;153(6):1194-217. Epub 2013/06/12.
74. Chan DC. Fusion and fission: interlinked processes critical for mitochondrial health. Annual review of genetics. 2012;46:265-87. Epub 2012/09/01.
75. Suarez-Rivero JM, Villanueva-Paz M, de la Cruz-Ojeda P, de la Mata M, Cotan D, Oropesa-Avila M, et al. Mitochondrial Dynamics in Mitochondrial Diseases. Diseases. 2016;5(1). Epub 2017/09/22.
76. Sebastian D, Palacin M, Zorzano A. Mitochondrial Dynamics: Coupling Mitochondrial Fitness with Healthy Aging. Trends in molecular medicine. 2017;23(3):201-15. Epub 2017/02/12.
77. Flotho A, Melchior F. Sumoylation: a regulatory protein modification in health and disease. Annual review of biochemistry. 2013;82:357-85. Epub 2013/06/12.
78. Wilkinson KA, Henley JM. Mechanisms, regulation and consequences of protein SUMOylation. The Biochemical journal. 2010;428(2):133-45. Epub 2010/05/14.
79. Enserink JM. Sumo and the cellular stress response. Cell division. 2015;10:4. Epub 2015/06/24.
80. Geiss-Friedlander R, Melchior F. Concepts in sumoylation: a decade on. Nature reviews Molecular cell biology. 2007;8(12):947-56. Epub 2007/11/15.
81. Hietakangas V, Anckar J, Blomster HA, Fujimoto M, Palvimo JJ, Nakai A, et al. PDSM, a motif for phosphorylation-dependent SUMO modification. Proceedings of the National Academy of Sciences of the United States of America. 2006;103(1):45-50. Epub 2005/12/24.
82. Yang SH, Galanis A, Witty J, Sharrocks AD. An extended consensus motif enhances the specificity of substrate modification by SUMO. The EMBO journal. 2006;25(21):5083-93. Epub 2006/10/13.
83. Matic I, Schimmel J, Hendriks IA, van Santen MA, van de Rijke F, van Dam H, et al. Site-specific identification of SUMO-2 targets in cells reveals an inverted SUMOylation motif and a hydrophobic cluster SUMOylation motif. Molecular cell. 2010;39(4):641-52. Epub 2010/08/28.
84. Jentsch S, Psakhye I. Control of nuclear activities by substrate-selective and protein-group SUMOylation. Annual review of genetics. 2013;47:167-86. Epub 2013/09/11.
85. Desterro JM, Rodriguez MS, Hay RT. SUMO-1 modification of IkappaBalpha inhibits NF-kappaB activation. Molecular cell. 1998;2(2):233-9. Epub 1998/09/12.
86. Shalizi A, Gaudilliere B, Yuan Z, Stegmuller J, Shirogane T, Ge Q, et al. A calcium-regulated MEF2 sumoylation switch controls postsynaptic differentiation. Science. 2006;311(5763):1012-7. Epub 2006/02/18.
87. Moldovan GL, Pfander B, Jentsch S. PCNA controls establishment of sister chromatid cohesion during S phase. Molecular cell. 2006;23(5):723-32. Epub 2006/08/29.
88. Psakhye I, Jentsch S. Protein group modification and synergy in the SUMO pathway as exemplified in DNA repair. Cell. 2012;151(4):807-20. Epub 2012/11/06.
89. Steinacher R, Schar P. Functionality of human thymine DNA glycosylase requires SUMO-regulated changes in protein conformation. Current biology : CB. 2005;15(7):616-23. Epub 2005/04/13.
90. Sriramachandran AM, Dohmen RJ. SUMO-targeted ubiquitin ligases. Biochimica et biophysica acta. 2014;1843(1):75-85. Epub 2013/09/11.
91. Chang CC, Tung CH, Chen CW, Tu CH, Chu YW. SUMOgo: Prediction of sumoylation sites on lysines by motif screening models and the effects of various post-translational modifications. Scientific reports. 2018;8(1):15512. Epub 2018/10/21.
92. Gong L, Sun Q, Li DW. Sumoylation in Cellular Senescence and Aging. Current molecular medicine. 2017;16(10):871-6. Epub 2016/12/27.
93. Scurr LL, Haferkamp S, Rizos H. The Role of Sumoylation in Senescence. Advances in experimental medicine and biology. 2017;963:215-26. Epub 2017/02/16.
94. Princz A, Tavernarakis N. The role of SUMOylation in ageing and senescent decline. Mechanisms of ageing and development. 2017;162:85-90. Epub 2017/01/16.

95. Moll L, Roitenberg N, Bejerano-Sagie M, Boocholez H, Carvalhal Marques F, Volovik Y, et al. The Insulin/IGF signaling cascade modulates SUMOylation to regulate aging and proteostasis in C. elegans. eLife. 2018;7. Epub 2018/11/08.
96. Pelisch F, Tammsalu T, Wang B, Jaffray EG, Gartner A, Hay RT. A SUMO-Dependent Protein Network Regulates Chromosome Congression during Oocyte Meiosis. Molecular cell. 2017;65(1):66-77. Epub 2016/12/13.
97. Pelisch F, Sonneville R, Pourkarimi E, Agostinho A, Blow JJ, Gartner A, et al. Dynamic SUMO modification regulates mitotic chromosome assembly and cell cycle progression in Caenorhabditis elegans. Nature communications. 2014;5:5485. Epub 2014/12/06.
98. Ferreira HC, Towbin BD, Jegou T, Gasser SM. The shelterin protein POT-1 anchors Caenorhabditis elegans telomeres through SUN-1 at the nuclear periphery. The Journal of cell biology. 2013;203(5):727-35. Epub 2013/12/04.
99. Kaminsky R, Denison C, Bening-Abu-Shach U, Chisholm AD, Gygi SP, Broday L. SUMO regulates the assembly and function of a cytoplasmic intermediate filament protein in C. elegans. Developmental cell. 2009;17(5):724-35. Epub 2009/11/20.
100. Zhang H, Smolen GA, Palmer R, Christoforou A, van den Heuvel S, Haber DA. SUMO modification is required for in vivo Hox gene regulation by the Caenorhabditis elegans Polycomb group protein SOP-2. Nature genetics. 2004;36(5):507-11. Epub 2004/04/27.
101. Leight ER, Glossip D, Kornfeld K. Sumoylation of LIN-1 promotes transcriptional repression and inhibition of vulval cell fates. Development. 2005;132(5):1047-56. Epub 2005/02/04.
102. Broday L, Kolotuev I, Didier C, Bhoumik A, Gupta BP, Sternberg PW, et al. The small ubiquitin-like modifier (SUMO) is required for gonadal and uterine-vulval morphogenesis in Caenorhabditis elegans. Genes & development. 2004;18(19):2380-91. Epub 2004/10/07.
103. Ward JD, Bojanala N, Bernal T, Ashrafi K, Asahina M, Yamamoto KR. Sumoylated NHR-25/NR5A regulates cell fate during C. elegans vulval development. PLoS genetics. 2013;9(12):e1003992. Epub 2013/12/19.
104. Roy Chowdhuri S, Crum T, Woollard A, Aslam S, Okkema PG. The T-box factor TBX-2 and the SUMO conjugating enzyme UBC-9 are required for ABa-derived pharyngeal muscle in C. elegans. Developmental biology. 2006;295(2):664-77. Epub 2006/05/17.
105. Huber P, Crum T, Clary LM, Ronan T, Packard AV, Okkema PG. Function of the C. elegans T-box factor TBX-2 depends on SUMOylation. Cellular and molecular life sciences : CMLS. 2013;70(21):4157-68. Epub 2013/04/19.
106. Fisher K, Gee F, Wang S, Xue F, Knapp S, Philpott M, et al. Maintenance of muscle myosin levels in adult C. elegans requires both the double bromodomain protein BET-1 and sumoylation. Biology open. 2013;2(12):1354-63. Epub 2013/11/29.
107. Kim SH, Michael WM. Regulated proteolysis of DNA polymerase eta during the DNA-damage response in C. elegans. Molecular cell. 2008;32(6):757-66. Epub 2008/12/30.
108. Brenner S. The genetics of Caenorhabditis elegans. Genetics. 1974;77(1):71-94. Epub 1974/05/01.
109. Wong D, Bazopoulou D, Pujol N, Tavernarakis N, Ewbank JJ. Genome-wide investigation reveals pathogen-specific and shared signatures in the response of Caenorhabditis elegans to infection. Genome biology. 2007;8(9):R194. Epub 2007/09/19.
110. Hofmann ER, Milstein S, Boulton SJ, Ye M, Hofmann JJ, Stergiou L, et al. Caenorhabditis elegans HUS-1 is a DNA damage checkpoint protein required for genome stability and EGL-1-mediated apoptosis. Current biology : CB. 2002;12(22):1908-18. Epub 2002/11/26.
111. Syntichaki P, Troulinaki K, Tavernarakis N. eIF4E function in somatic cells modulates ageing in Caenorhabditis elegans. Nature. 2007;445(7130):922-6. Epub 2007/02/06.
112. Artal-Sanz M, Tavernarakis N. Prohibitin couples diapause signalling to mitochondrial metabolism during ageing in C. elegans. Nature. 2009;461(7265):793-7. Epub 2009/10/09.

113. Palikaras K, Lionaki E, Tavernarakis N. Coordination of mitophagy and mitochondrial biogenesis during ageing in C. elegans. Nature. 2015;521(7553):525-8. Epub 2015/04/22.
114. Rieckher M, Markaki M, Princz A, Schumacher B, Tavernarakis N. Maintenance of Proteostasis by P Body-Mediated Regulation of eIF4E Availability during Aging in Caenorhabditis elegans. Cell reports. 2018;25(1):199-211 e6. Epub 2018/10/04.
115. Pelisch F, Hay RT. Tools to Study SUMO Conjugation in Caenorhabditis elegans. Methods Mol Biol. 2016;1475:233-56. Epub 2016/09/16.
116. Pelisch F, Bel Borja L, Jaffray EG, Hay RT. Sumoylation regulates protein dynamics during meiotic chromosome segregation in C. elegans oocytes. Journal of cell science. 2019;132(14). Epub 2019/06/28.
117. Shen L, Tatham MH, Dong C, Zagorska A, Naismith JH, Hay RT. SUMO protease SENP1 induces isomerization of the scissile peptide bond. Nature structural & molecular biology. 2006;13(12):1069-77. Epub 2006/11/14.
118. Palikaras K, Tavernarakis N. Intracellular Assessment of ATP Levels in Caenorhabditis elegans. Bio-protocol. 2016;6(23). Epub 2017/02/15.
119. Palikaras K, Tavernarakis N. Measuring Oxygen Consumption Rate in Caenorhabditis elegans. Bio-protocol. 2016;6(23). Epub 2017/02/28.
120. Cristina D, Cary M, Lunceford A, Clarke C, Kenyon C. A regulated response to impaired respiration slows behavioral rates and increases lifespan in Caenorhabditis elegans. PLoS genetics. 2009;5(4):e1000450. Epub 2009/04/11.
121. Andreou AM, Tavernarakis N. Roles for SUMO modification during senescence. Advances in experimental medicine and biology. 2010;694:160-71. Epub 2010/10/05.
122. Ficulle E, Sufian MDS, Tinelli C, Corbo M, Feligioni M. Aging-related SUMOylation pattern in the cortex and blood plasma of wild type mice. Neuroscience letters. 2018;668:48-54. Epub 2018/01/13.
123. Rytinki MM, Lakso M, Pehkonen P, Aarnio V, Reisner K, Perakyla M, et al. Overexpression of SUMO perturbs the growth and development of Caenorhabditis elegans. Cellular and molecular life sciences : CMLS. 2011;68(19):3219-32. Epub 2011/01/22.
124. Broday L. The SUMO system in Caenorhabditis elegans development. The International journal of developmental biology. 2017;61(3-4-5):159-64. Epub 2017/06/18.
125. Fraser AG, Kamath RS, Zipperlen P, Martinez-Campos M, Sohrmann M, Ahringer J. Functional genomic analysis of C. elegans chromosome I by systematic RNA interference. Nature. 2000;408(6810):325-30. Epub 2000/12/01.
126. Jones D, Crowe E, Stevens TA, Candido EP. Functional and phylogenetic analysis of the ubiquitylation system in Caenorhabditis elegans: ubiquitin-conjugating enzymes, ubiquitin-activating enzymes, and ubiquitin-like proteins. Genome biology. 2002;3(1):RESEARCH0002. Epub 2002/01/25.
127. Syntichaki P, Troulinaki K, Tavernarakis N. Protein synthesis is a novel determinant of aging in Caenorhabditis elegans. Annals of the New York Academy of Sciences. 2007;1119:289-95. Epub 2007/12/07.
128. Tabara H, Sarkissian M, Kelly WG, Fleenor J, Grishok A, Timmons L, et al. The rde-1 gene, RNA interference, and transposon silencing in C. elegans. Cell. 1999;99(2):123-32. Epub 1999/10/27.
129. Alic N, Tullet JM, Niccoli T, Broughton S, Hoddinott MP, Slack C, et al. Cell-nonautonomous effects of dFOXO/DAF-16 in aging. Cell reports. 2014;6(4):608-16. Epub 2014/02/11.
130. Timmons L, Court DL, Fire A. Ingestion of bacterially expressed dsRNAs can produce specific and potent genetic interference in Caenorhabditis elegans. Gene. 2001;263(1-2):103-12. Epub 2001/02/27.
131. Calixto A, Chelur D, Topalidou I, Chen X, Chalfie M. Enhanced neuronal RNAi in C. elegans using SID-1. Nature methods. 2010;7(7):554-9. Epub 2010/06/01.
132. Winston WM, Molodowitch C, Hunter CP. Systemic RNAi in C. elegans requires the putative transmembrane protein SID-1. Science. 2002;295(5564):2456-9. Epub 2002/02/09.

133. Hertweck M, Gobel C, Baumeister R. C. elegans SGK-1 is the critical component in the Akt/PKB kinase complex to control stress response and life span. Developmental cell. 2004;6(4):577-88. Epub 2004/04/08.
134. Li W, Gao B, Lee SM, Bennett K, Fang D. RLE-1, an E3 ubiquitin ligase, regulates C. elegans aging by catalyzing DAF-16 polyubiquitination. Developmental cell. 2007;12(2):235-46. Epub 2007/02/06.
135. Bossis G, Melchior F. Regulation of SUMOylation by reversible oxidation of SUMO conjugating enzymes. Molecular cell. 2006;21(3):349-57. Epub 2006/02/04.
136. Stankovic-Valentin N, Drzewicka K, Konig C, Schiebel E, Melchior F. Redox regulation of SUMO enzymes is required for ATM activity and survival in oxidative stress. The EMBO journal. 2016;35(12):1312-29. Epub 2016/05/14.
137. Labbadia J, Morimoto RI. Repression of the Heat Shock Response Is a Programmed Event at the Onset of Reproduction. Molecular cell. 2015;59(4):639-50. Epub 2015/07/28.
138. Ghose P, Park EC, Tabakin A, Salazar-Vasquez N, Rongo C. Anoxia-reoxygenation regulates mitochondrial dynamics through the hypoxia response pathway, SKN-1/Nrf, and stomatin-like protein STL-1/SLP-2. PLoS genetics. 2013;9(12):e1004063. Epub 2014/01/05.
139. Back P, De Vos WH, Depuydt GG, Matthijssens F, Vanfleteren JR, Braeckman BP. Exploring real-time in vivo redox biology of developing and aging Caenorhabditis elegans. Free radical biology & medicine. 2012;52(5):850-9. Epub 2012/01/10.
140. Regmi SG, Rolland SG, Conradt B. Age-dependent changes in mitochondrial morphology and volume are not predictors of lifespan. Aging. 2014;6(2):118-30. Epub 2014/03/20.
141. Chaudhari SN, Kipreos ET. Increased mitochondrial fusion allows the survival of older animals in diverse C. elegans longevity pathways. Nature communications. 2017;8(1):182. Epub 2017/08/05.
142. Kanazawa T, Zappaterra MD, Hasegawa A, Wright AP, Newman-Smith ED, Buttle KF, et al. The C. elegans Opa1 homologue EAT-3 is essential for resistance to free radicals. PLoS genetics. 2008;4(2):e1000022. Epub 2008/05/06.
143. Zunino R, Braschi E, Xu L, McBride HM. Translocation of SenP5 from the nucleoli to the mitochondria modulates DRP1-dependent fission during mitosis. The Journal of biological chemistry. 2009;284(26):17783-95. Epub 2009/05/05.
144. Figueroa-Romero C, Iniguez-Lluhi JA, Stadler J, Chang CR, Arnoult D, Keller PJ, et al. SUMOylation of the mitochondrial fission protein Drp1 occurs at multiple nonconsensus sites within the B domain and is linked to its activity cycle. FASEB journal : official publication of the Federation of American Societies for Experimental Biology. 2009;23(11):3917-27. Epub 2009/07/30.
145. Guo C, Hildick KL, Luo J, Dearden L, Wilkinson KA, Henley JM. SENP3-mediated deSUMOylation of dynamin-related protein 1 promotes cell death following ischaemia. The EMBO journal. 2013;32(11):1514-28. Epub 2013/03/26.
146. Prudent J, Zunino R, Sugiura A, Mattie S, Shore GC, McBride HM. MAPL SUMOylation of Drp1 Stabilizes an ER/Mitochondrial Platform Required for Cell Death. Molecular cell. 2015;59(6):941-55. Epub 2015/09/20.
147. Fang EF, Hou Y, Palikaras K, Adriaanse BA, Kerr JS, Yang B, et al. Mitophagy inhibits amyloid-beta and tau pathology and reverses cognitive deficits in models of Alzheimer's disease. Nature neuroscience. 2019;22(3):401-12. Epub 2019/02/12.
148. Henley JM, Craig TJ, Wilkinson KA. Neuronal SUMOylation: mechanisms, physiology, and roles in neuronal dysfunction. Physiological reviews. 2014;94(4):1249-85. Epub 2014/10/08.
149. Anderson DB, Zanella CA, Henley JM, Cimarosti H. Sumoylation: Implications for Neurodegenerative Diseases. Advances in experimental medicine and biology. 2017;963:261-81. Epub 2017/02/16.
150. Henley JM, Carmichael RE, Wilkinson KA. Extranuclear SUMOylation in Neurons. Trends in neurosciences. 2018;41(4):198-210. Epub 2018/03/14.

151. Gill G. Something about SUMO inhibits transcription. Current opinion in genetics & development. 2005;15(5):536-41. Epub 2005/08/13.
152. Enserink JM. Regulation of Cellular Processes by SUMO: Understudied Topics. Advances in experimental medicine and biology. 2017;963:89-97. Epub 2017/02/16.
153. Wotton D, Pemberton LF, Merrill-Schools J. SUMO and Chromatin Remodeling. Advances in experimental medicine and biology. 2017;963:35-50. Epub 2017/02/16.
154. Cossec JC, Theurillat I, Chica C, Bua Aguin S, Gaume X, Andrieux A, et al. SUMO Safeguards Somatic and Pluripotent Cell Identities by Enforcing Distinct Chromatin States. Cell stem cell. 2018;23(5):742-57 e8. Epub 2018/11/08.
155. Cai R, Yu T, Huang C, Xia X, Liu X, Gu J, et al. SUMO-specific protease 1 regulates mitochondrial biogenesis through PGC-1alpha. The Journal of biological chemistry. 2012;287(53):44464-70. Epub 2012/11/16.
156. Anderson CA, Blackstone C. SUMO wrestling with Drp1 at mitochondria. The EMBO journal. 2013;32(11):1496-8. Epub 2013/05/02.
157. Buchan JR. mRNP granules. Assembly, function, and connections with disease. RNA biology. 2014;11(8):1019-30. Epub 2014/12/23.
158. Senchuk MM, Dues DJ, Schaar CE, Johnson BK, Madaj ZB, Bowman MJ, et al. Activation of DAF-16/FOXO by reactive oxygen species contributes to longevity in long-lived mitochondrial mutants in Caenorhabditis elegans. PLoS genetics. 2018;14(3):e1007268. Epub 2018/03/10.
159. Schaar CE, Dues DJ, Spielbauer KK, Machiela E, Cooper JF, Senchuk M, et al. Mitochondrial and cytoplasmic ROS have opposing effects on lifespan. PLoS genetics. 2015;11(2):e1004972. Epub 2015/02/12.
160. Dues DJ, Schaar CE, Johnson BK, Bowman MJ, Winn ME, Senchuk MM, et al. Uncoupling of oxidative stress resistance and lifespan in long-lived isp-1 mitochondrial mutants in Caenorhabditis elegans. Free radical biology & medicine. 2017;108:362-73. Epub 2017/04/11.
161. Ivanschitz L, Takahashi Y, Jollivet F, Ayrault O, Le Bras M, de The H. PML IV/ARF interaction enhances p53 SUMO-1 conjugation, activation, and senescence. Proceedings of the National Academy of Sciences of the United States of America. 2015;112(46):14278-83. Epub 2015/11/19.
162. Xia N, Cai J, Wang F, Dong B, Liu S, Chen F, et al. SENP1 Is a Crucial Regulator for Cell Senescence through DeSUMOylation of Bmi1. Scientific reports. 2016;6:34099. Epub 2016/09/24.
163. McManus FP, Bourdeau V, Acevedo M, Lopes-Paciencia S, Mignacca L, Lamoliatte F, et al. Quantitative SUMO proteomics reveals the modulation of several PML nuclear body associated proteins and an anti-senescence function of UBC9. Scientific reports. 2018;8(1):7754. Epub 2018/05/19.
164. Sonenberg N, Gingras AC. The mRNA 5' cap-binding protein eIF4E and control of cell growth. Current opinion in cell biology. 1998;10(2):268-75. Epub 1998/04/30.
165. Culjkovic B, Topisirovic I, Borden KL. Controlling gene expression through RNA regulons: the role of the eukaryotic translation initiation factor eIF4E. Cell Cycle. 2007;6(1):65-9. Epub 2007/01/25.
166. Decker CJ, Parker R. P-bodies and stress granules: possible roles in the control of translation and mRNA degradation. Cold Spring Harbor perspectives in biology. 2012;4(9):a012286. Epub 2012/07/06.
167. Hubstenberger A, Courel M, Benard M, Souquere S, Ernoult-Lange M, Chouaib R, et al. P-Body Purification Reveals the Condensation of Repressed mRNA Regulons. Molecular cell. 2017;68(1):144-57 e5. Epub 2017/10/03.
168. Andrei MA, Ingelfinger D, Heintzmann R, Achsel T, Rivera-Pomar R, Luhrmann R. A role for eIF4E and eIF4E-transporter in targeting mRNPs to mammalian processing bodies. RNA. 2005;11(5):717-27. Epub 2005/04/21.
169. Ferraiuolo MA, Basak S, Dostie J, Murray EL, Schoenberg DR, Sonenberg N. A role for the eIF4E-binding protein 4E-T in P-body formation and mRNA decay. The Journal of cell biology. 2005;170(6):913-24. Epub 2005/09/15.

170. Hoyle NP, Castelli LM, Campbell SG, Holmes LE, Ashe MP. Stress-dependent relocalization of translationally primed mRNPs to cytoplasmic granules that are kinetically and spatially distinct from P-bodies. The Journal of cell biology. 2007;179(1):65-74. Epub 2007/10/03.
171. Lejbkowicz F, Goyer C, Darveau A, Neron S, Lemieux R, Sonenberg N. A fraction of the mRNA 5' cap-binding protein, eukaryotic initiation factor 4E, localizes to the nucleus. Proceedings of the National Academy of Sciences of the United States of America. 1992;89(20):9612-6. Epub 1992/10/15.
172. Strudwick S, Borden KL. The emerging roles of translation factor eIF4E in the nucleus. Differentiation; research in biological diversity. 2002;70(1):10-22. Epub 2002/04/20.
173. Culjkovic-Kraljacic B, Borden KL. Aiding and abetting cancer: mRNA export and the nuclear pore. Trends in cell biology. 2013;23(7):328-35. Epub 2013/04/16.
174. Culjkovic B, Topisirovic I, Skrabanek L, Ruiz-Gutierrez M, Borden KL. eIF4E promotes nuclear export of cyclin D1 mRNAs via an element in the 3'UTR. The Journal of cell biology. 2005;169(2):245-56. Epub 2005/04/20.
175. Topisirovic I, Siddiqui N, Lapointe VL, Trost M, Thibault P, Bangeranye C, et al. Molecular dissection of the eukaryotic initiation factor 4E (eIF4E) export-competent RNP. The EMBO journal. 2009;28(8):1087-98. Epub 2009/03/06.
176. Culjkovic B, Topisirovic I, Skrabanek L, Ruiz-Gutierrez M, Borden KL. eIF4E is a central node of an RNA regulon that governs cellular proliferation. The Journal of cell biology. 2006;175(3):415-26. Epub 2006/11/01.
177. Culjkovic-Kraljacic B, Baguet A, Volpon L, Amri A, Borden KL. The oncogene eIF4E reprograms the nuclear pore complex to promote mRNA export and oncogenic transformation. Cell reports. 2012;2(2):207-15. Epub 2012/08/21.
178. Osborne MJ, Borden KL. The eukaryotic translation initiation factor eIF4E in the nucleus: taking the road less traveled. Immunological reviews. 2015;263(1):210-23. Epub 2014/12/17.
179. Borden KL. The eukaryotic translation initiation factor eIF4E wears a "cap" for many occasions. Translation (Austin). 2016;4(2):e1220899. Epub 2017/01/17.
180. Volpon L, Culjkovic-Kraljacic B, Osborne MJ, Ramteke A, Sun Q, Niesman A, et al. Importin 8 mediates m7G cap-sensitive nuclear import of the eukaryotic translation initiation factor eIF4E. Proceedings of the National Academy of Sciences of the United States of America. 2016;113(19):5263-8. Epub 2016/04/27.
181. Cohen N, Sharma M, Kentsis A, Perez JM, Strudwick S, Borden KL. PML RING suppresses oncogenic transformation by reducing the affinity of eIF4E for mRNA. The EMBO journal. 2001;20(16):4547-59. Epub 2001/08/14.
182. Kentsis A, Dwyer EC, Perez JM, Sharma M, Chen A, Pan ZQ, et al. The RING domains of the promyelocytic leukemia protein PML and the arenaviral protein Z repress translation by directly inhibiting translation initiation factor eIF4E. Journal of molecular biology. 2001;312(4):609-23. Epub 2001/09/29.
183. Jankowska-Anyszka M, Lamphear BJ, Aamodt EJ, Harrington T, Darzynkiewicz E, Stolarski R, et al. Multiple isoforms of eukaryotic protein synthesis initiation factor 4E in Caenorhabditis elegans can distinguish between mono- and trimethylated mRNA cap structures. The Journal of biological chemistry. 1998;273(17):10538-42. Epub 1998/05/30.
184. Keiper BD, Lamphear BJ, Deshpande AM, Jankowska-Anyszka M, Aamodt EJ, Blumenthal T, et al. Functional characterization of five eIF4E isoforms in Caenorhabditis elegans. The Journal of biological chemistry. 2000;275(14):10590-6. Epub 2000/04/01.
185. Mangio RS, Votra S, Pruyne D. The canonical eIF4E isoform of C. elegans regulates growth, embryogenesis, and germline sex-determination. Biology open. 2015;4(7):843-51. Epub 2015/05/17.
186. Friday AJ, Henderson MA, Morrison JK, Hoffman JL, Keiper BD. Spatial and temporal translational control of germ cell mRNAs mediated by the eIF4E isoform IFE-1. Journal of cell science. 2015;128(24):4487-98. Epub 2015/11/07.

187. Friday AJ, Keiper BD. Positive mRNA Translational Control in Germ Cells by Initiation Factor Selectivity. BioMed research international. 2015;2015:327963. Epub 2015/09/12.
188. Dinkova TD, Keiper BD, Korneeva NL, Aamodt EJ, Rhoads RE. Translation of a small subset of Caenorhabditis elegans mRNAs is dependent on a specific eukaryotic translation initiation factor 4E isoform. Molecular and cellular biology. 2005;25(1):100-13. Epub 2004/12/17.
189. Kosugi S, Hasebe M, Tomita M, Yanagawa H. Systematic identification of cell cycle-dependent yeast nucleocytoplasmic shuttling proteins by prediction of composite motifs. Proceedings of the National Academy of Sciences of the United States of America. 2009;106(25):10171-6. Epub 2009/06/13.
190. Chisnell P, Parenteau TR, Tank E, Ashrafi K, Kenyon C. The mTOR Target S6 Kinase Arrests Development in Caenorhabditis elegans When the Heat-Shock Transcription Factor Is Impaired. Genetics. 2018;210(3):999-1009. Epub 2018/09/20.